

Geologic controls on element concentrations
in
the Upper Freeport coal bed

C. B. Cecil, R. W. Stanton, S. D. Allshouse, R. B. Finkelman,
and L. P. Greenland

U.S. Geological Survey, National Center, Reston, VA 22092

Introduction

The primary objective of this investigation was to determine the geologic controls on variations of mineral matter in the Upper Freeport coal bed near Homer City, Pa. (fig. 1). Mineral matter consists of the inorganic constituents of coal, including mineral phases and elements other than organically bound hydrogen, oxygen, nitrogen, and sulfur [1]. By this definition, organic sulfur is not part of the mineral matter; however, variations of all sulfur forms including organic sulfur were considered in this study.

The concentrations of 70 elements were determined on 75 bench-channel and 21 complete bed-channel samples from two deep mines in the study area (fig. 2). Ultimate, proximate, sulfur forms, maceral, and pyrite morphological analyses were also conducted on these samples. Scanning electron microscope [2] and electron microprobe [3] analyses were conducted on selected channel and column samples to determine element-mineral and maceral associations.

Results

The Upper Freeport coal bed of the Homer City study area is divisible in the field into five zones (fig. 3). In the northern part of the area where all five zones are present, the coal bed averages 83 inches (211 cm) in thickness; in the southern part where only three zones are present, the coal bed averages 48 inches (122 cm) in thickness. Laboratory analyses show that each of the five zones consists of distinct mineral matter-maceral associations. Elements that tend to be concentrated in the upper and/or basal zones of the bed include As, Cd, Cl, Fe, Hg, Mn, Pb, Se, S, and Zn.

Linear regression analysis was used to determine relationships among elements, sulfur (total, pyritic, and organic), ash, and maceral concentrations on the 75 bench-channel samples. On the basis of this statistical analysis, element concentrations in the coal can be related to three variables: ash, pyritic sulfur, and calcium (reported as CaO). The elements (some of which are reported as oxides) that positively correlate with each of the three variables are shown in figure 4. Only manganese is positively correlated with all three variables. The fusinite-semifusinite maceral concentrations correlate with the ash content.

Discussion

The mineral-matter content of the Upper Freeport coal bed of the Homer City area was controlled by interrelated geologic, geochemical, and paleobotanical variables. The elements that positively correlate with the ash (fig. 4) probably accumulated contemporaneously with the peat. Possible sources include: 1) mineral matter incorporated by plants, or 2) detrital minerals and dissolved elements incorporated during the peat stage of coal formation. Element concentrations resulting from mixed sources such as deposition of detrital minerals, sorption of dissolved ionic species, and mineral matter of plant origin would not lead to a strongly interrelated assemblage. Fusinite and semifusinite are generally believed to be the coalified products of partially oxidized peat and plant material. Oxidation results in a loss of organic matter and a concentration of residual mineral matter;

therefore, as the fusinite-semifusinite content of the coal increases, the ash and statistically related element contents also increase. Plant inorganic matter must be the major source of the ash-related elements. This interpretation is consistent with 1) the moderate ash content (8-15%), 2) the positive correlation between ash and fusinite-semifusinite content, and 3) the element-ash correlations illustrated in figure 4.

The calcium in the coal bed is primarily in authigenic calcite. Fixation of the calcium in the peat by ion exchange and/or as calcium salts of humic acids with subsequent liberation of CO₂ and organically bound calcium during coalification may have resulted in the formation of calcite in macerals and cleats. The buffering effect of calcium carbonate species supplied to the ancestral peat partially controlled the pH. Sulfate-reducing bacterial activity is greatest at neutral pH and minimal or nonexistent at pH 4.0 or less [4]. Therefore, pH values near neutral favor 1) bacterial generation of sulfide species if sulfate ions are present, 2) bacterial degradation of peat that could result in the concentration of mineral matter, and 3) retention of mineral matter because of decreasing solubilities as pH increases.

Low pH (<4.0) would favor a low-ash (<8%), low-sulfur (<1%) coal. Partial neutralization of waters of the ancestral peat of the Upper Freeport coal is indirectly indicated by the presence of 1) calcite in coal macerals and cleats and 2) mixed carbonate and clastic sediments directly under the coal bed. The Upper Freeport coal studied is a medium ash (8-15%), medium sulfur (1-3%) coal that is consistent with partial neutralization of peat waters.

The pyrite in the Upper Freeport coal is usually concentrated in the upper and/or basal zones of the bed throughout the area. Genetically, pyrite and the associated trace elements As and Hg appear unrelated to the bulk of the coal ash. Although pH conditions were suitable for pyrite deposition, pyrite concentrations were controlled by the availability of ferrous iron and appropriate sulfur species.

Summary

The elements in the Upper Freeport coal bed of the area can be genetically related to three variables (i.e., ash content, pyritic sulfur content, and calcium content). The buffering effect of dissolved calcium carbonate species may have been sufficient to maintain a pH of 4 or greater. Under these pH conditions, sulfate-reducing bacteria generated sulfide species, which reacted to form minerals such as pyrite, sphalerite, chalcocopyrite, and galena. During coalification, the calcium salts of humic acids decomposed to form calcite and carbon compounds that may account for the calcite in coal macerals and cleats. The pH conditions that existed during peat formation were conducive to the retention of mineral matter, the bulk of which was of plant origin.

References

- [1] C. P. Rao, and H. J. Gluskoter, Occurrence and distribution of minerals in Illinois coals. Illinois Geol. Survey Cir. 476 (1973).
- [2] R. B. Finkelman, R. W. Stanton, C. B. Cecil and J. A. Minkin, Modes of occurrence of selected trace elements in several Appalachian coals, (1979), this session.
- [3] J. A. Minkin, E. C. T. Chao and C. T. Thompson, Distribution of elements in coal macerals and minerals: determination by electron microprobe, (1979), this session.
- [4] J. E. Zajic, Microbial biogeochemistry, Academic Press (1969).

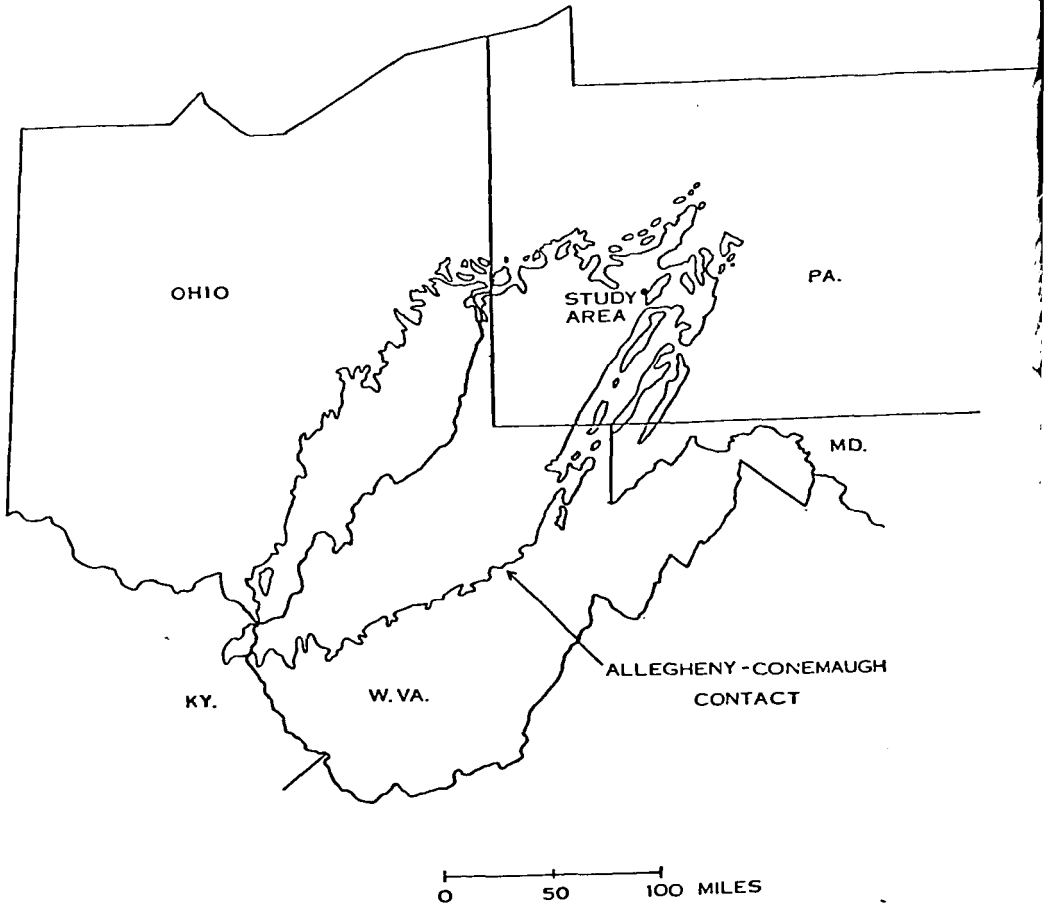
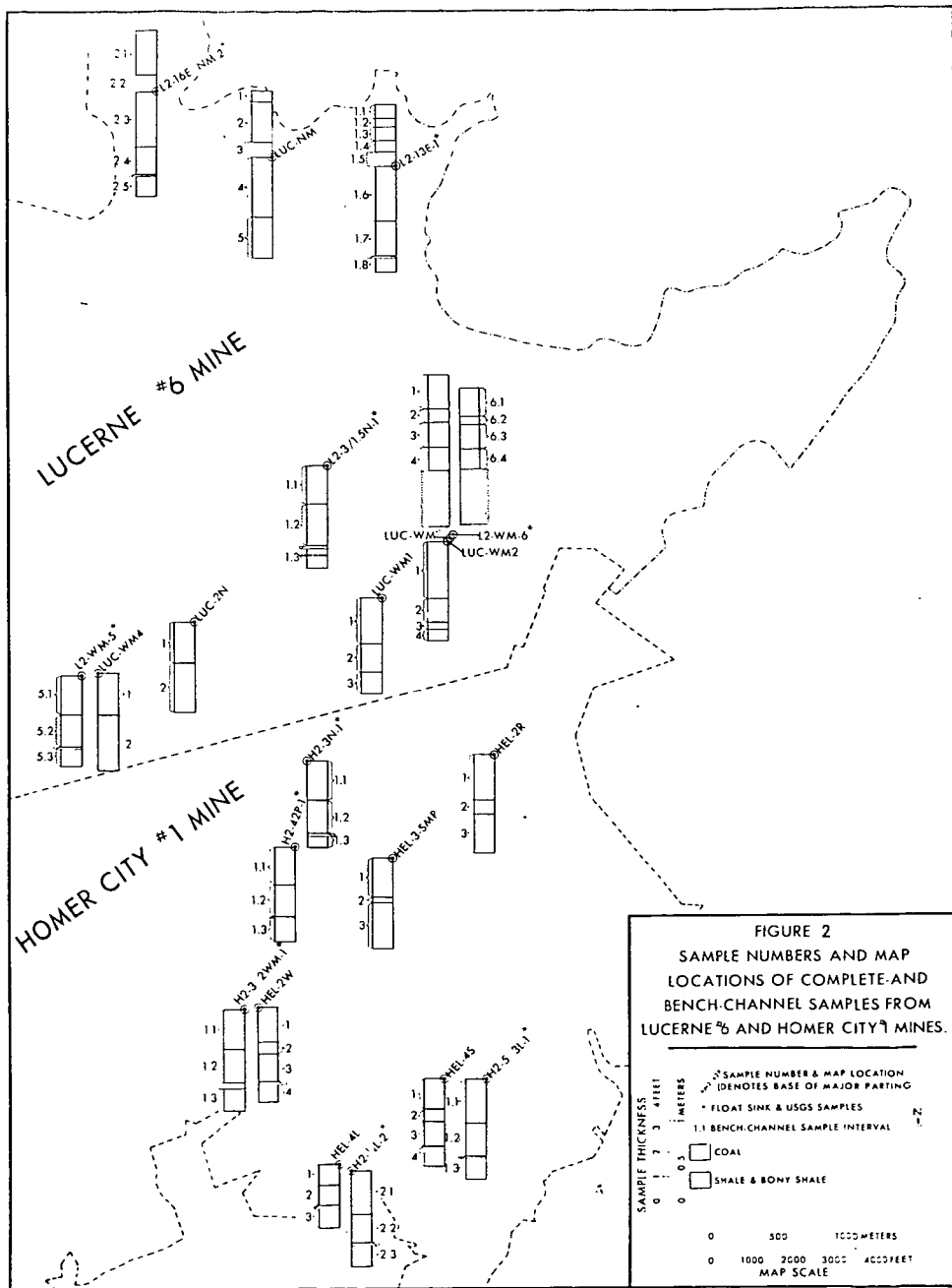
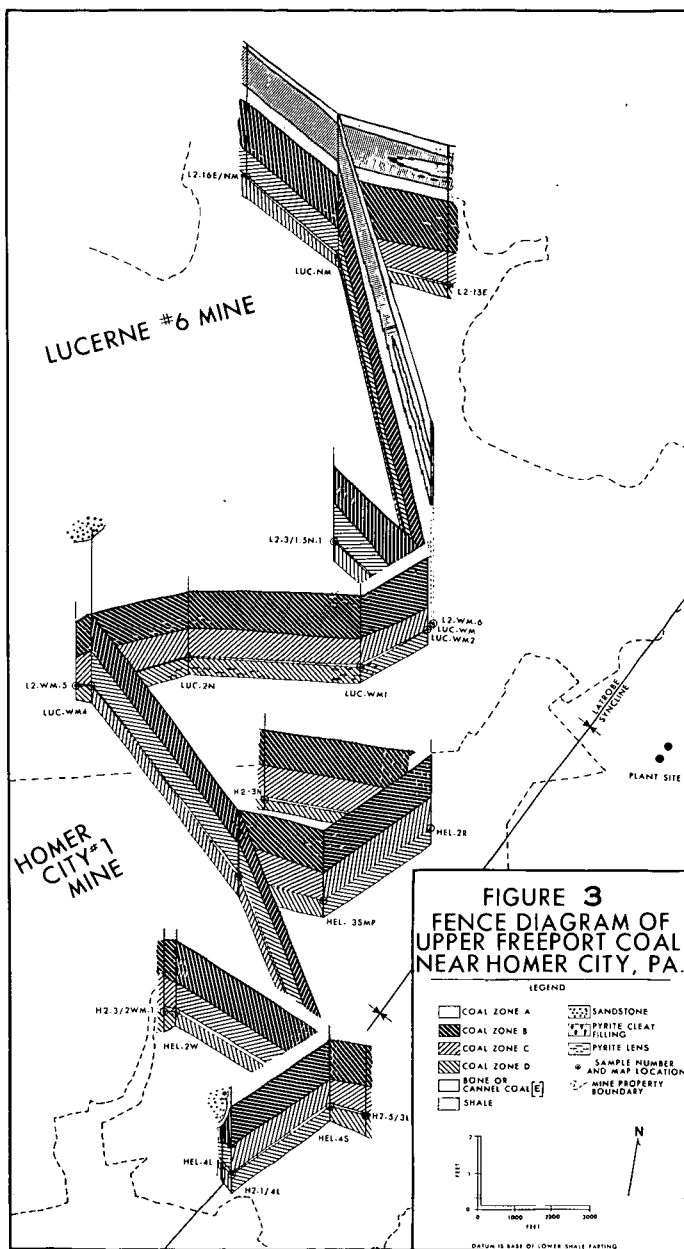


Figure 1. - Index map of Homer City, Pa., study area and Allegheny Group-Conemaugh Group contact.





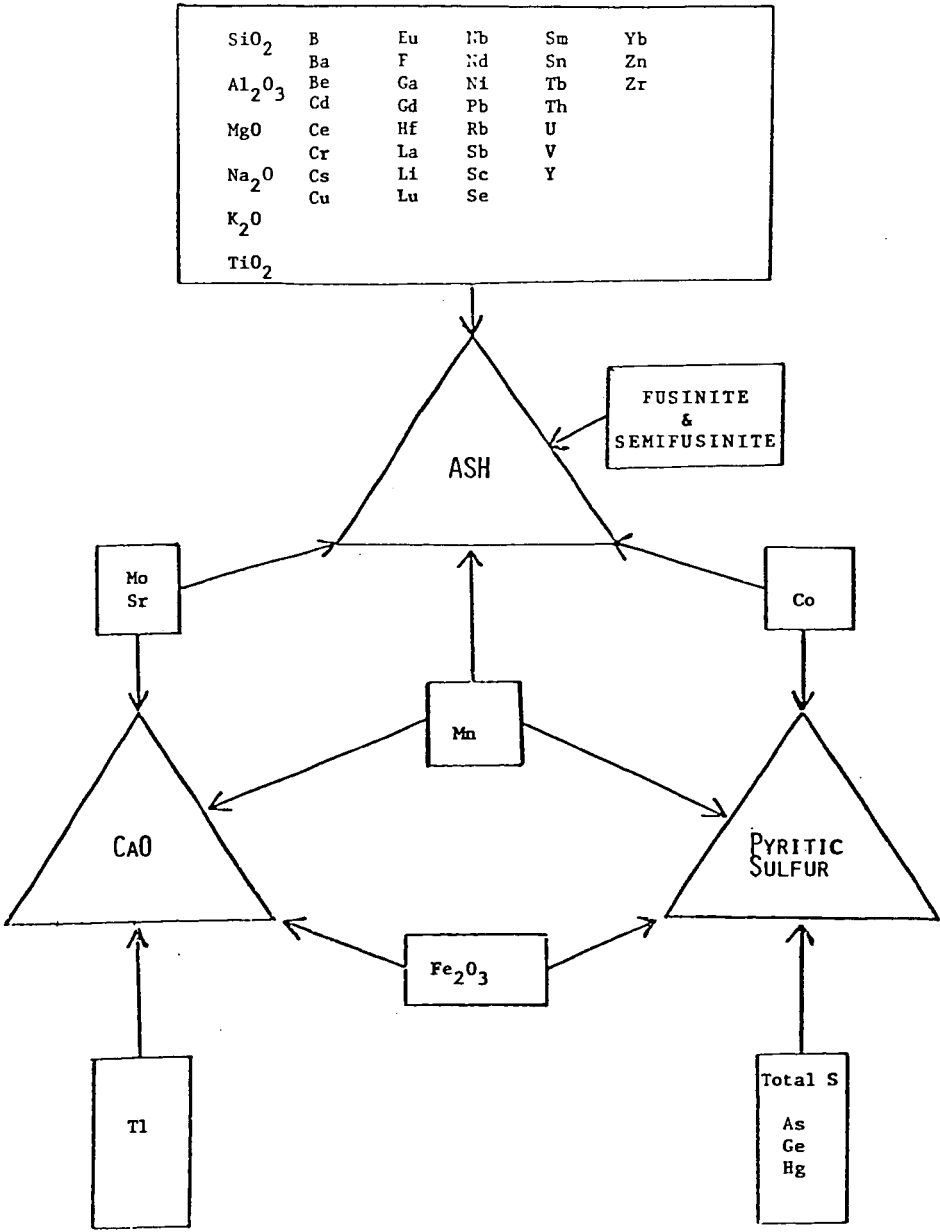


Figure 4. Mineral matter constituents and macerals of the Upper Freeport coal that statistically positively correlate with ash, pyritic sulfur, and calcium.

Modes of Occurrence of Selected Trace Elements
in
Several Appalachian Coals

Robert B. Finkelman, Ronald W. Stanton,
C. Blaine Cecil and Jean A. Minkin

U.S. Geological Survey, National Center, Reston, VA 22092

Most coal-cleaning processes are predicated on differences in physical properties between the coal and the included mineral matter believed to contain the undesirable elements. However, as the mode of occurrence of most elements in coal (particularly the trace elements) is not clearly understood, the effectiveness of the coal-cleaning procedures in removing these trace elements is uncertain. By combining detailed chemical, mineralogical, and petrographic techniques we have determined how various trace elements, particularly those of environmental interest occur in several Appalachian bituminous coals.

This study was conducted primarily on polished blocks of coal using a scanning electron microscope (SEM) with an energy dispersive X-ray detector. With this system individual *in situ* mineral grains as small as 0.5 μm can be observed and analyzed for all elements of atomic number 11 (Na) and greater that are present in concentrations as low as about 0.5 weight percent [Finkelman (1), and Finkelman and Stanton (2)].

On the basis of the abundance of the accessory minerals in the Waynesbury coal, Finkelman (1) calculated the concentrations for 10-15 trace elements. The calculated values for many of these elements, including Zn and Cu, correlated well with their analytical values. These data suggest that the trace elements occur in this coal predominantly as specific accessory minerals. For example, zinc occurs as zinc sulfide (sphalerite; Figure 1) and copper as copper iron sulfide (chalcopyrite; Figure 2). SEM analysis of other coals from the Appalachian Basin appears to substantiate this conclusion. Preliminary estimates based on the new data suggest that most of the selenium in these coals and much of the lead occur as 1 to 3 μm particles of lead selenide (clausthalite?), which are often associated with cadmium-bearing sphalerite and chalcopyrite, (Figure 3). These fine-grained mineral intergrowths occur exclusively within the organic constituents and in all probability formed in place. Experiments by Bethke and Barton (3) on the chemical partitioning of selenium between sphalerite, galena (PbS) and chalcopyrite suggest that the sphalerite-chalcopyrite-clausthalite assemblage would be the expected assemblage at low temperature (300°C).

If all the selenium in these coals occurred as lead selenide this would tie up about half the available lead. Although galena is not found associated with sphalerite or chalcopyrite it does occur as micrometer-sized particles on the edges of pyrite grains (Figure 4). This mode of occurrence may account for the lead in excess of that tied up by the selenium.

Because substantial amounts of Zn, Cu, Pb, Cd, and Se occur as finely dispersed mineral grains in the organic matrix, considerable amounts of these elements can be retained in the lighter specific gravity fractions of cleaned coal (4).

Figure 5 illustrates the concentration of Zn in a size-gravity separation of the Upper Freeport coal. Similar results have been obtained for Cd, Cu, and Pb on six samples of this coal. The divergence of these curves in the high specific gravity range is consistent with the observation that these elements occur as fine-grained minerals which are increasingly released from their organic matrix with fine grinding.

It is evident from Figure 5 that the concentrations, on a whole coal basis, of Zn (this would apply to Cu, Cd, and Pb as well) are much greater for the higher specific gravity (Sp. G.) fractions. However, the bulk of the coal generally floats at the lower Sp. G. levels. Recalculating these data to show the proportion of each element in each Sp. G. fraction reveals that substantial amounts of these

elements are retained in the lighter (<1.50) fractions (Table 1). Similar results were obtained in a washability study of these coals by Cavallaro and others (5). Not all the Upper Freeport samples demonstrated this type of behavior. In several samples more than 50 weight percent of the coal sank in Sp. G. 1.60 liquids, carrying with it as much as 85 percent of these trace elements.

Figure 6 illustrates the concentration of Zn in the high-temperature ash of one of the size-gravity fractions. Similar results have been obtained for Cd, Cu, and Zn in many of the Upper Freeport samples. The highest concentrations of these elements commonly occur in the ash of the lightest fraction of the coal. This reflects the association of fine-grained sphalerite, chalcopyrite, and clausthalite (?) with the organic matrix. The high concentrations in the sink 1.8 fractions are probably due to the release of some of these minerals during grinding.

Many of the trace elements of environmental interest (e.g. As, Cd, Cu, Hg, Pb, Tl, Se, Zn) occur as sulfides. In coal the most prominent sulfide mineral is pyrite (FeS₂). The crystal chemistry of pyrite allows for only a small amount of solid solution with most of the above mentioned elements (6). Indeed, preliminary electron microprobe and ion microprobe analyses of pyrite and its dimorph marcasite from several coals suggest that most pyrite is free of trace constituents to concentrations as low as 100 ppm.

Arsenic is one chalcophile element whose mode of occurrence and behavior differs from that of Zn, Cd, Pb, Cu, and Se. Although arsenic sulfide has been observed in coals, the bulk of the As in the Upper Freeport coal appears to be associated with pyrite. The distribution of As in the Upper Freeport coal appears to be controlled, to a large extent, by the fractures within the coal and within the pyrite. Thus far, arsenic has been found only in pyrite horizons that are associated with fractured coal, although not all such pyrite occurrences had detectable arsenic. Within these favorable sites As was found only along the outer rims of pyrite grains or along fractures within the pyrite. Optically, the As-bearing pyrite always appears "dirty" due to abundant microfractures, perhaps caused by reactions with epigenetic As-bearing solutions. Pyrite without microfractures did not have detectable arsenic (>0.01 weight percent).

In the size-gravity separations, As was found to concentrate in the sink 1.8 fraction along with pyrite.

Correlation coefficients based on statistical analyses of analytical data from 96 Upper Freeport coal samples indicate that As and pyrite correlate well with each other (7). Mercury, the only other element with which arsenic and pyrite have a strong positive correlation, behaves similarly to arsenic in the size-gravity separations (Table 1). In all probability the mode of occurrence of mercury is similar to that of arsenic.

With this type of information on mode of occurrence, coal-cleaning procedures can be devised to effectively remove the undesirable trace elements.

References

- (1) R. B. Finkelman, Scanning Electron Microscopy/1978/vol. 1, 143, (1978).
- (2) R. B. Finkelman and R. W. Stanton, Identification and significance of accessory minerals from a bituminous coal. Fuel (in press).
- (3) P. M. Bethke and P. B. Barton, Jr. Econ. Geol., 66, 140, (1971).
- (4) C. B. Cecil, R. W. Stanton, S. D. Allshouse and R. B. Finkelman, Preparation characteristics of the Upper Freeport coal, Homer City, PA. R & D Program Report (in press).
- (5) J. A. Cavallaro, A. W. Deurbrouck, H. Schults, G. A. Gibbon, and E. A. Hattman. A washability and analytical evaluation of potential pollution from trace elements in coal. EPA interagency Energy/ Environmental R & D Program Report EPA-60017-78-038, (1978).
- (6) W. A. Deer, R. A. Howie and J. Zussman; Rock Forming Minerals, vol. 5, non-silicates, 1962, J. Wiley and Sons Inc.
- (7) C. B. Cecil, R. W. Stanton, S. D. Allshouse, R. B. Finkelman and L. P. Greenland. Mineral matter in the Upper Freeport Coal Bed, Homer City, Pa., EPA, Inter-agency Energy/Environmental R & D Program Report (in press).

Table 1. Trace element concentrations in size-gravity splits of two Appalachian coals. Values are in percentages of the element in each Sp. G. fraction of a size split.

Upper Freeport (H2-42P-1.1)

Mesh size	Cd		Cu		Pb		Zn		Hg		As	
	+1/4"	8x100	+1/4"	8x100	+1/4"	8x100	+1/4"	8x100	+1/4"	8x100	+1/4"	8x100
Float 1.275	36	9	20	10	19	13	5	28	21	0.5	8	tr
1.300	17	16.5	33	30	18	9	12.5	27	13	3.5	10.5	6
1.325	10	0.5	18	12	4	2	11	4	2	3.5	7	1
1.400	6	6.5	13	12	10	10	7.5	4.5	4	5	8	2.5
Cumulative percent	(69)	(42.5)	(67)	(45)	(71)	(33)	(35)	(63.5)	(40)	(12.5)	(33.5)	(15.5)
1.600	9	4	11	8.5	14	10	5	7	10	4	4	6
1.80	9	14.5	32	5	5	4	65	9	15	10	4	2.5
Sink 1.80	12.5	49.5	42	10	10	53	21	40	4	87	46.5	75
												99
												69.5
												78

Waynesburg

Mesh size	Cu		Pb		Zn		As*	
	>10	10-20	>10	10-20	>10	10-20	>10	10-20
Sp. G.								
1.30	33	18	34	15.5	28.5	27	15	34.5
1.50	65.5	79	53	60.5	41.5	59.5	62.5	33
Cumulative percent	(98.5)	(97)	(91)	(94.5)	(85)	(70)	(86.5)	(77.5)
1.70	0.5	1.5	3	1.5	4.5	9	2.5	6
Sink 1.70	0.5	1.5	6	4	10	21	11	17
								25
								<150
								<150
								1500
								990
								610

*ppm
tr = trace

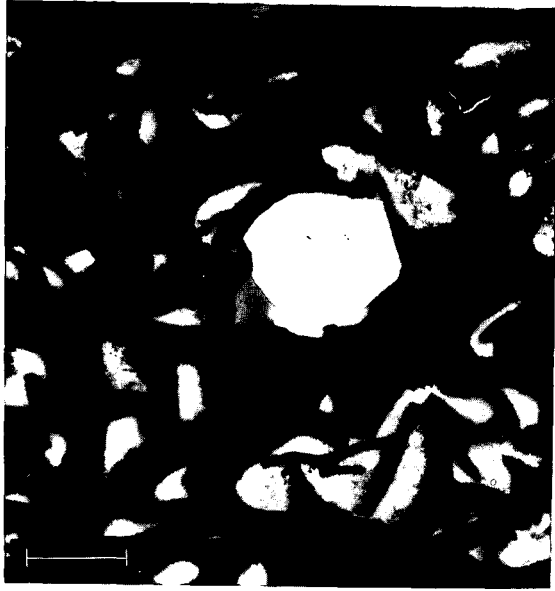


Figure 1. SEM photomicrograph of a sphalerite crystal in semifusinite.
Scale bar = 10 μm .



Figure 2. SEM photomicrograph of a chalcopyrite grain.
Scale bar = 10 μm .



Figure 3. SEM photomicrograph of a grain consisting of sphalerite (right rim), chalcopyrite (left rim), and lead selenide (bright cap).
Scale bar = 10 μm .



Figure 4. SEM photomicrograph of galena (light gray) on pyrite (medium gray). Backscattered electron image.
Scale bar = 1 μm .

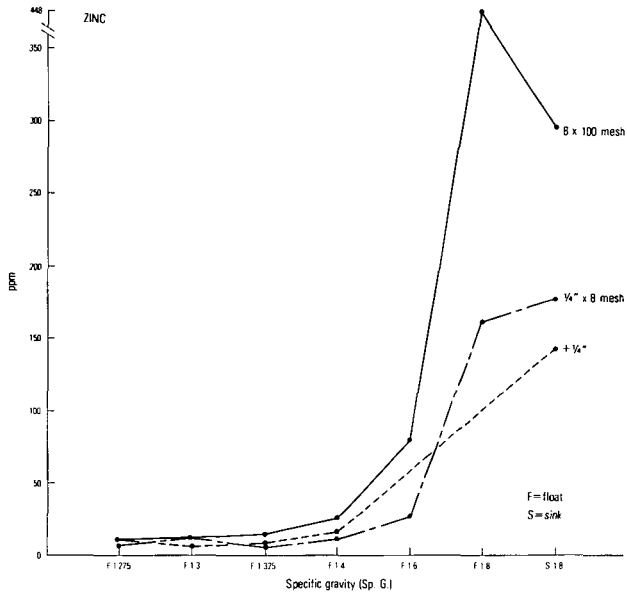


Figure 5. Concentration of zinc (whole-coal basis) in size-gravity separates of the Upper Freeport coal sample H2-42P-1.1.

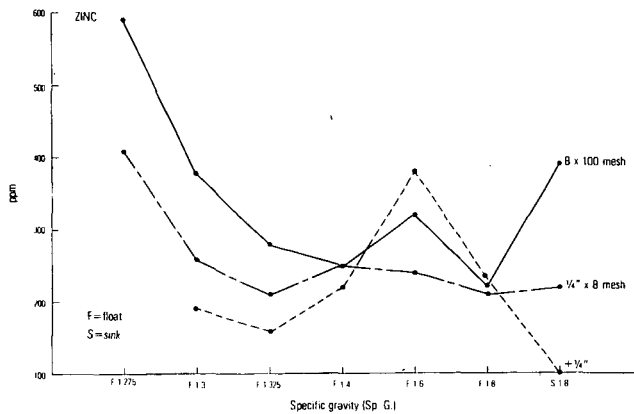


Figure 6. Concentration of zinc in the ash of size-gravity separates of Upper Freeport coal sample H2-53L-1.0.

Distribution of Elements in Coal Macerals and Minerals:
Determination by Electron Microprobe

Jean A. Minkin, E. C. T. Chao and Carolyn L. Thompson

U. S. Geological Survey, National Center, Reston, Va. 22092

Systematic study of elemental abundances in coal macerals and minerals is vital to understanding the genetic history and geological significance of particular coal beds, in correlating coal beds for coal mine planning, in assessing the environmental impact of utilization of coal from a particular source, and in evaluating the potential for recovery of waste by-products and for catalytic action in coal conversion. In-situ determinations of elemental concentrations in macerals and in clays, sulfides and other mineral constituents may help to establish the primary vs. secondary emplacement of particular elements, i.e. elements which were fixed when the coal precursors were deposited vs. mobile elements which may have been introduced and/or redistributed by ground water circulation and other diagenetic processes. Furthermore, determination of the distribution of elements between macerals and minerals is essential in evaluating the possibility of removal of contaminants by grinding and washing, because elements in macerals cannot be effectively removed by these procedures.

Application of electron microprobe analysis to coal-related studies is still in the developmental stage (1). We report here preliminary results of intensive study of one columnar coal sample to indicate the nature of the data on elemental distribution that are readily obtainable through use of the electron microprobe. In order to preserve the stratigraphic relationships of the different coal facies, polished blocks (Figure 1) and polished thin sections were prepared to represent the total thickness of the coal bed. These blocks and thin sections were first studied petrographically with the optical microscope, and areas representative of the principal lithologic units (Figure 2) were designated for analysis by the electron microprobe. A 118-cm thick columnar sample of medium volatile bituminous Upper Freeport coal used for this study was collected in the Helen Mine, Indiana County, Pa. Petrographic analysis (E. C. T. Chao et al., unpublished data) indicates that the coal bed is composed of two cycles of organic-matter deposition and five major lithologic coal types (Figure 3). The division between the two cycles of deposition is the base of one major lithologic unit, a carbonaceous shale parting with bands of vitrite between depths 85 and 92.5 cm. This carbonaceous shale, characterized by water-transported depositional features, may be a key stratigraphic marker. Above the shale parting three major lithologic coal types are discernible: one from the top of the coal to 30 cm depth, another from 30 to 50 cm, and a third from 50 to 85 cm. The fifth is the column interval from 92.5 to 118 cm.

The electron microprobe has been used for in-situ determinations of abundances of 23 elements in the macerals and for analyses of discrete mineral grains present at representative depths of the column. The instrument at the Reston laboratories of the U. S. Geological Survey is routinely capable of wavelength dispersive analysis of all elements stable in vacuum and of atomic number 9 (fluorine) and greater. Limit of detectability for most elements is about 100 ppm, and the minimum target area which can be analyzed is approximately $3 \times 3 \mu\text{m}$. Penetration depth of the electron beam into the target is from 1 to $5 \mu\text{m}$.

Table 1 summarizes the range of abundance of the 23 elements analyzed in macerals of the five major lithologic coal types of the column. At the sites where these elements were detected by probe analysis, discrete minerals were not observed optically down to the limit of resolution (about $0.5 \mu\text{m}$). Strehlow et al. (2), in a transmission electron microscope study of Illinois No. 6 coal, reported a profusion of mineral particles in vitrinite in the size range from 30nm to approximately $0.2 \mu\text{m}$. Thus it is probable that some of the elements detected in our electron microprobe maceral analyses are associated with submicron-sized mineral

matter. In particular, silicon and aluminum, which vary in abundance in a parallel manner are probably associated with extremely finely dispersed clay minerals.

Two elements, sulfur and chlorine, clearly seem organically associated in the macerals of this coal. Sulfur appears to be homogeneously distributed throughout a given maceral, implying an association on the molecular level. Furthermore, a comparable amount of iron is not present, as would be true if this were submicron-sized pyrite or marcasite. The amounts of organic sulfur determined by electron microprobe analysis (Table 1) tend to be greater in the lower depositional unit and are in good agreement with analyses of this coal by conventional methods (3,4). The amount of sulfur in inertinite tends to be about half that in vitrinite, while the sulfur content of the exinites analyzed (this coal contains very little exinite (Figure 3)), more closely approaches the level in vitrinite. Harris et al. in a suite of coals they studied (5) found that exinites always have more sulfur than do vitrinites but determinations by Raymond and Gooley (1) generally agree with our results. In the Upper Freeport sample, chlorine like sulfur, seems homogeneously distributed in a given maceral. In addition, comparable levels of cations such as sodium or potassium were not detected (Table 1), as would be expected if the chlorine were associated with mineral inclusions. Gluskoter and Ruch (6) also concluded that in coals from the Illinois Basin weakly bound chlorine in organic combination was a likely mode of occurrence. Chlorine concentrations in the Upper Freeport sample tend to be higher for the upper cycle of deposition (Table 1). X-ray fluorescence data on ash from this coal show a similar trend (3). This trend perhaps implies greater salinity of the swamp water during the period of growth and deposition of the coal precursors of the upper depositional cycle, compared with the lower.

A systematic study has also been made of the composition of the clays over the full 118-cm depth of the column (Table 2). Identification of the clay minerals is based on their chemical compositions. Those with $K_2O > 2.5$ wt. % are tentatively designated as illites, those with $Al_2O_3 > 30$ wt. %, $SiO_2 > 40$ wt. % and $K_2O \leq 1.5$ wt. % are labeled kaolinites, and "mixed layer" clays are those with K_2O between 1.6 and 2.5 wt. %. In the upper unit of deposition, illites are distinctly dominant and kaolinites occur mostly in shale. "Mixed layer" clays are found only below 92.5 cm depth. Clays in the shales are generally lower in silicon and higher in iron than those in the rest of the coal column. Illites tend to be higher in titanium and lower in aluminum than the other two clay types.

Electron microprobe analyses of iron sulfides determined that arsenic is present in pyrite only from depth 5 to 20 cm in this coal column. The mode of arsenic occurrence is discussed by Finkelman et al. (7).

Because much of this sample of Upper Freeport coal is vitrinite-rich (Figure 3), even small amounts of non-volatile elements in the vitrinite (Table 1) will contribute significantly to the coal ash. The clay and quartz optically observed in vitrinite generally is less than $30\mu m$ in grain size; thus, the elements shown in the analyses of Table 2 will also probably remain in the coal even after fine grinding and washing.

These preliminary elemental studies using the electron microprobe have documented variations in sulfur and chlorine abundance in macerals, clay compositions, and presence of arsenic in pyrite which clearly indicate differences in the depositional and subsequent environmental characteristics of the upper and lower depositional units of this coal. It is hoped that after refinement of our methods of study, more complete evaluation of the abundance of particular elements in a given coal bed will be possible through correlation of modal analyses of maceral-mineral composition (E. C. T. Chao et al., unpublished data) with in-situ chemical data for macerals and minerals obtained by electron microprobe and proton-induced X-ray emission (the latter for elements at concentrations less than 100 ppm) techniques.

References

- (1) R. Raymond and R. Gooley, Scanning Electron Microscopy, 1978/1, p. 93-108 (1978), Scanning Electron Microscopy, Inc. AMF O'Hare, Ill. 60666.
- (2) R. A. Strehlow, L. A. Harris, and C. S. Yust, Fuel 57, 185 (1978).

- (3) C. B. Cecil, R. W. Stanton, S. D. Allshouse, R. B. Finkelman, and L. P. Greenland, "Mineral matter in the Upper Freeport Coal Bed, Homer City, Pa.", EPA Interagency Energy/Environment R & D Program Report (1979). In press.
- (4) ASTM (1977). Annual Book of ASTM Standards. Designation D2492-77. Amer. Soc. Testing and Materials, Phila., Pa., p. 322-326.
- (5) L. A. Harris, C. S. Yust, and R. S. Crouse, Fuel 56, 456 (1977).
- (6) H. J. Gluskoter and R. R. Ruch, Fuel 50, 65 (1971).
- (7) R. B. Finkelman, R. W. Stanton, C. B. Cecil, and J. A. Minkin, "Modes of Occurrence of Selected Trace Elements in Several Appalachian Coals" (1979), this session.

Table 1. Electron Microprobe Determinations of Minor and Trace Element Concentrations (Wt. %) in Macerals of the Five Major Lithologic Coal Types, Upper Freeport Column Sample H2-42P-1.

	0 - 30 cm		30 - 50 cm		50 - 85 cm	
	V	E and I	V	E and I	V	E and I
Al	0-0.11	0-0.14	0.03-0.05	0.09-8.3	0-0.48	0-8.0
Ba	n.d.	n.d.	0	0	0-0.03	0-0.10
Bi	0	0	0-0.07	0-0.06	0	0-0.07
Ca	0.02-0.07	0-0.11	0-0.05	0-2.6	0-0.07	0-6.2
Cl	0.25-0.28	0-0.15	0.24-0.32	0.09-0.48	0.15-0.31	0-2.2
Co	0	0	0-0.05	0-0.08	0-0.04	0-0.04
Cr	0-0.02	0	0-0.05	0-0.05	0-0.03	0-0.08
Cu	0-0.06	0-0.03	0	0	0-0.08	0-0.10
F	0	0-0.08	0	0-0.02	0-0.05	0-0.12
Fe	0-0.05	0-0.41	0-0.04	0-0.20	0	0-0.09
K	0	0-0.36	0	0-0.12	0-0.06	0-0.92 (I) 0-0.05 (E)
Mg	0	0-0.11	0	0-0.04	0	0-0.79 (I) 0-0.06 (E)
Mn	0	0	0	0-0.09	0-0.03	0-0.07
Na	0	0-0.07	0	0-0.07	0-0.03	0-0.35
Ni	0	0	0-0.04	0-0.04	0	0-0.08
P	0	0-0.11	0	0	0	0-0.09
Pb	0	0-0.03	0	0-0.02	0-0.04	0
S	0.46-0.57	0.09-0.40 (I) 0.45-0.48 (E)	0.37-0.49	0.16-0.29 (I) 0.34-0.43 (E)	0.43-0.63	0.13-0.29 (I) 0.23-0.42 (E)
Si	0-0.29	0-0.25	0.04-0.07	0.15-10.9	0-0.30	0-1.80 (I) 0-9.4 (E)
Sr	0	0	0	0	0	0
Ti	0-0.03	0	0.02-0.05	0-0.02	0.02-0.25	0-0.02
V	0-0.02	0-0.03	0	0	0-0.04	0-0.03
Zn	n.d.	n.d.	0	0-0.02	0	0-0.07

V: Vitrinite E: Exinite I: Inertinite
n.d. = not determined

"0" = < 0.01 wt. %.

Table 1. continued

	85 - 92.5 cm		92.5 - 118 cm	
	V	E and I	V	E and I
Al	0.09-0.30	0.14-3.3	0-0.47	0-8.9 (I) 0-0.03 (E)
Ba	0	0	0-0.07	0-0.16
Bi	0	0	0-0.08	0-0.07
Ca	0-0.07	0-0.09	0-0.10	0-0.89
Cl	0.02-0.24	0	0.21-0.27	0.02-0.12
Co	0	0	0	0-0.03
Cr	0-0.02	0-0.04	0-0.02	0-0.04
Cu	0	0-0.02	0	0
F	0-0.04	0-0.02	0-0.05	0-0.78
Fe	0.04-0.13	0.05-0.34	0-0.07	0-1.78 (I) 0-0.14 (E)
K	0-0.06	0-0.04	0	0-0.03
Mg	0	0-0.06	0-0.02	0-0.17
Mn	0-0.03	0-0.04	0-0.04	0-0.08
Na	0	0-0.71 (I) 0-0.03 (E)	0-0.02	0-0.34 (I) 0-0.05 (E)
Ni	0-0.05	0	0-0.02	0
P	0	0	0	0-0.30
Pb	0	0	0-0.02	0-0.06
S	0.63-0.66	0.28-0.38 (I) 0.41 (E)	0.59-0.69	0.18-0.42 (I) 0.44-0.56 (E)
Si	0-0.26	0.20-0.48	0.04-0.77	0.03-10.7 (I) 0-0.09 (E)
Sr	0	0	0	0
Ti	0.22-0.39	0-0.02	0.02-0.17	0 (I) 0-0.42 (E)
V	0-0.05	0	0-0.03	0
Zn	0	0-0.03	0-0.03	0-0.05

V: Vitrinite E: Exinite I: Inertinite "0" = < 0.01 wt. %.
n.d. = not determined

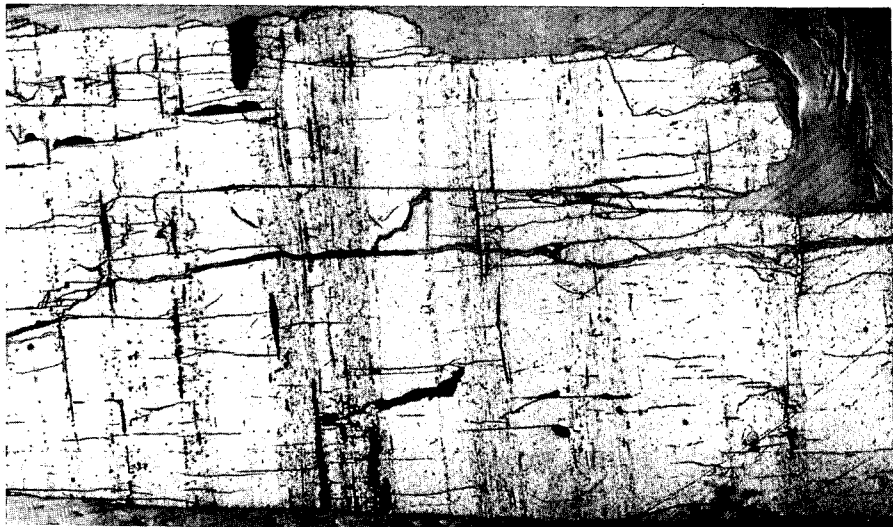
Table 2. Electron Microprobe Analyses of Clay Minerals in Upper Freeport Coal Column Sample HZ-42P-1

Depth (cm.)	ILLITES		KAOLINITES		"MIXED LAYER" CLAYS	
	56	88	88	112	96	112
SiO ₂	48.9	45.2	44.6	44.6	47.2	47.6
Al ₂ O ₃	32.4	35.4	36.0	38.1	36.9	36.2
FeO*	1.42	2.69	3.2	0.63	1.22	1.73
MgO	1.70	0.43	0.85	0.15	0.60	0.87
CaO	0	0	0	0	0.05	0.05
K ₂ O	6.6	8.2	0.16	0.10	1.71	1.83
Na ₂ O	0.23	0.69	0.09	0.07	0.18	0.55
TiO ₂	0.49	0.18	0.03	0	0.07	0.03
MnO	0	0	0	0	n.d.	0
Total Oxide Wt. %	91.7	92.8	84.9	83.6	87.9	88.9

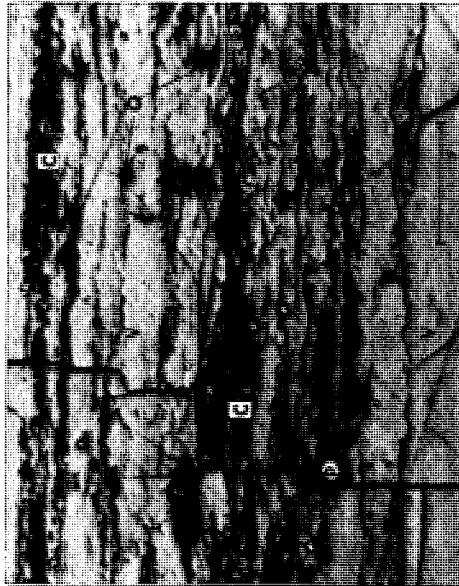
*O = < 0.01 wt. %.

n.d. = not determined.

*Total Fe as FeO.



(left) Figure 1. Vertical-illumination photograph of a polished block from depths 27-30.5 cm, Upper Freeport column sample H2-42P-1. Light gray bands are vitrinite; darker bands are assemblages containing 90-95 volume % vitrinite, 5% exinite and lesser amounts of inertinite and mineral matter. Very dark lenses at depth 28-28.5 cm are inertinites (fusinite and semifusinite). Bar scale 0.5 cm.



(Above) Figure 2. Photomicrograph of an area at depth 96.5 cm, same column, showing mineral matter dispersed in vitrinite. Vitrinite is labeled V, quartz Q, clay C, pyrite P, and inertinite I. Taken in reflected light using an oil-immersion contrast objective lens. Bar scale 0.1 mm.

RAPID, EASY MULTIELEMENT ANALYSIS OF WHOLE COAL VIA SLURRY-INJECTION ATOMIC ABSORPTION SPECTROPHOTOMETRY

James E. O'Reilly and Donald G. Hicks

Department of Chemistry, University of Kentucky, Lexington, Ky., 40506; and The Institute for Mining & Minerals Research, Kentucky Center for Energy Research Laboratory, P.O. Box 13015, Lexington, Ky., 40583.

INTRODUCTION

In recent years, a few laboratories have reported on the use of flame atomic absorption/emission methods for the analysis of solids directly, bypassing normal ashing and dissolution steps(1-5). However, not all these workers made attempts to achieve quantitative results. For example, although the early paper by Harrison(4) and the recent one by Willis(5) are quite significant, neither reported any quantitative analyses of standard or non-standard analyzed samples! Furthermore, no efforts have been made thus far to determine functional limits of detection and analysis for a wide variety of elements in any one particularly significant solid matrix such as coal. Atomic absorption(AA) procedures involving non-flame furnace atomization techniques seem to have been more widely investigated(6-13).

The need to analyze coal for major, minor, and trace-level elements has been underscored by the Clean Air Act of 1970(14) and the Toxic Substances Control Act of 1976(15,16). Concentrations of trace elements are of great interest in the geological characterization of coals(17), and Hook(18) has emphasized the significance of metals content of coal in determining the quality of industrial products such as coke, iron, and steel. Moreover, the U.S. National Bureau of Standards has recently introduced bituminous and sub-bituminous coal Standard Reference Materials (19,20) having certified concentration values for 14 trace metals. A survey has shown that 70 % of the millions of geochemical exploration samples collected annually have been analyzed by AA procedures(21). But conventional AA analysis procedures are plagued by lengthy sample preparation steps, usually involving a high or low-temperature ashing for many hours, followed by a prolonged dissolution in mixed acids. Even for a "rush" analysis, the turnaround time is nearly 2 days from receipt of samples.

Therefore, we have developed an atomic absorption method for the direct analysis of whole coal by injection of powdered coal slurries into either flames or graphite furnaces. This paper greatly expands the preliminary observations of O'Reilly(22) on the slurry-injection approach to flame AA analysis of coal. Our work is oriented toward a comprehensive exploration of the capabilities of this general approach for determining a wide variety of elements in some difficult-to-digest solid matrices such as coal, coal ash, oil shale, limestone, pigments, glasses, and selected ores. That is, solid matrices with "relatively" constant major component compositions.

EXPERIMENTAL

Apparatus and Reagents: All absorption and emission signals were measured using a non-modified Varian Model AA-6 atomic absorption spectrophotometer equipped with a Model BC-6 H₂-lamp background corrector, Model CRA-90 graphite tube/cup atomizer system, and a high quality strip chart recorder capable of expanding the 100 mv output absorbance signal by 100x in several steps. A standard Varian premix

burner with single-slot "high solids" heads was used throughout for flame atomization studies. As supplied, nebulizer intake capillaries had quite variable I.D. values. To minimize clogging, only those with I.D. greater than 35 μ m were utilized. To decrease the frequency of removing solid particles constantly collecting therein, a large conical suction flask was filled with water and used as a burner "drain trap" at floor level. A length of 8 mm glass tubing was inserted through a one-hole rubber stopper to a point about 5 inches below the water surface, and also connected to the burner chamber. A plastic tube ran from the flask side arm to a drain in the floor. The critical, final comminution of analytical samples was accomplished by use of a swing-mill (Spex Model 8510 Shatterbox) with 3.7 x 2.5 inch hardened steel or tungsten carbide(WC) grinding containers.

Certified atomic absorption standard solutions (Fisher Scientific) were used to prepare aqueous standards. A 10 % by weight stock solution of Triton X-100(Rohm & Haas scintillation grade) wetting agent was prepared and diluted daily as needed to 0.2 % or 0.5 % with distilled and doubly deionized water. Other materials were reagent grade.

Reference standard coals of nominal sub-60 mesh(-250 μ m) particle size were prepared from several eastern Kentucky bituminous coal samples. Ten to twenty pounds of each of these raw coals was put through (a) a standard jaw crusher, (b) a roller-mill, and (c) a Holmes Model 500 rotor-beater type of pulverizer equipped with a screen allowing output particles of 60-mesh or smaller. After tumbling each total sample 2 hrs, they were dried briefly at 110°C to remove surface moisture. The reference standard coals were then analyzed for content of several elements by conventional AA procedures involving 24-hr low-temperature oxygen-plasma ashing(23,24) and dissolution of the ash after treatment with aqua regia/HF in a teflon bomb(25,26) or fusion with lithium tetraborate (27,28). Analysis of NBS-SRM coal as an unknown and studies on the linearity of AA signals versus concentration made use of these samples.

Analysis Procedure: The grinding chamber of the Spex swing-mill was "dry-cleaned" initially, and also between samples, by a 2-min milling of about 6 mL of the new coal sample to be analyzed. After discarding the resulting powder, the chamber was quickly wiped with laboratory tissue and blown out with a jet of dry air. Roughly 10 mL of the new coal sample was then added to the container and pulverized for 10 minutes. The majority of the powdered sample was dumped into a 325-mesh(44 μ m) metal screen sieve with a 3-inch brass body, then shaken and bumped by hand for 1.5 minutes. Two-thirds or more of the solid typically passed the screen. The -44 μ m powder which collected in the bottom pan was covered with a snug-fitting lid, shaken vigorously for about 10 sec, and tumbled 10-12 times. Analytical samples in the range of 0.1 to 2.5 g were placed in 150-mL beakers. Using graduated cylinders or repipets, 30 to 100 mL of 0.5 % Triton X-100 slurring solution was gently added to produce slurries containing 0.1 to 8.0 grams coal per 100 mL slurring liquid(0.1 % to 8 % wt/vol solids). Actually, with the burner slot parallel to the light beam, most elements in most coal samples could be determined using slurries of 0.3 %, 5 %, or 8 % solids. Slurries of reference standard coals and unknowns were always prepared to contain approximately the same % solids. Samples were then stirred magnetically for about 30 minutes prior to aspiration into the burner. Absorbance measurements, made while stirring the slurries gently, were corrected for non-atomic "background" absorption using broad-band emission from an H₂-arc lamp. Absorbances of standard and unknown

coal slurries were normalized to the same % solids value which was chosen to be near the solids level of the slurries actually prepared. Element concentrations in the unknowns were determined from best-fit calibration curves constructed from standards, or from simple ratios of absorbances of standards and unknowns with subsequent averaging.

When analyzing coal by non-flame graphite furnace atomization techniques, suspensions containing 0.2 to 8.0 g of unsieved powdered coal per 100 mL total slurry volume were prepared by dilution in volumetric containers. After brief mixing, slurries were transferred to wide mouth containers and stirred a few minutes. Adding 5 to 25 μ L of the slurries to the graphite tube or cup provides a functionally accurate and rapid method to measure 10 to 2000 μ g of powdered coal sample.

RESULTS AND DISCUSSION

Sample Comminution Studies: Of several types of grinding devices examined, a swing-mill (Spex "Shatterbox") was found to be generally superior after considering such factors as (a) production of a very high percentage of really fine (-325 mesh) particles, (b) grinding 7 to 45 grams of sample, (c) short milling time, (d) number of samples milled simultaneously, and (e) general ease of operation and reproducibility. Table I illustrates that absorbances of samples ball-milled 60 min are significantly lower than those for samples pulverized 12 min in any swing-mill container. Usually, slurries made from unsieved coal ground in the swing-mill WC chamber did not clog burner capillaries. But clogging did occur often enough for us to recommend a brief partial sieving in the analytical procedure. The optimum time (Fig. 1) to grind 12 mL of coal having a 44-250 μ m starting range of particle sizes was found to be 12-15 minutes, although grinding times as short as 5 min will produce suitable samples when sieved. Since absorption has been shown to increase with decreasing particle size(5), 12 min in a swing-mill WC dish apparently results in a maximum state of subdivision of particles. Prior to this maximum absorbance grinding time, the -325 mesh powder exhibits a signal slightly greater than that of the unsieved samples. But after 12 minutes, the two types of samples show no difference in signal. To minimize clogging, 30-min of intermittent stirring is recommended after first mixing the slurry, particularly for water-based slurries of higher solids content. However, analytically useful slurries are obtainable after only 5-10 min stirring of either water-based suspensions with lower % solids or organic solvent mixtures of any solids level. Slurries having 8 % solids in a water base or 20 % solids in organic solvents have been aspirated a few minutes without clogging a 0.4 mm I.D. burner capillary. Regardless of the % solids, the rate of slurry aspiration is essentially the same as the uptake rate of the particular slurrying liquid (within 1 % to 2 %). Although clogging factors are discussed here, it is emphasized that it rarely happened when following routine analysis procedures.

Analysis By Flame Atomization: Best-fit calibration curves, obtained at some particular % solids level, are generally linear over a reasonable concentration range---as illustrated by Figures 2 and 3. Individual points resulting from different standard coals show a small, but highly reproducible, scatter about the line. We interpret this to be caused by relatively small matrix variation effects. For elements tested, slurry calibration curves have the same general shape. That is, they exhibit the same relative positioning of data points whether obtained (a) in $N_2O-C_2H_2$ or air- C_2H_2 flames, (b) from unsieved or partially sieved powders, (c) after 15 min milling in a swing-mill or 2 hr in a

rolling-jar ball-mill, or (d) after 20 min or 3 hrs stirring. Strong emission signals for several elements were obtained from coal slurries. In the case of sodium, the AA calibration curve had the same shape as one obtained from atomic emission measurements. Precisions attainable by this slurry-injection AA approach are quite good as seen in Table II, and are similar to those observed for replicate determinations on purely aqueous standards. Relative standard deviations (RSD) are typically 1 % of the mean for elements with strong signals, and 3-4 % when scale expansion is required.

For some elements whose coal slurry AA signals are quite small, considerable scale expansion is necessary and non-atomic "background" absorbance becomes significant (Fig. 3). Experimental observations shown in Table III suggest that this apparent absorption is primarily caused by light scattering from the solid particles. This "background" signal increases linearly with increasing solids level, is relatively constant from one coal to another, is greater when measured near the top of the burner, is much greater when the slurry is aspirated by non-burning gases (Table III), decreases gradually as wavelength changes from 200 nm to 600 nm (Table III), has the same magnitude whether measured with line or broadband light sources (Table III), increases with increasing slurry aspiration rate, is greater for coal sieved through a screen with larger openings (i.e. larger particles), is much less in the $N_2O-C_2H_2$ flame than in the air- C_2H_2 flame, and has a maximum observed absorbance of 0.002/1 % solids---this latter data in accord with Willis' (5) value for pulverized rocks.

Figure 4 indicates that conventional atomic absorption sensitivities (ppm at which $Abs. = 0.0044$) for elements in the NBS-1632 coal matrix increase in the same general order as AA sensitivities determined in aqueous solution. Atomization efficiencies relative to water media were determined as $\% \text{ atomization} = (100)(\text{slurry absorbance})/(\text{aqueous solution absorbance})$ at equal effective concentrations of the test element. These efficiencies for coal ranged between 16 % and 24 % of those obtainable from aqueous solution. Apparently, the NBS-1632 coal matrix (and perhaps others) does not drastically affect the signal of one element relative to another.

Flame response profile studies have shown that elements generally exhibit a maximum absorbance at a point higher in a flame when slurries are fed in than when aqueous solutions are aspirated (Fig. 5). As can be seen in Figure 6, the relative atomization efficiency in a flame also increases with increasing height above the burner. The % atomization of slurries increases more rapidly with increasing height in the $N_2O-C_2H_2$ vs air- C_2H_2 flame, and, the height of maximum absorbance is nearer the top of the burner in the $N_2O-C_2H_2$ vs air- C_2H_2 flame; both observations being in contrast with the greater aspiration rate of the $N_2O-C_2H_2$ burner. Along with the fact of lower non-atomic background absorbance therein, these data indicate that the $N_2O-C_2H_2$ flame is more efficient than the air- C_2H_2 flame in decomposing solid particles.

Of 33 elements studied, 23 were found to have sufficient sensitivity to be determined by flame atomization at levels normally encountered in coal (Al, Si, Fe, K, Ca, Mg, Na, Ti---Ba, Be, Cu, Cr, Co, Eu, Li, Mn, Ni, Pb, Rb, Sr, V, Yb, and Zn). Eu and Yb were detected by their emission signals from $N_2O-C_2H_2$ flames. Ag, As, Bi, Cd, Mo, P, Pd, Se, Sn, and Te were not detected with sufficient sensitivity. Utilizing

flame atomization, concentrations of 16 elements have been determined in NBS-1632 SRM coal with moderate accuracies of ± 5 to 25% error (Table IV). Although NBS-1632 is a relatively uniform blend of several coals, it is to be noted that the eastern Kentucky coals used as standards were not uniform. When considering sample-to-sample variations, it has been observed that slurry absorbances of Si and Al increase as ash content of the coal increases. But, correlations are not linear. Some other elements tested (Fe, Ti, Mg, Ca, K, Na, Ba, Sr) do not consistently show a similar correlation. Analysis of high speed photographs of flames has shown that the rise velocity of the larger of the $-44 \mu\text{m}$ coal particles near the top of the burner is essentially the same as the streaming velocity of the gases through the burner slot.

SUMMARY AND CONCLUSIONS

Most of our work has concerned flame atomization AA procedures, which are generally faster and more convenient than non-flame electrothermal atomization techniques. A recent brief report by Gladney(10) showed that Be in coal could be accurately determined by graphite furnace techniques, with observed precisions around 7.5 % RSD. Our work confirms determination of this particular element, and also shows that injection of μL amounts of slurries into a graphite cup/tube is a rapid and very reproducible way to circumvent microbalance weighings! In general, it appears that powdered coal slurries may be analyzed (in these devices) for elements which allow higher ashing and atomization cycle temperatures. Using a 2.5 mm I.D. graphite cup for atomization, 8 replicate determinations on 10- μL aliquots from a 1 % solids slurry ($-44 \mu\text{m}$ coal) resulted in a relative standard deviation of 3.2%.

Ease of sample preparation plus greatly increased speed of analysis using a commonly available instrument are the main advantages of this slurry injection AA method for coal analysis. As an example, the turnaround time for determining the concentrations of 4 elements in 6 samples can be reduced to 2 hrs from the current 2 days required by conventional AA procedures! Some operator time is also saved. The technique is useful for extremely fast single element scanning, which would allow more frequent and widespread sampling of coal shipped in large vessels. Although multielement scanning is a sequential process, it is rapid and does compete in total analysis time with X-ray fluorescence techniques, for instance. Assuming 10-12 min XRF instrument time per sample count period, and high and low energy counting on each sample, the XRF and slurry-injection AA methods both need about $\frac{1}{2}$ day to determine 12 elements in 6 samples. The price paid for this speed is the achievement of only modest accuracy. However, slurry-injection AA accuracies might be improved over those implied by the data in Table IV if standards and unknowns are matched somewhat better with respect to approximate ash content or general type of coal. Accuracies are certainly good enough for geochemical explorations, and are actually in the range of values reported(17) for conventional AA determinations.

ACKNOWLEDGEMENTS

We are grateful to Henry E. Francis, Karen Moore, and Sayra Russell for selected analyses, and to Dennis Sparks for initial preparation of some coal samples. Financial support for this project was provided by the Kentucky Center for Energy Research and the Institute for Mining and Minerals Research, and by Georgia State University (sabbatical leave for DGH).

REFERENCES

1. P. T. Gilbert, Anal. Chem., **34**, 1025 (1962).
2. J. L. Mason, Anal. Chem., **35**, 874 (1963).
3. V. I. Lebedev, Zh. Anal. Khim., **24**, 337 (1969).
4. W. W. Harrison and P. O. Juliano, Anal. Chem., **43**, 248 (1971).
5. J. B. Willis, Anal. Chem., **47**, 1752 (1975).
6. F. J. Langmyhr, J. R. Stubergh, Y. Thomassen, J. E. Hanssen, and J. Dolezal, Anal. Chim. Acta, **71**, 35 (1974).
7. F. J. Langmyhr, R. Solberg, and L. T. Wold, Anal. Chim. Acta, **69**, 267 (1974).
8. E. L. Henn, Anal. Chim. Acta, **73**, 273 (1974).
9. D. A. Lord, J. W. McLaren, and R. C. Wheeler, Anal. Chem., **49**, 257 (1977).
10. E. S. Gladney, At. Absorpt. Newsl., **16**, 42 (1977).
11. D. D. Siemer and H. Wei, Anal. Chem., **50**, 147 (1978).
12. B. V. L'vov, Talanta, **23**, 109 (1976).
13. F. J. Langmyhr, Talanta, **24**, 277 (1977).
14. U. S. Clean Air Act of 1970, Public Law 91-604, Dec 31, 1970.
15. U. S. Toxic Substances Control Act of 1976, Public Law 94-469, Sec. 4, 10, 27.
16. R. M. Druley and G. L. Ordway, Eds., "The Toxic Substances Control Act," Bureau of National Affairs, Washington, D.C., 1977.
17. H. J. Gluskoter, R. R. Ruch, W. G. Miller, R. A. Cahill, G. B. Dreher, and J. K. Kuhn, "Trace Elements in Coal: Occurrence and Distribution," Illinois State Geological Survey Circular 499, 154 pp., 1977.
18. W. Hook, Pure Appl. Chem., **49**, 1465 (1976).
19. NBS-1632a and NBS-1635 SRM Data sheets, National Bureau of Standards, U. S. Department of Commerce, Washington, D.C., 1978.
20. J. M. Ondov, W. H. Zoller, L. Olmez, N. K. Aras, G. E. Gordon, L. A. Rancitelli, K. H. Abel, R. H. Filby, K. R. Shah, and R. C. Ragaini, Anal. Chem., **47**, 1102 (1975).
21. J. S. Webb and M. Thompson, Pure Appl. Chem., **49**, 1507 (1976).
22. J. E. O'Reilly and M. A. Hale, Anal. Lett., **10**, 1095 (1977).
23. H. J. Gluskoter, Fuel, **44**, 285 (1965).
24. C. E. Gleit and W. D. Holland, Anal. Chem., **34**, 1454 (1962).
25. B. Bernas, Anal. Chem., **40**, 1683 (1968).
26. B. Bernas, Amer. Lab., **5** (8), 41 (1973).
27. R. B. Muter and L. L. Nice, in "Trace Elements in Fuel," S. P. Babu, Ed., American Chemical Society, Washington, D.C., 1975.
28. J. H. Medlin, N. H. Suhr, and J. B. Bodkin, At. Absorpt. Newsl., **8**, 25 (1969).

FIGURE CAPTIONS

- Figure 1. Effect of grinding time in a Spex Shatterbox (tungsten-carbide container) on the atomic absorbance of several elements in one coal sample that was originally 60/325 mesh (44-250 μm particle diameters). The solid circles are for unsieved final samples, the open circles for a final sample partially screened through a 325-mesh sieve. Conditions: nitrous oxide-acetylene flame; 1% wt/vol coal slurry; wavelengths = 285.2, 248.3, and 213.9 nm for Mg, Fe, and Zn.
- Figure 2. Calibration curve for analysis of zinc in whole coal. Conditions: air-acetylene flame, 0.4% wt/vol coal slurry in 0.2% Triton X-100, coal ground in a tungsten-carbide swing-mill.
- Figure 3. Calibration curve for analysis of manganese in whole coal illustrating correction for background absorbance. A: Absorbance of coal slurries without correction for background absorbance. B: Flame background absorption (particulate scattering) of aspirated coal slurries at 380 nm measured separately with a hydrogen-arc lamp mounted in place of a hollow-cathode lamp. C: The resultant background-corrected calibration curve. Conditions: air-acetylene flame, 3% wt/vol coal slurry in 0.2% Triton X-100, coal samples ball-milled, -325-mesh fraction.

Figure 4. Atomic absorption sensitivities ($A = 0.0044$) for a number of elements in NBS-1632 coal slurry versus the experimental sensitivity for those elements in purely aqueous standard solutions. The two lines represent effective atomization efficiencies of an element in a coal slurry of 16 and 24% that in aqueous solution. Conditions: nitrous oxide-acetylene flame except for Rb; coal slurries were of different solids levels in 0.2% Triton X-100; coal ground in a tungsten-carbide swing-mill.

Figure 5. Effect of measurement height in the flame on the atomic absorbance of iron in aqueous solution and in a coal matrix. Circles--in an air/acetylene flame; triangles--in a nitrous oxide-acetylene flame. Solid points--0.50% coal slurry in 0.5% Triton X-100; open points--aqueous 5 ppm iron solution. Conditions: The coal (1.07% Fe content) was ground 15 min in a steel swing-mill and sieved through a 200-mesh (75 μ m) screen.

Figure 6. Effect of measurement height in the flame on the relative atomization efficiency ($\epsilon_{rel} \times 100$) of iron in a coal matrix. Conditions same as in Figure 5.

Table I. Atomic Absorbance of Certain Elements vs. Grinding-Preparation Method^a

Grinding-Preparation Method	Grinding Time, min	Sieving ^b	Element ^c				
			Mg(NA)	Al(NA)	Si(NA)	Fe(NA)	Fe(AA)
Ball mill	60	yes	0.661	0.299	0.212	0.148	0.290
Swing-mill (steel)	12	yes	0.831	0.533	0.301	0.188	0.468
Swing-mill (WC)	12	yes	0.860	0.575	0.314	0.198	0.504
Swing-mill (WC)	12	no	0.862	0.577	0.317	0.195	0.504

^aThe same sample of coal was used in all grinding tests. ^bAfter grinding, the subsample was partially sieved through a 325-mesh screen (44 μ m diameter particles). Conditions: 2% wt/vol coal slurries in 0.2% Triton X-100. ^cAbsorbances are the average of at least three measurements; AA = air-acetylene, NA = nitrous oxide-acetylene flame. The normal atomic absorption wavelengths were used for the four elements studied. WC = tungsten carbide grinding chamber.

Table II. Precision of Atomic-Absorption Signal Intensities^a

Element	Series A RSD ^b	Series B RSD	Series C RSD
Fe	1.1	0.90	0.95
Zn	2.5	2.7	2.3
Mg	0.72	-	0.76
K	-	-	0.93

^aIn the A series of replicate analyses, nine 15-mL subsamples of a particular -60 mesh coal were milled 15 min in the swing-mill hardened-steel container and sieved 1.5 min by hand through a 200-mesh (75 μm) screen. Series B was 10 subsamples of the same coal pulverized 2 hr in a rolling-jar ball-mill, and then sieved 2 min by hand through a 400-mesh (38 μm) screen. Series C consisted of nine 12-mL subsamples of a different coal milled 10 min in the Shatterbox WC container, and then sieved 1.5 min by hand through a 325-mesh (44 μm) screen. Series A and C employed an air-C₂H₂ flame while series B used the N₂O-C₂H₂ flame.

^bRSD = relative standard deviation as percent of the average.

Table III. Background Absorbance of a Coal Slurry at Several Wavelengths^a

Wavelength, nm	Lamp ^b	Absorbance, $\times 10^3$		
		N ₂ O-C ₂ H ₂ Flame	Air-C ₂ H ₂ Flame	Air-C ₂ H ₂ No Flame ^c
207.5	HC	1.5	4.7	12.4
214	H ₂	---	4.8	---
231.7	HC	1.3	4.9	12.9
267.3	HC	1.1	3.3	11.9
280	H ₂	---	3.2	---
326.1	HC	---	2.9	---
358	H ₂	---	2.2	---
391.0	HC	0.6	2.6	9.5
450	H ₂	---	1.8	---
459.3	HC	---	2.0	---
610.4	HC	---	1.6	---

^a5% wt/vol slurry in 0.5% Triton X-100. Coal was ground 15 min in a steel swing-mill, and sieved through a 200-mesh sieve. Dash means measurement not made. ^bHC = isolated line from a hollow-cathode lamp; H₂ = Hydrogen arc lamp. ^cFlame not lit, but gases flowing on the air-C₂H₂ burner head; zero absorbance set with 0.5% Triton X-100 aspirating.

Table IV. Analysis of NBS-1632 Bituminous Coal SRM by Slurry-Injection Atomic Absorption Spectrophotometry^a

Element	NBS	Slurry-AA	Error, % of NBS
	Concentration, ^b µg/g	Concentration, µg/g	
Si	<u>32000</u>	26000	19
Al	17300*	15700	9
Fe	8700	9200	6
Ca	4340*	4950	14
K	2790*	2570	8
Ti	<u>800</u>	690	13
Na	396*	480	21
Sr	128*	99	22
Cu	18	20	11
Zn	37	34	8
Mn	40	38	5
Ni	15	14	7
Cr	20.2	23	14
Pb	30	24	20
V	35	43	23
Co	5.6*	4.4	21

^aVarious analyzed Kentucky coals were used as standards.

^bUnmarked values are NBS certified, underlined values are NBS provisional;

*values are averages of several reported in the 1977 Illinois State Geological Survey Circular 499 (17).

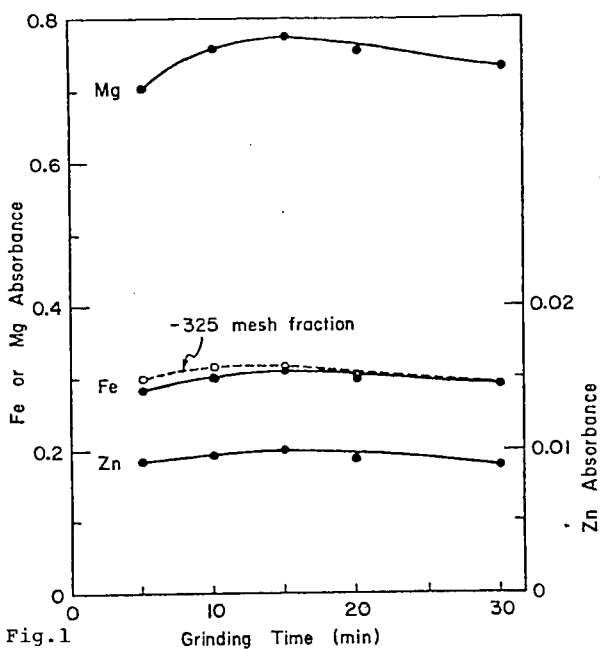


Fig. 1

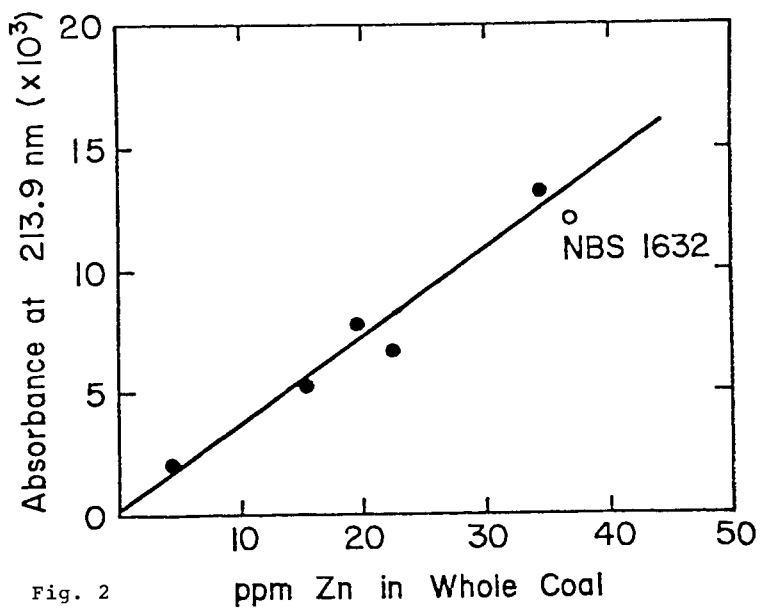
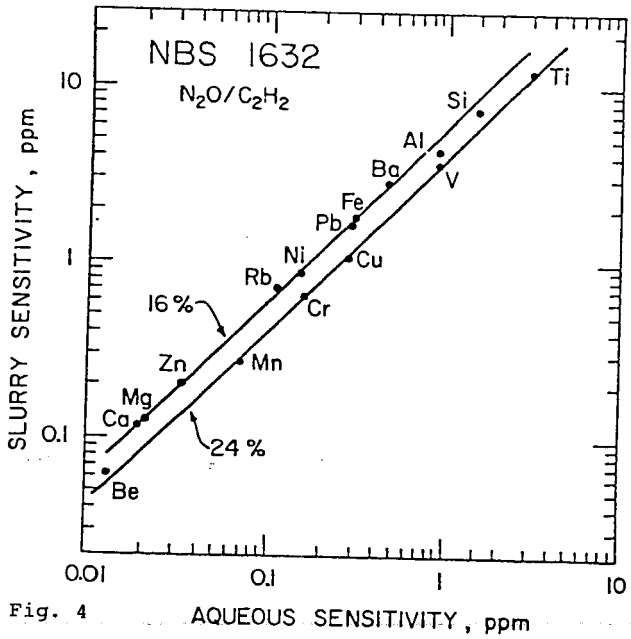
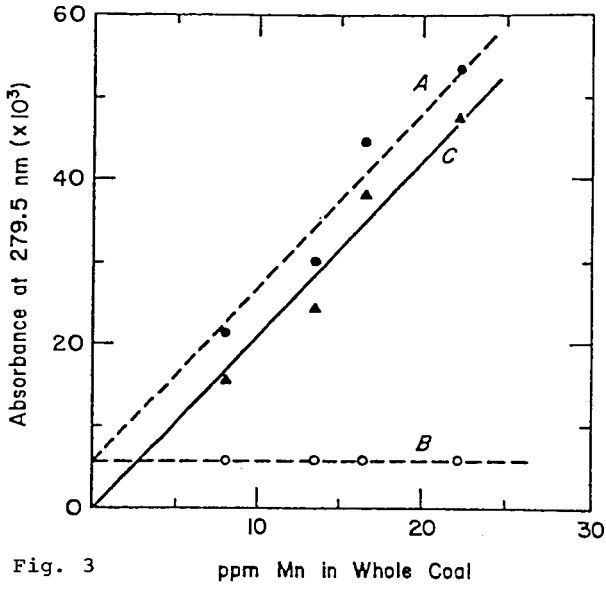


Fig. 2



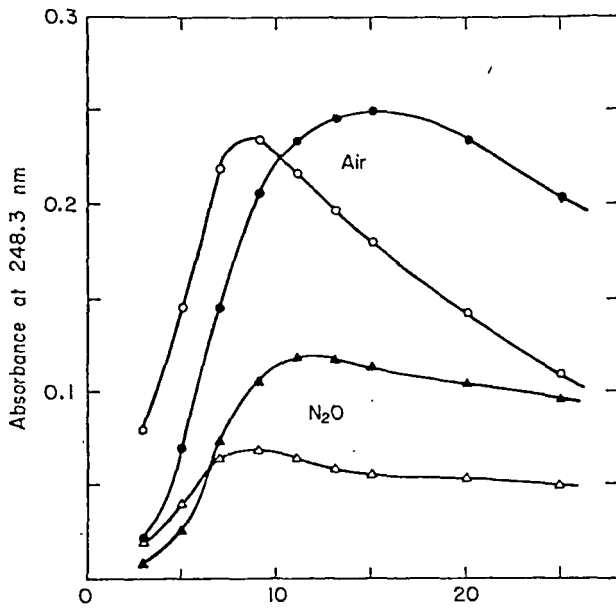


Fig. 5 Height of Measurement, mm above Burner Top

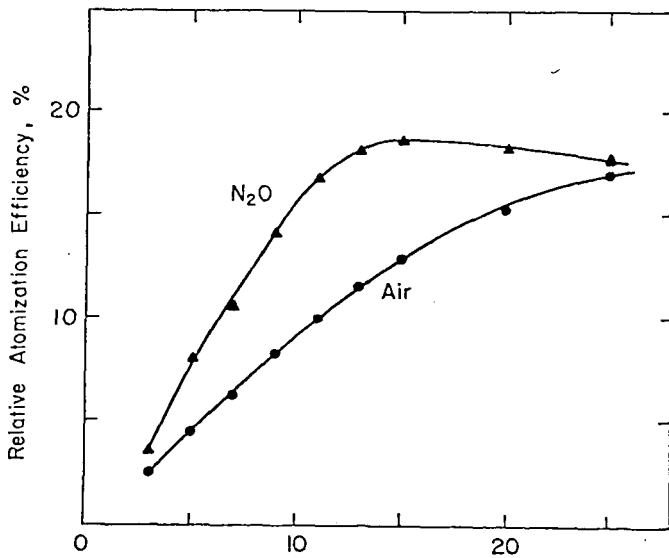


Fig. 6 Height of Measurement, mm above Burner Top

Precision on the Determination of Trace Elements in Coal

Mutsumi Ihida, Teruaki Ishii, Rieko Ohnishi

Nippon Kokan K.K., Chemical Analysis Laboratory, Technical Research Center
1-1, Minamiwatarida-cho, Kawasaki-ku, Kawasaki, 210 Japan

1 Introduction

The quantity of mineral matter contained in coal is generally 5 to 25 per cent of the total contents. Most of the mineral matter are contained in the form of silicate, while the rest of a few per cent are trace elements with more than 20 kinds including zinc, cadmium, lead, nickel, chromium, copper, and vanadium etc..

At the present moment, it would not be so important to find out the quantity of these trace elements in coal for the purpose of recovering raw materials except certain materials such as germanium and gold, however to know the quantity of trace elements in coal is becoming more important for the purpose of the environmental chemistry.

There are following problems in conducting the determination of trace elements;

- 1) Concentration of the elements are slight.
- 2) Coal is composed of organic matter.
- 3) Difficulty in obtaining a standard sample required for the determination.

To cope with these problems, the Sample Research Committee, JUSE, has conducted a Round-Robin study with cooperation of seven laboratories and tried to evaluate the precision of the determination of trace elements in coal and coke. Besides, it was considered that volatility loss at the stage of pretreatment of sample might have occurred for the elements with inferior reproducibility such as zinc.

The result of the study is described hereinafter.

2 Experimental

2-1 Design of Experiment

Three kind of test samples crushed under 250 μ m, shown in Table 1, were analyzed at seven laboratories by the analytical method described below. Each kind of sample was analyzed two times and the measurement by the atomic absorption method was performed twice respectively.

Analytical procedure was as follows;

Transfer 1g of the sample, weighed to the nearest 0.1mg, to a platinum dish. Add 5ml of HF and 10ml of HNO₃. Evaporate to white fumes to expel all HF. Transfer the sample to 200ml beaker, add 30ml of HNO₃, and 10ml of HClO₄. Cover the beaker, and heat until the solution becomes clear. Evaporate to dense white fumes. Cool, and approximately 50ml of water. Filter through a texture paper, and wash the residue with warm HCl (2+100). Transfer the residue to a platinum crucible, ignite, fuse with 2g of Na₂S₂O₇, and then add to the original solution. Transfer to a 100ml volumetric flask, and dilute exactly to the mark with water. Measure the absorption of an aliquat by an atomic absorption apparatus.

2-2 Result of Experiment

Original data obtained are shown in Table 2. About 600 data obtained are statistically analyzed, and the precision calculated by using ANOVA (nested design) are summarized in Fig. 1, Fig. 2, and Fig. 3 respectively. (See formulas (1), (2)

and (3)).

Repeatability (Error due to A.A. method only),

$$\sigma_E = \sqrt{v_E}, \quad \text{C.V.} \cdot \sigma_E = \sigma_E / \bar{x} \times 100 \quad \dots\dots\dots (1)$$

Repeatability (Error due to pretreatment),

$$\sigma_P = \sqrt{(v_L - v_P) / 4}, \quad \text{C.V.} \cdot \sigma_P = \sigma_P / \bar{x} \times 100 \quad \dots\dots\dots (2)$$

Reproducibility (Error among different laboratories),

$$\sigma_{\bar{x}} = \sqrt{\sigma_L^2 + \sigma_E^2 / 2 + \sigma_P^2 / 2}, \quad \text{C.V.} \cdot \sigma_{\bar{x}} = \sigma_{\bar{x}} / \bar{x} \times 100 \quad \dots (3)$$

2-3 Discussion

2-3-1 Repeatability within same laboratory

As is evident from Fig. 3, C.V. of repeatabilities (C.V. σ_E) are less than 10% except cadmium and lead. These inferior repeatability of the above two elements may be due to the contents of them closing to the detection limit of the A.A. method as shown in Table 3.(1) In such a case, pre-extraction procedure may be effective to improve the precision.(2)

2-3-2 Error due to pretreatment

As is evident from Fig. 1, C.V. of pretreatment (C.V. σ_P) for zinc is inferior than that of other elements. It suggests that volatility loss of zinc may be occurred during decomposition.

The supplemental experiment using seven samples, therefore, has been carried out to study the effect of pretreatment for the determination of zinc. The following three pretreatments have been compared on the zinc. In addition, nickel has also been determined from the same solution as a reference, because it has higher boiling point than that of zinc.

- 1) Low temperature ashing method.
- 2) High temperature ashing method.
- 3) Wet oxidation method employed on the above Round-Robin Study.

As is evident from Fig. 4 showing the effect of pretreatments, significant loss during incineration was observed technically compared to the wet oxidation method in case of zinc. On the other hand, no significant bias was observed among the three methods in case of nickel. Anyway, the volatility loss of zinc during pretreatment should be studied more precisely because it may results the inferior precision.

2-3-3 Reproducibility between different laboratories

As is evident from Fig. 2, the C.V. of reproducibilities (C.V. $\sigma_{\bar{x}}$) calculated using all of the data including outliers, were almost more than 20%. Even if the outliers are excluded, most of the elements still show inferior reproducibility.

3 Conclusion

- 1) The precisions (repeatability and reproducibility) on the determination of trace elements in coal and coke (zinc, nickel, chromium, copper, lead, cadmium, and vanadium) are insufficient on the viewpoint of coefficient of variance ($\sigma_x / \bar{x} \times 100$) on the most elements are more than 20% when outliers are not rejected.
- 2) C.V. of cadmium and lead are inferior because of substantial difficulties on the

A.A.method. That is, the contents of cadmium are close to the detection limit, and the lack of sensitivity for the determination of lead may cause these inferior precision respectively.

- 3) In case of the determination of zinc, the more precise studies on the pre-treatment should be carried out in the future.

Afterwords

These studies were carried out in Japan prior to the first international Round-Robin Study of ISO/TC 27/WG 14 (Trace elements). A part of the statistical analysis on the above experiment was reported in a document ISO/TC 27/WG 14, No. 6 (Japan-6).

Literature cited

- (1) "Atomic Absorption Spectrophotometry in the Steel Industry", The Iron and Steel Institute of Japan, (1975) P. 52 - P. 53.
- (2) "Round-Robin Studies for the Estimation of Accuracy and Precision of Pollution and Environment Control Analysis", The fourth SAC Conference (1977).

Table 1 Proximate Analysis of the Samples

% of the Air-Dried Coal and Coke

Samples	Moisture	Ash	*V.M.	**F.C.
U.S. Massey H.V. Coal	1.4	13.2	32.4	52.6
Japanese Miike Coal	9.9	6.5	38.3	54.2
Metallurgical Coke	0.1	11.6	0.5	87.8

* Volatile Matter ** Fixed Carbon

Table 2 Trace Elements in Coal and Coke

PPM in Air-Dried Whole Coal and Coke

(1) Sample ; U.S. Massey H.V. Coal

Lab.	Zn		Cd		Pb		Ni		Cr		Cu		V		
	P ₁	P ₂													
A	m ₁	29.0	17.2	0.26	0.26	5.15	3.83	11.2	11.9	15.2	17.2	16.9	16.5	34.3	30.4
	m ₂	27.7	17.2	0.13	0.26	6.47	5.15	10.6	10.6	17.2	17.2	15.3	15.3	29.0	27.1
B	m ₁	27.1	26.0	0.34	0.45	8.58	8.32	12.5	12.5	20.5	19.4	17.2	19.3	32.1	30.8
	m ₂	27.3	26.4	0.34	0.43	8.05	8.05	12.5	12.5	20.7	19.4	17.2	18.3	32.1	30.8
C	m ₁	11.6	23.0	<u>0.95</u>	<u>2.09</u>	4.22	0.26	18.6	12.7	14.7	22.7	16.6	26.6	30.6	33.4
	m ₂	12.0	20.7	<u>0.66</u>	<u>1.25</u>	5.15	8.18	9.6	12.4	19.5	23.4	17.2	14.5	23.2	26.0
D	m ₁	16.9	22.0	0.95	0.40	7.52	7.26	12.3	12.3	19.7	19.7	20.5	20.5	32.7	31.9
	m ₂	17.0	20.7	0.75	0.63	11.9	9.50	15.0	13.2	16.5	16.9	19.8	20.7	30.6	30.5
E	m ₁	23.9	18.6	0.48	0	10.6	11.9	<u>20.6</u>	<u>20.9</u>	<u>7.5</u>	<u>8.6</u>	21.6	23.5	25.2	28.1
	m ₂	21.6	18.6	0.48	0	10.6	11.9	<u>20.6</u>	<u>20.9</u>	<u>7.7</u>	<u>8.3</u>	20.9	21.9	25.2	29.1
F	m ₁	19.7	12.2	0.21	0.21	5.15	4.49	10.4	10.0	21.3	19.1	17.4	18.2	29.6	26.4
	m ₂	18.7	22.0	0.17	0.17	5.02	4.49	10.3	9.8	21.3	19.3	17.4	18.2	28.5	26.4
G	m ₁	21.8	18.1	0.32	0.18	3.34	5.41	11.9	11.5	17.7	18.9	19.0	16.8	31.2	31.9
	m ₂	21.6	18.2	0.26	0.22	2.38	5.68	12.1	11.7	17.4	18.5	18.5	16.4	31.2	31.7

p ; pretreatment , m ; measurement

— Outliers

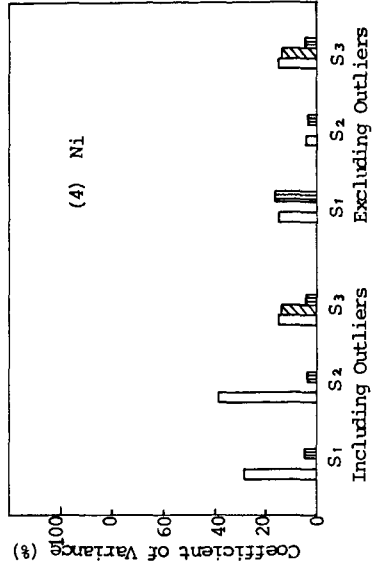
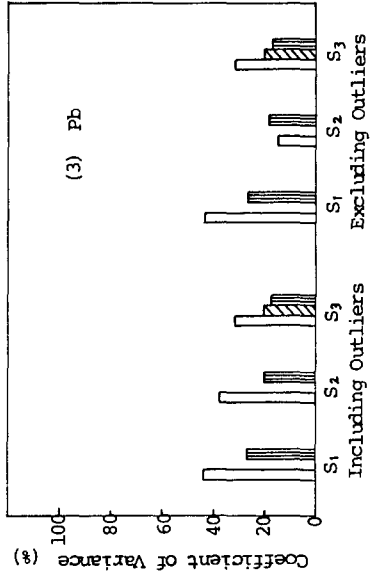
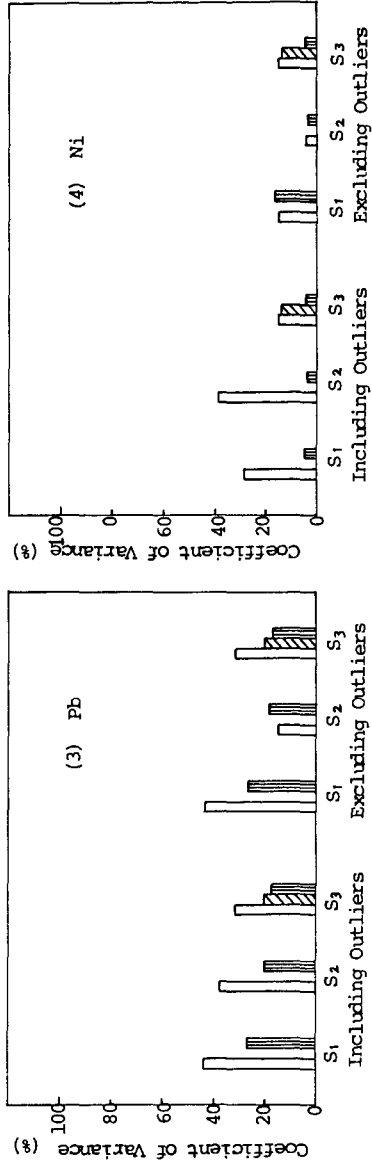
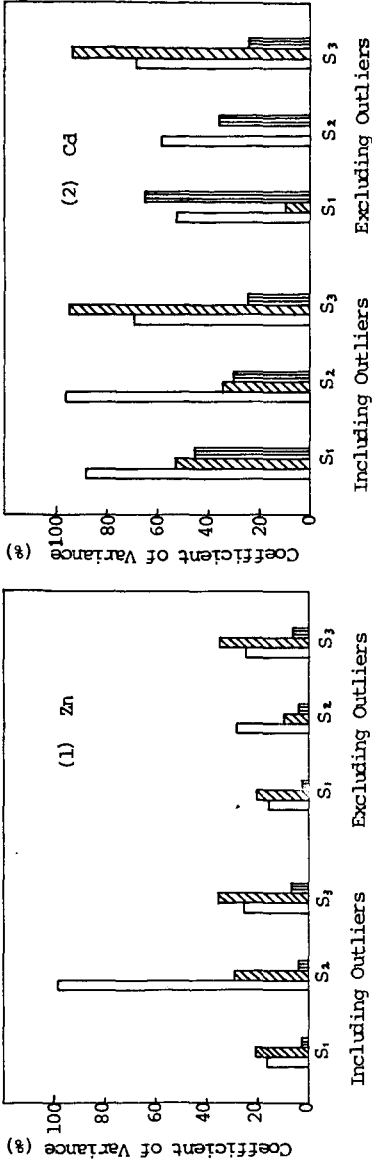
Table 2 Concluded

(2) Sample ; Japanese Miike Coal

Lab.	Zn		Cd		Pb		Ni		Cr		Cu		V		
	P ₁	P ₂													
A	m ₁	3.58	3.90	0.13	0.13	3.19	1.89	18.9	18.5	8.45	8.45	5.72	5.59	<u>4.55</u>	<u>4.55</u>
	m ₂	2.93	3.58	0.07	0	3.19	3.19	18.5	18.5	8.45	8.45	5.07	5.07	<u>4.55</u>	<u>4.55</u>
B	m ₁	<u>27.0</u>	<u>26.7</u>	0.20	0.21	2.99	3.51	20.3	20.6	10.4	9.62	6.24	6.50	7.15	7.15
	m ₂	<u>27.1</u>	<u>26.8</u>	0.20	0.21	3.06	3.45	20.2	20.5	10.4	9.55	6.24	6.31	7.22	7.02
C	m ₁	<u>35.4</u>	<u>21.5</u>	<u>0.56</u>	<u>0.81</u>	3.25	3.45	49.4	7.5	8.13	11.0	5.59	5.46	4.62	6.96
	m ₂	<u>23.8</u>	<u>23.1</u>	<u>0.39</u>	<u>0.73</u>	2.21	1.56	22.8	13.0	9.75	11.4	5.72	6.24	4.75	10.9
D	m ₁	4.29	4.36	0.18	0.20	<u>4.42</u>	<u>4.03</u>	19.9	19.8	9.43	10.9	6.50	6.63	5.92	6.57
	m ₂	4.42	4.36	0.31	0.34	<u>5.33</u>	<u>5.33</u>	22.1	21.4	8.84	9.10	6.37	6.37	4.75	5.92
E	m ₁	5.20	4.10	0.12	0.12	3.90	3.25	25.3	23.7	<u>2.86</u>	<u>2.86</u>	6.70	6.70	4.68	8.00
	m ₂	4.75	4.23	0.12	0.12	3.90	3.25	25.3	25.3	<u>2.86</u>	<u>2.86</u>	6.70	6.63	8.00	4.86
F	m ₁	4.55	4.42	0.07	0.07	3.25	2.80	19.3	19.0	9.62	10.7	5.59	5.72	<u>4.23</u>	<u>4.23</u>
	m ₂	4.55	4.36	0.07	0.07	3.38	2.80	19.2	19.2	9.69	10.5	5.66	5.86	<u>4.42</u>	<u>4.23</u>
G	m ₁	9.00	6.50	0.10	0.10	<u>0.78</u>	<u>1.56</u>	13.7	14.0	9.62	9.69	5.66	6.11	5.98	6.50
	m ₂	7.67	6.50	0.11	0.11	<u>1.56</u>	<u>1.76</u>	14.0	13.3	8.71	8.58	8.85	6.11	5.98	6.50

(3) Sample ; Metallurgical Coke

Lab.	Zn		Cd		Pb		Ni		Cr		Cu		V		
	P ₁	P ₂													
A	m ₁	24.4	14.5	0.23	1.16	4.52	5.68	41.8	43.5	22.6	19.1	24.4	24.4	47.6	46.4
	m ₂	24.4	13.3	0	1.16	6.73	7.89	40.6	42.3	22.6	20.9	21.8	22.9	55.1	51.0
B	m ₁	16.2	16.0	0.25	0.34	5.92	6.38	44.7	44.7	24.9	24.0	24.9	25.8	55.3	54.9
	m ₂	16.2	16.2	0.24	0.34	6.03	6.38	44.4	45.2	25.1	24.0	24.9	25.8	55.1	54.3
C	m ₁	10.2	12.1	0.37	1.30	4.41	2.20	78.3	7.0	19.7	34.8	24.2	21.5	30.2	45.8
	m ₂	10.3	17.6	0.41	1.31	6.73	4.87	41.8	23.2	20.3	24.4	24.8	24.0	36.0	48.7
D	m ₁	15.2	13.5	0.43	0.38	9.05	9.63	44.3	44.3	22.9	21.9	26.8	26.9	56.0	53.2
	m ₂	14.6	13.9	0.58	0.57	10.4	8.70	50.6	50.2	18.7	21.7	25.8	25.8	55.3	55.0
E	m ₁	16.7	15.3	0.42	0	9.28	5.92	48.4	50.7	7.5	7.5	28.8	28.8	41.8	42.8
	m ₂	16.1	15.3	0.42	0.21	6.96	5.92	51.2	54.8	7.5	7.5	28.8	29.0	33.4	34.1
F	m ₁	14.0	13.9	0.14	0.14	4.99	4.64	47.8	71.3	27.8	25.3	25.9	25.3	50.8	51.3
	m ₂	14.0	13.9	0.21	0.21	4.99	4.87	48.0	71.6	27.5	24.9	25.9	25.5	49.9	52.0
G	m ₁	15.3	15.5	0.17	0.21	6.26	2.09	39.9	40.4	23.3	23.9	24.8	24.1	61.2	49.2
	m ₂	15.5	15.1	0.15	0.19	5.92	1.74	39.4	39.4	23.0	23.9	26.4	26.0	55.2	58.0



□ Repeatability C.V. σ_x , ▨ Repeatability C.V. σ_p , ▩ Repeatability C.V. σ_w
 Sample: S₁; U.S. Massey H.V. Coal, S₂; Japanese Miike Coal, S₃; Metallurgical Coke

Fig. 1 Precision on the Determination of Trace Elements

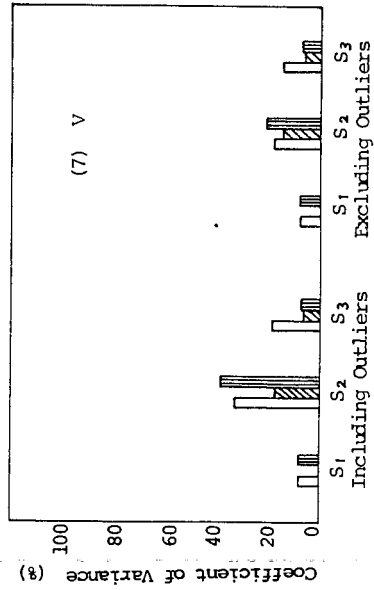
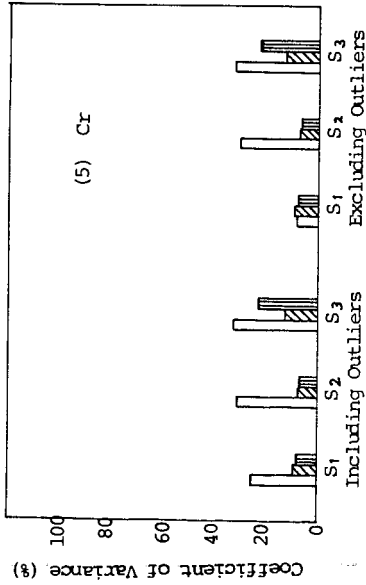
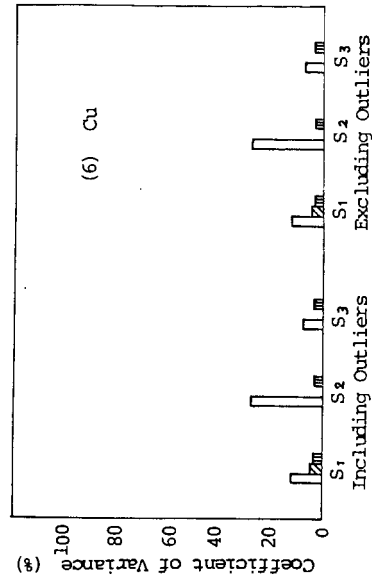


Fig. 1 Concluded

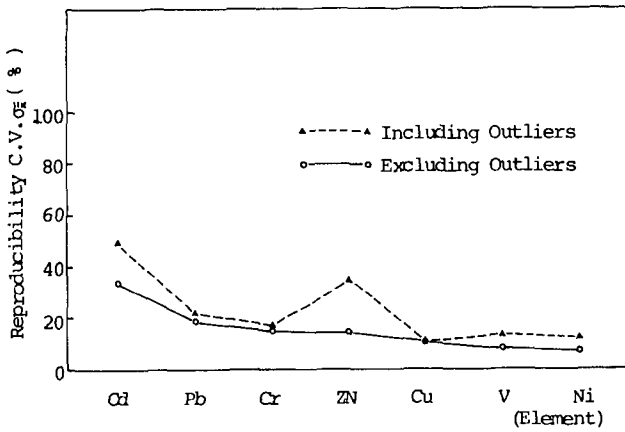


Fig. 2 Error among Different Laboratories

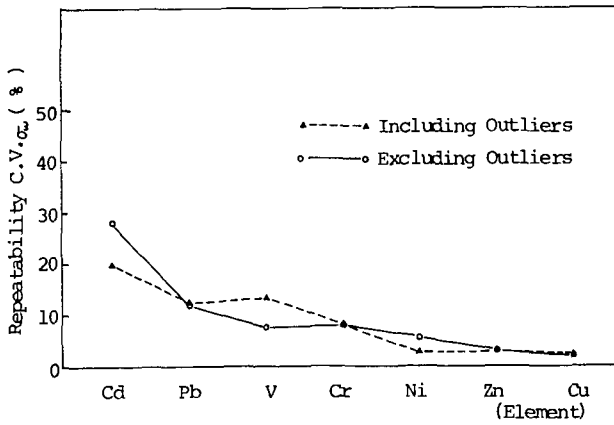
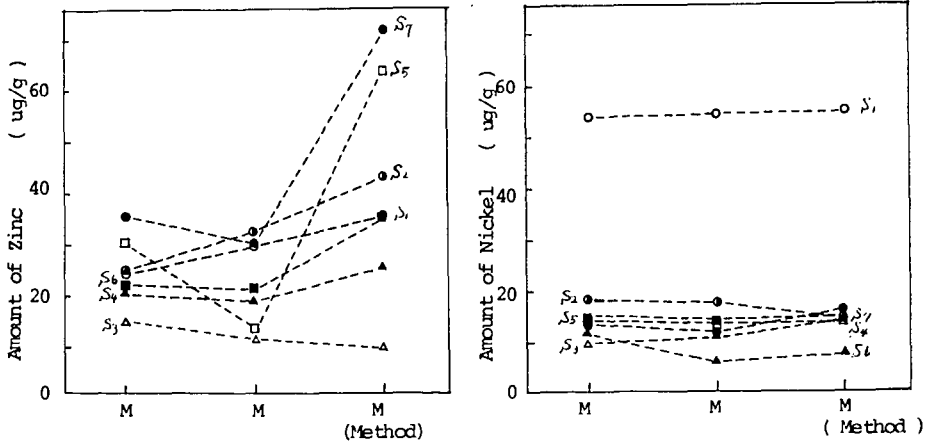


Fig. 3 Error due to Atomic Absorption Analysis

Table 3 Detection Limit and Sensitivity of the Atomic Absorption Method

Element	Line Å	Detection Limit µg/ml	Sensitivity 1% Absorption µg/ml	Analytical Rang of Sample µg/ml
Zn	2138	0.02	0.04	0.1~0.2
Cd	2288	0.002	0.02	0.02~0.04
Pb	2833	0.03	0.5	0.03~0.07
Ni	2320	0.005	0.1	0.06~0.2
Cr	3579	0.003	0.08	0.03~0.2
Cu	3247	0.005	0.1	0.06~0.2
V	3514	0.04	1.3	0.06~0.3



M₁: Low temperature ashing method, M₂: High temperature ashing method
M₃: Wet oxidation method
S₁: Metallurgical coke, S₂: Hongei coal, S₃: Beatrice coal, S₄: Vicary coal
S₅: Pittoston coal, S₆: Black water coal, S₇: Yutoku coal

Fig. 4 Comparison of Analytical Values of Zinc and Nickel in Coal and Coke by Three Decomposition Method

Trace Element Variations in an
Oil-Shale Retorting Operation

Thomas R. Wildeman
Department of Chemistry/Geochemistry
Colorado School of Mines
Golden, Colorado 80401

and

Robert N. Heistand
Development Engineering Inc.
Box A, Anvil Points
Rifle, Colorado 81650

Experiments were conducted jointly between Colorado School of Mines (CSM) and Development Engineering, Inc. (DEI) using raw shale feed to the Paraho Semi-Works retort. (1,2) A schematic diagram of the 10-1/2 foot O.D. Semi-Works retort is shown in Figure 1. The Direct Mode operation, where combustion occurs within the retort to provide necessary heat, is portrayed in this schematic diagram. Operations are continuous and flows are countercurrent. Gases flow upward. The downward flow of shale is controlled by a hydraulically-operated grate mechanism. Shale is distributed evenly across the top of the bed by a rotating distributor. Here, the shale is preheated by rising hot gases in the mist formation zone. Next, the preheated shale passes through the retorting zone where the organic kerogen is decomposed into oil, gas, and coke. The coke remaining on the retorted shale serves as fuel in the combustion zone. Air is distributed evenly across the bed in an air-gas mixture in this zone. In the lower section of the retort, the shale is cooled by bottom recycle gas and this gas, in turn, is preheated before entering the combustion zone. The oil, as a stable mist, is carried out the top of the retort through the off-gas collector and is separated from the gas in a coalescer-electrostatic precipitator system.

In the Indirect Mode operation, the gas blower is replaced by an external heater. The middle and upper recycle gas is passed through this heater to provide heat needed for retorting. In this mode, the product gas is not diluted with products of combustion and nitrogen from the air, and the carbon remaining on the retorted shale is not utilized.

Uniform flow of solids and gases within the retort is essential in order to maintain a continuous operation and a high efficiency. In the Paraho Semi-Works retort, the bottom grate, the air-gas distributors, and the rotating shale distributor are designed to assure uniform flows. In addition, the raw shale feed is carefully screened and handled to a uniform feed. Feedstock for the retort consists of + 1/2 inch to - 3 inch nominal size. Fines and non-uniform shale size can result in gas channeling, high pressure drops, and uneven bed temperatures. These problems cause low oil yields and could, eventually, result in a retort shutdown. In addition to providing good operations and high efficiencies within the retort, the resulting lump-size retorted shale reduces considerably the environmental impact caused by dusting.

Although lump-size feed improves retort operation, minimizes environmental impacts, and reduces crushing costs, this feed creates problems in securing a representative sample for laboratory analysis. A raw

shale sampling system was designed to meet the accepted criteria for sampling this lump-size, non-homogeneous material. (3) A diagram of the Paraho sampling system is shown in Figure 2. A motorized gate diverts flow from the retort at preset intervals (usually 30-50 minutes). Approximately 200 pounds of material is taken in a single cut. The sample is crushed to -3/4 inch and passed through a four-stage splitter. The retained sample is crushed to - 1/4 inch and passed through a second four-stage splitter. This system provides a 24-hour composite laboratory sample (20-30 lbs, - 1/4 inch) from the 2 1/2-4 tons of the lump material sampled from the raw shale feed. An examination of the Paraho raw shale sampling system showed it to be unbiased. (4) Careful analyses of the grade (gallons oil/ton shale) indicated no significant differences between reject streams A and B and the laboratory sample. This laboratory sample was used in the studies presented in this paper.

Sampling Program

The objective of this research is to determine the concentrations of trace elements in the Paraho oil-shale feedstock and to study the fate of those trace elements during retorting. Elements of particular interest are B, F, As, Se, and Mo (5). In this regard, sampling the Paraho feedstock presents a problem. Lumps of rock -3 inches to +1/2 inch in size is not an ideal size of sample. One or two lumps is all that would be needed for most analyses, but that can hardly be considered representative. However, if the Paraho sampler were used to secure a sample, the amount would be about 6 kg. The sample is obviously physically heterogeneous. Does this also mean that it will be chemically heterogeneous? In addition, mining, hauling, crushing and retorting are a continuous operation at Anvil Points, little stockpiling is done. Does this mean that feedstock sampled on one day will differ significantly from that used in the retort on another day? Fundamental sampling questions such as this require a sampling program that is based on a strong foundation of statistical theory.

The statistical model followed in the sampling was a hierarchical or nested analysis of variance (6,7). In this case, one month of 30 days in which the retort was operating was subdivided or nested into 24 hour, 8 hour, and 1 hour periods. Of these 30 days, 6 were chosen as test days. Samples were taken on each of the three 8 hour periods. Then, on one randomly chosen 8 hour shift, eight 1 hour samples of oil shale feedstock were taken. This nested sampling design is shown in Figure 3. Now, for some constituent, such as iron, if all the samples were the same then

$$\text{concentration of Fe}_i = \mu_{\text{Fe}} \quad (1)$$

where μ_{Fe} is the mean of Fe concentrations and i designates the i^{th} sample. This is not the case. There can be a deviation or error due to the time in which the sample was taken and the imprecision of the analysis. So the equation 1 becomes

$$\% \text{Fe}_{ijkm} = \mu_{\text{Fe}} + \alpha_i + \beta_{ij} + \gamma_{ijk} + \delta_{ijkm} \quad (2)$$

Mean + 24 hr + 8 hr + 1 hr + analysis

where i designates the retort day and α_i is the deviation from the mean due to the sample being taken on that day. Similarly, β_{ij} represents the deviation due to the sample being taken in the j^{th} 8 hr shift of the i^{th} day, γ_{ijk} means the same for the 1 hr period; and δ_{ijkm} is the error for the analysis. By carefully setting up a nested sampling design and randomly selecting the sampling periods, an estimate of magnitude of the error or deviation for each time

period can be obtained. Certainly, if more periods were sampled, the estimates of error would be better, but the design choice is such that a minimum of samples yields meaningful estimates on all the error parameters.

One can not actually determine the errors and deviations; but if the sampling design is properly constructed, estimates of the errors can be estimated (6,7). Such an estimate is called a variance, the variance equation corresponding to equation 2 is

$$s_{Fe}^2 = s_{\alpha}^2 + s_{\beta}^2 + s_{\gamma}^2 + s_{\delta}^2 \quad (3)$$

These variances are similar to estimates of the standard deviation but in this case, the variance is partitioned among several components. The partitioning of the variance allows the following questions to be answered:

1. Is the mean of all the samples representative of the whole retort month or is there a trend over the month?
2. Is there significant scatter in any one of the 24 hr; 8 hr; or 1 hr time periods?
3. Are the analytical procedures precise enough or do they contribute to most of the scatter in the concentration values?

Analysis Program

DEI performed the Fischer assay analyses by a procedure that has been described previously (4). The precision of the analyses has been determined to be 2% relative standard deviation for the oil yield and 15% and 20% relative standard deviation for the water yield and gas plus loss yield. All 70 oil shale feedstock samples that were collected were analyzed for oil yield.

The elemental analyses were done by energy dispersive x-ray fluorescence (EXRF) analysis. The details of the analytical procedure have been previously published (8,9). In this procedure, four samples were chosen for analysis in each of the six hourly sample sections and three of the eight hour shift samples were analyzed for each day for a total of 37 samples. Also, duplicates of eight samples were analyzed to determine the variance of the analysis procedure. The relative standard deviation for the analysis for each element is listed in Table I. They range from above 10% for light elements to below 5% for heavier elements. These results are typical of the precision of the EXRF method. Comparison of analyses of NBS standard coal (SRM 1632) and round robin analyses done on oil shales show the accuracy of the analyses to be within $\pm 10\%$ (10,11). K and Se concentrations do not compare well with other analytical methods; the results are aberrant by about 30%.

Results and Conclusions

In Table I, the results for the Fischer assays and EXRF analyses are listed. The average, mean, range, standard deviation of the mean, and relative standard deviation of the mean are based on all samples. The average analysis relative standard deviation is based on the variations found in the eight samples for which multiple analyses were performed. The percent of variance for 24 hr, 8 hr, 1 hr and analysis level is determined from the analysis of variance program. The meaning of the variances requires an explanation.

For each level (i) analytical, 1 hour, 8 hour, 24 hour, and analysis,

a variance S_i^2 is determined for each element. Then, the percent of total variance for the level for the concentration of Fe is:

$$\% (S_{Fe})_i^2 = \left(\frac{(S_{Fe})_i^2}{\sum_{i,j,k,m} (S_{Fe})_n^2} \right) \times 100$$

This parameter measures where the majority of the variation lies for each concentration in the 4 level sampling scheme design. For example, for oil yield, the % variance is greatest on the 24 hr level, the value being 63%. This implies that the samples taken on the 1 hr and 8 hr periods each day did not change significantly with respect to the day-to-day changes. Thus, the samples taken on one day are appreciably different from the samples taken on other days. The 24 hr averages for oil yield for the 6 days were 23.8, 25.8, 30.4, 24.5, 31.2, and 26.9 gallons per ton respectively. The daily variation is readily apparent. For day 3 where the 24 hr average is 25.8, the 8 hr oil yields are 25.2, 26.7, and 25.4 gpt and the 1 hr oil yields are 25.5, 22.4, 27.8, 21.2, 26.7, 27.4, 25.3, and 25.0 gpt. These results are about typical. The tight range of the 8 hr samples is obvious; the 1 hr samples range a bit more but not as much as the daily averages. The percent of variance for the 1 hr level is 37%. Thus, the percent of variance is a measure of how much scatter there is in the concentration of a substance at each level.

The first conclusion that appears from the results in Table I is that the oil yield measurably changed from day to day. The percent of variance is 63% for the daily level, 0% for the 8 hr level, and 37% for the 1 hr level. The oil yield is a reasonable measure of the organic content of the shale. So, this implies that for the retort month there were measurable differences from day to day in the organic content. This also implies that an average organic content for the month is probably not meaningful, but that a daily average for organic content can be reasonably estimated.

The elemental concentration results show these samples to be quite interesting. A geochemist would expect concentration ranges for trace elements to range by about a factor of 10 over a section of a formation. Here the range is only a factor of 2. For some elements like Rb and Sr, the relative standard deviation over all the samples is less than 10%. For most of the elements, the analytical precision is at 10% or less. This can be considered to be quite respectable for a multi-element analytical technique. Nevertheless, for Ca, Mn, Fe, Cu, and Se the analytical precision contributions most of the error as can be seen by the percent of variance for the analysis for these elements. This implies that more precise techniques should be used to obtain the concentrations of these elements in oil shale. Finding techniques with uniform precision significantly below 10% is difficult. For none of the elements does the daily or 8 hr percent of variance exceed 33%. This implies that a representative sample for the retort month for the inorganic elements can be calculated. The grand mean for each element represents a reasonable average for the whole month. For the elements listed, the results are not statistically different from those of other laboratories who were conducting other experiments at Anvil Points at the same time. So thus, the mean concentration values for the elements represent an accurate estimate of the feedstock that month within the constraints of the analytical scheme and the sampling design.

The contrast in conclusions for the organic and inorganic portions of the oil shale feedstock is obvious. Since great care was taken in the consideration of the sampling design, one has to conclude that this difference is real. To test this further, the concentration of all the substances listed in Table I for all the samples analyzed were tested by a linear correlation program. The results for the correlation coefficients are listed in Table II. None of the coefficients relating the oil yield to the elements rises above 0.5. This also shows the basic dissimilarity between organic and inorganic portions of this oil shale.

Several implications arise from this organic and inorganic difference. The primary conclusion is that on a production level none of the above elements vary in the same general way as the organic content of the oil shale. This conclusion allows the situation of variability in layers in the formation; but if there is mining, then hauling and crushing blend out any variations. This conclusion also will allow the possibility of some minor amount of an element such as As or Pb to be associated with the organic portion of the shale but the majority of amount of that element cannot be associated with organics in the shale. Another implication of this dicotomy is that the results of analyses on the organic content which would typically be performed by an oil analysis laboratory will not yield information about the inorganic elements. This implication means that specific analyses for the inorganic elements will have to be made if their concentrations are of interest. Fortunately, the results shown for Table I for the inorganic elements show the feedstock to be quite uniform. This means that careful analysis of a sample taken once a week will yield more information on elemental concentrations than less accurate analyses taken on samples collected every hour or every shift.

References

1. Jones, J. B., Jr. (1977) Technical Evaluation of the Paraho Process, 11th Israel Conf. on Mechanical Engineering, Technion, Haifa, Israel.
2. Jones, J. B., Jr. (1976) The Paraho oil-shale retort. Quart. Colo. School of Mines, vol. 71, No. 4, pp. 39-48.
3. Taggart, A. F. (ed.) (1967) Handbook of Mineral Dressing, J. F. Wiley & Sons, New York,
4. Heistand, R. N. (1976) The Fischer Assay: Standard for the oil shale industry. Energy Sources, vol. 2, pp. 397-405.
5. Chappell, W. R. (1978) Toxic trace elements and shale oil production. Proc. 11th Oil Shale Symp. Colo. School of Mines, Golden, CO., In Press.
6. Miesch, A. T. (1976) Sampling designs for geochemical surveys-syllabus for a short course. U. S. Geol. Survey, Open-File Report 70-772, 132 pp.
7. Miesch, A. T. (1976) Geochemical survey of Missouri - Methods of sampling, laboratory analysis, and statistical reduction of data. U. S. Geol. Survey Prof. Paper 954-A, 39 pp.

8. Alfrey, A. C., Nunnelley, L. L., Rudolph, H., and Smythe, W. R. (1976) Medical Applications of small x-ray Fluourescence System. In: Adv. in X-ray Analysis, vol. 19, Kendall/Hunt, Dubuque, Iowa, pp 497-509.
9. Kubo, H., Bernthal, R. and T. R. Wildeman (1978) Energy dispersive x-ray fluourescence spectrometric determination of trace elements in oil samples. Anal. Chem., vol. 50, pp 899-903.
10. Wildeman, T. R., and Meglen, R. R., (1978) The analysis of oil-shale materials for element balance studies. In. Analytical Chemistry of oil shale and tar sands, Adv. in Chem. Series.
11. Fox, J. P., Fruchter, J. S., and T. R. Wildeman (1979) Inter-laboratory study of elemental abundances in raw and spent oil shales. Oil shale sampling, analysis and quality assurance symposium. March 26-28, 1979, Denver, Colorado.

Table I. Concentration parameters of Paraho oil shale. The sampling period is from August 23, 1977 through September 20, 1977.

Substance	Conc. Unit	Grand Mean	Grand Standard Deviation	Grand Rel. Std. Dev. %	Range	Avg. Analysis Rel. Dev. %	% OF VARIANCE			
							24 hr Level	8 hr Level	1 hr Level	
Oil	gpt	27.0	3.2	11.9	22-39	2	63	0	37	-
Water	gpt	4.4	1.7	39	1.6-11.4	15	0	93	7	-
Gas & Loss	gpt	2.2	0.6	28	1.0-3.7	20	0	26	74	-
Ca	%	12.3	1.5	12	7.2-15	13	3	0	0	97
Mn	ppm	313	34	11	191-380	10	12	0	0	88
Fe	%	2.13	0.21	10	12.2-25	9.2	6	0	0	94
Ni	ppm	32	3	9.5	18-36	6.6	0	0	55	45
Cu	ppm	35	4	10.1	20-40	6.6	8	22	2	68
Zn	ppm	83	24	29	40-180	9.8	14	0	68	18
Ga	ppm	7.0	0.8	12	4-8	7.6	18	0	32	50
As	ppm	44	5.6	13	26-58	8.7	25	0	23	52
Se	ppm	1.5	0.26	17	1.0-2.3	15	7	0	0	93
Rb	ppm	80	6	7.4	45-85	1.7	24	0	73	3
Sr	ppm	770	66	8.6	410-830	2.2	32	0	62	6
Y	ppm	12	1.2	10.6	6.2-14	4.9	8	0	49	43
Zr	ppm	56	14	25	26-120	8.3	10	0	80	10
Nb	ppm	5.7	0.5	9.7	3.3-6.6	2.4	19	0	72	9
Mo	ppm	23	2.5	10.8	13-28	2.3	0	0	89	11
Ba	ppm	480	67	14	240-670	1.7	14	0	84	2
Pb	ppm	24	3.1	13	15-35	3.2	0	26	65	9

Ca	Mn	Fe	Ni	Cu	Zn	Ga	As	Se	Rb	Sr	Y	Zr	Nb	Mo	Ba	Pb	Oil	Water	Gas & Loss
1.00	0.88	1.00																	
0.82	0.72	0.83	1.00																
0.90	0.53	0.70	0.82	1.00															
0.79	0.36	0.35	0.40	0.18	1.00														
0.71	0.84	0.74	0.68	0.49	0.38	1.00													
0.26	0.38	0.52	0.62	0.67	0.24	0.32	1.00												
0.49	0.27	0.34	0.52	0.50	-0.08	0.35	0.40	1.00											
0.68	0.84	0.89	0.76	0.64	0.33	0.80	0.46	0.35	1.00										
0.49	0.84	0.82	0.66	0.53	0.33	0.76	0.42	0.23	0.95	1.00									
0.38	0.58	0.59	0.51	0.36	0.29	0.68	0.30	0.29	0.75	0.71	1.00								
0.75	0.02	0.16	0.20	0.31	0.04	0.26	0.20	0.18	0.24	0.16	0.30	1.00							
0.70	0.77	0.79	0.61	0.52	0.18	0.67	0.36	0.25	0.82	0.84	0.73	0.16	1.00						
0.38	0.36	0.50	0.61	0.80	0.18	0.36	0.61	0.48	0.55	0.52	0.35	0.30	0.52	1.00					
0.05	0.65	0.58	0.46	0.34	0.22	0.67	0.27	0.19	0.65	0.67	0.43	0.36	0.59	0.21	1.00				
0.60	0.39	0.49	0.47	0.57	0.09	0.14	0.56	0.27	0.43	0.38	0.11	0.01	0.30	0.50	0.25	1.00			
0.39	-0.39	-0.18	0.11	0.38	-0.13	-0.39	0.28	0.28	-0.33	-0.46	-0.35	0.15	-0.43	0.28	-0.42	0.29	1.00		
-0.09	-0.12	-0.05	-0.04	0.04	0.07	-0.01	0.12	-0.03	0.00	0.03	0.07	-0.04	0.04	0.12	-0.05	0.09	0.04	1.00	
0.08	0.00	0.11	0.13	0.11	0.10	-0.07	0.10	-0.01	0.09	0.11	-0.10	0.03	0.00	0.16	0.06	0.16	0.14	0.02	1.00
Loss																			

Table II. Correlation coefficients of the concentrations of various substances in Paraho shale.

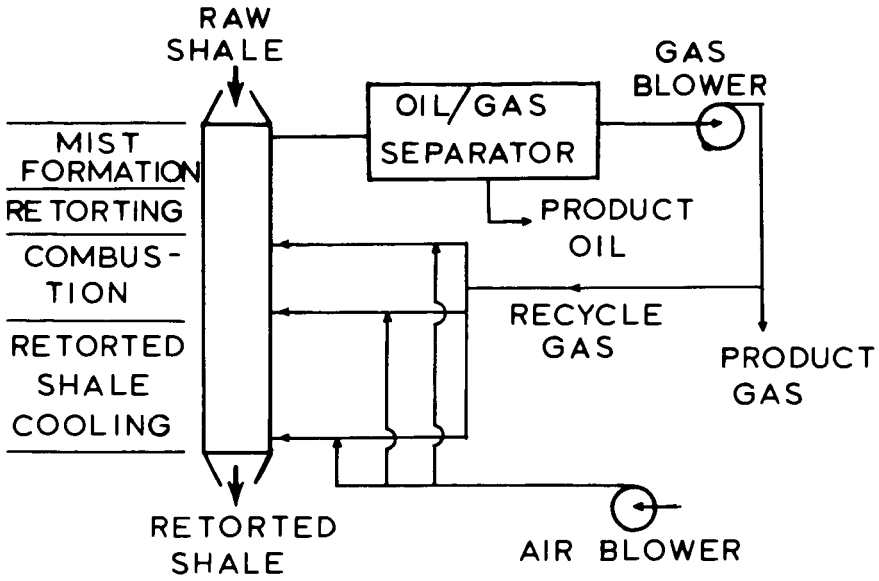


FIGURE 1. SCHEMATIC OF PARAHO RETORT FOR THE DIRECT HEATED MODE.

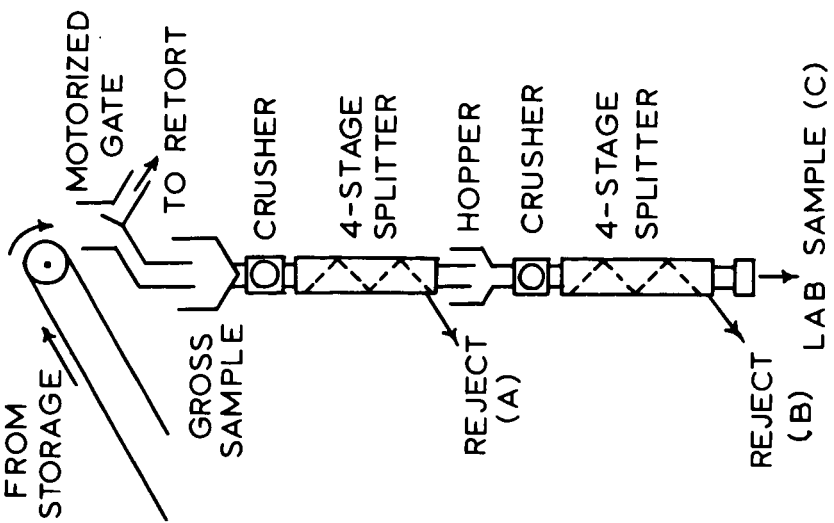


FIGURE 2. FEEDSTOCK SAMPLING SYSTEM FOR THE PARAHO RETORT.

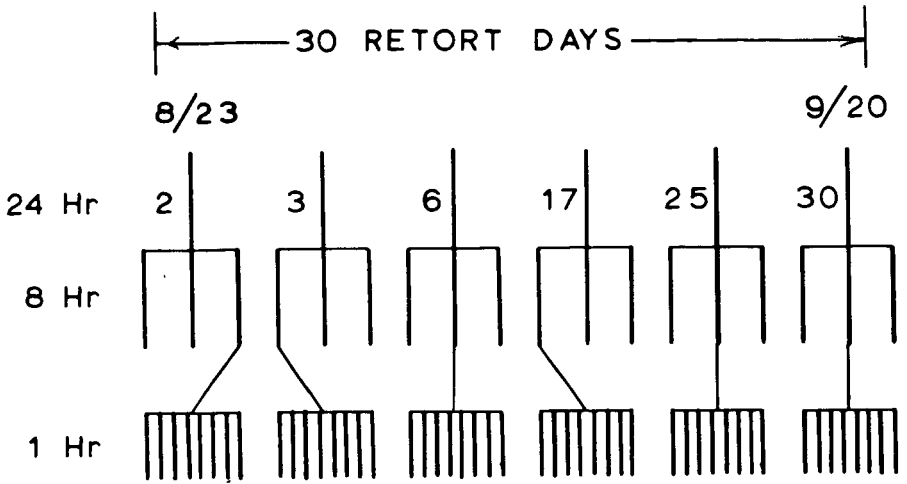


FIGURE 3 TIME NESTED PARAHO SAMPLING DESIGN.

Aromatic Nitrogen Compounds in Fossil Fuels - A Potential Hazard?

C.-h. Ho, B. R. Clark, M. R. Guerin, C. Y. Ma,¹ and T. K. Rao*

Analytical Chemistry and Biology Divisions*
Oak Ridge National Laboratory, Oak Ridge, TN 37830

Introduction

To achieve energy independence in the United States, converting coal to oil or extracting oil from shale will be required. Before commercial scale fossil fuel conversion facilities become a reality, chemical and biological studies of currently available synfuel samples derived from coal or shale are urgently needed in order to determine what the potential health problems, such as from occupational exposure, might be.

The nitrogen content either of shale oil (1-2%) (1) or coal derived oil (1-1.5%) (2) is far higher than that in petroleum (average N-content in petroleum is 0.05-0.1%) (3). This means enormous amounts of nitrogen containing species will be produced and found in crude synfuels, and this could lead to significant health or environmental impact. Clearly, a thorough characterization of nitrogen compounds in synfuels is an important pursuit.

Aromatic nitrogen compounds such as basic aza-arenes, neutral aza-arenes, and aromatic amines are considered environmentally important and several members of these classes of compounds possess biological activity. For example, dibenz(a,h)acridine, 7 H-dibenzo(c,g)carbazole, and 2-naphthylamine (4), are well known as carcinogens. In this paper, the methods used to isolate the basic aromatic nitrogen compounds and neutral aza-arenes from one shale oil and one coal-derived oil will be discussed. The mutagenic activities of these fractions, based on the Ames Salmonella typhimurium test, will be compared.

Experimental

Samples

A shale oil was obtained from the Laramie Energy Research Center's 150-ton retort operated for above ground simulation of *in-situ* retorting. The raw oil from the retort was an intimate emulsion of solids, water and oil; the emulsion was collapsed by centrifugation at 2500 RPM for about 20 min. at room temperature. Three phases were produced: an oily top phase (~50% vol.), a gelatinous intermediate phase (~20% vol.), and an aqueous phase (~30% vol.). The oil phase has been studied in this laboratory (5,6) and similar samples from other retort runs have been examined by others, principally by workers at the Laramie Energy Research Center (1,7,8).

A crude coal liquid (not necessarily representative of any final production scale product) was obtained from the Pittsburgh Energy Research Center. This material was very viscous, contained no water, and had a small amount of filterable solids (>5 μ m range).

Separation Procedures

Neutral aza-arenes. Figure 1 shows the separation scheme for isolation of neutral aza-arenes from synfuels. After removing acidic and basic components from the whole sample, the neutral fraction was loaded onto a Sephadex LH-20 gel column. The column was eluted sequentially with 250 ml of isopropanol (Fraction AP) and 600 ml of acetone (Fraction AROM). Pentadecane and naphthalene were used to indicate the appropriate cut between elution of aliphatic compounds and 2-ring aromatic compounds.

¹Faculty Research Member, University of Mississippi.

Acetone was removed from Fraction AROM and the residue was separated into three sub-fractions on a silicic acid column: Fraction I (PAH), eluate from 1200 ml benzene/hexane (1/3); Fraction II (neutral aza-arenes), eluate from 600 ml benzene/hexane (2/1); and Fraction III (polar), eluate from 600 ml ethanol. A mixture of a number of PAH compounds (pyrene, C¹⁴-carbazole and 7 H-dibenzo(c,g)carbazole) were chromatographed in establishing this procedure.

Basic components. Basic fractions of the oils were produced by first dissolving the oils in diethyl ether and extracting the acids with a 1 M NaOH solution. A second extraction with 1 M HCl removed the basic components which were further partitioned between an aqueous/ether phase at pH 11. The basic fractions are contained in this ether phase. Further details of this procedure are reported elsewhere (9). Figure 2 shows the subfractionation scheme used to further separate basic fraction constituents. The basic fraction was placed onto a basic alumina column. The column was eluted with 500 ml benzene (benzene subfraction) followed by 700 ml ethanol. Ethanol was removed and the residue was separated further on a Sephadex LH-20 gel column. The column was eluted sequentially with 250 ml of isopropanol (isopropanol subfraction) and 600 ml of acetone (acetone subfraction).

Column packings and reagents. Basic alumina (100-200 mesh, AG-10, Bio-Rad Laboratories), Sephadex LH-20 gel (25-100 μ , Pharmacia Fine Chemicals) and silicic acid (100 mesh, Mallickrott, washed successively with hexane, acetone, and methanol; activated in 150°C oven for 16 hours) were used for column packings. Forty grams of alumina were added to 75 ml of benzene in a modified 50 ml buret column. A Sephadex column was prepared by swelling 75 g of the gel in isopropanol with sufficient excess to form a pourable slurry. The slurry was poured into the 250 ml buret column and allowed to compact by the gravity elution of 50-100 ml of isopropanol. A silicic acid column was made by pouring a slurry of 100 g of silicic acid in hexane into a 2.5 cm (O.D.) x 50 cm glass column.

All solvents were reagent grade and were freshly distilled except for the absolute ethanol. Reagents prepared for the microbial mutagenesis bioassay are described elsewhere (10,11).

GC/MS

GC/MS data were obtained using a Perkin-Elmer Model 3920 gas chromatograph interfaced to a DuPont 21-490B mass spectrometer via a glass jet separator. An effluent splitter provided about a 2:1 split between the mass spectrometer and a flame ionization detector, respectively. A Hewlett-Packard 21-094B data system interfaced to the mass spectrometer provided for the generation of mass spectra, mass chromatograms, library searches, etc. A glass GC column of 20 ft. x 1/8-in. O.D. was packed with 3% Dextsil 400 on 100/120 mesh Chromosorb 750 and installed with graphite ferrules. GC temperature programming was from 100°C (8 minutes hold) to 320°C at a linear rate of increase of 1°/min. Injector and detector temperatures were set at 320°C, helium gas inlet pressure at 100 psig, MS ionization voltage at 70 eV, mass scan rate at 2 seconds/decade and the MS resolution at about 600.

Microbial Mutagenesis Assay. Salmonella typhimurium bacteria, strain TA98, were generally employed. The experimental procedures are described by Ames et al. (10). Briefly, the bacteria are added to a soft agar containing nutrients and in some cases, enzyme activation preparations along with the substance being tested. The essential condition is that the amino acid, histidine, is absent. The suspension, containing approximately 2×10^8 bacteria, is overlaid on minimal agar plates and incubated. If the test substance is a mutagenic agent in this system, then large colonies (which have reverted to the wild type) are evident on the plate and can be counted, i.e., by mutation they can produce their own histidine and grow in a

histidine-free medium. If no colonies form except for a control background level, then no mutations have occurred. A test consists of assays at several concentrations of test substance in order to obtain a dose-response curve. Some potential mutagens require metabolic activation with liver homogenate preparations.

Results and Discussion

Neutral Aza-arenes

The procedures used for the isolation of neutral aza-arenes from synthetic crude oils evolved in part from an extraction scheme and a gel filtration chromatographic scheme (5, 12) developed in this laboratory. The silicic acid adsorption chromatography step was developed by Snook et al. (13) to isolate indole/carbazole from cigarette smoke condensate. But the silicic acid chromatography has been evaluated and some modifications have been made to make the system compatible with a gravity flow column. A good separation between PAHs and neutral aza-arenes was achieved by eluting the column with 1/3 (benzene/hexane) followed by 2/1 (benzene/hexane). However when large quantities of aliphatic compounds are present in the sample, these contaminate all the eluate fractions. It is necessary to remove major portions of aliphatic components prior to the silicic acid step. Gel filtration chromatography with a Sephadex LH-20 column eluted with isopropanol is effective for removing a major portion of aliphatic and polymeric compounds while retaining aromatic compounds of two rings and higher. Further elution of the column with acetone results in the quantitative recovery of aromatic components in order of increasing aromaticity (5). Silicic acid chromatography produced a relatively pure neutral aza-arene fraction (Fraction II), suitable for GC/MS analysis and bioassay. The separation of PAH and neutral aza-arene fractions was further confirmed by a chromatographic study of oil samples spiked with large excesses of benzo(a)pyrene along with carbazole. Tracer studies of oil samples spiked with C^{14} -carbazole showed that carbazole was not eluted from the column with even as much as 1600 ml 1/3 (benzene/hexane). The recovery of C^{14} -carbazole from the silicic acid column with 2/1 (benzene/hexane) was 97% for the coal derived oil and 75% for the shale oil. This agrees well with data on cigarette smoke condensate (13).

The presence of indole/carbazole analogues in Fraction II from both oil samples is also supported by their IR spectra. These fractions have a sharp band at 3430 cm^{-1} which is normally found in the IR spectrum of carbazole and is characteristic of the N-H group in these compounds.

In a peak by peak comparison of GC profiles of Fraction II obtained with an FID and an NPD, we found the majority of the GC peaks were nitrogen containing compounds.

The proton NMR spectrum of Fraction II gave a ratio of aliphatic protons to aromatic protons close to unity (1.06) indicating that only a few alkyl groups are contained in Fraction II. This result seems to be consistent with the observation from GC/MS analysis in which the biggest alkyl substituent was six carbons.

The odd m/e values of molecular ions obtained from GC/MS data confirmed the predominant presence of nitrogen compounds in Fraction II. Tentatively identified components are C_1 - C_3 phenylpyrroles, indole, C_1 - C_6 indoles, C_1 - C_3 phenylindoles, carbazole, C_1 - C_5 carbazoles, benzocarbazoles, and C_1 - C_3 benzocarbazoles.

The weight distribution of aliphatic and aromatic subfractions are listed in Table 1. N-heterocyclic material is much less than aromatic hydrocarbon material in the shale oil. The quantities of carbazole in the original oil samples were estimated by external standard calibration based on GC peak height. They

are 147 ppm for the shale oil and 268 ppm for the coal-derived oil. Because of lack of standard neutral nitrogen-heterocyclic compounds, the quantitative data, except for carbazole, are not available at this time.

Table 2 summarizes the mutagenicity test data on the four neutral subfractions of coal-derived oil and several commercially available neutral aza-arenes. Indole and carbazole, exhibit no mutagenicity. Highly carcinogenic 7 H-dibenzo(c,g)-carbazole gave a slight but definite positive mutagenic activity at a low dose range (below 25 µg/plate). Specific activity could not be determined for this compound due to the toxic effect at a higher dose range. Benzocarbazoles and their alkyl-substituted compounds were not available for this study. Despite the incompleteness of this study, the correlation between chemical structure and mutagenic activity is expected to be in general agreement with that observed with PAH (14). Fraction AP which contains mostly aliphatic and polymeric constituents shows no mutagenic activity as expected. PAH subfractions exhibit the lowest specific activity among the three subfractions. The neutral aza-arene fractions, which are normally isolated with PAH fractions, have more than two times the specific activity of the PAH fraction. This indicates that the analysis of neutral aza-arene fractions of synfuels are as important as PAH analysis. The higher specific activity of the neutral aza-arene fraction may contain substantial quantities of multi-ring compounds. The further sub-fractionation of the neutral aza-arene fractions into fractions with aza-arenes of approximately the same ring sizes is presently being undertaken.

Basic nitrogen compounds. To further understand what classes or types of basic nitrogen compounds are the most bioactive among compounds in the basic fraction, we recently developed a separation method which isolates the mutagenically active compounds from the bulk of the base fraction (15). The subfractionation scheme is shown in Figure 2. This separation method was devised using a microbial mutagenesis bioassay as a liquid chromatographic detector in the development of the chromatographic subfractionation procedure. Table 3 summarizes the mutagenicity test data on the three basic subfractions of the synfuels. The bioactivities of several commercially available compounds and three that were synthesized in this laboratory are listed in Table 4 for comparison. About 90% of the basic mutagenic activity is recovered in the acetone subfraction which comprises about 10% of the basic fraction. That suggests that the method can be used for isolation of basic mutagenic components from samples of different origins (in this case oil shale or coal). To demonstrate the utility of the method, 3 different kinds of cigarette smoke condensates were fractionated using this scheme and the mutagenic compounds were also concentrated in the acetone subfraction. GC/MS data indicate that the major compound type of the benzene subfractions is C₃-C₁₃ alkyl substituted pyridines. Mutagenic activities of some commercially available pure pyridines (such as pyridine and C₁-C₃ pyridines) and one specially synthesized C₉-pyridine are essentially zero in agreement with these results. The major compounds in the isopropanol fractions are partially hydrogenated 1-2 ring aza-arenes. Biological data on compounds of this type are not available for comparison.

The acetone subfraction of shale oil was about half as mutagenic as benzo(a)pyrene while the coal-derived oil subfraction was about four times more active. GC/MS data indicate multi-ring aza-arenes comprised a large portion of the acetone subfraction, e.g. aza-benzoperylene, aza-indenopyrene, and aza-coronene have been identified. This finding is consistent with bioactivity data from a few multi-ring aza-arene compounds such as dibenz(a,j)acridine (13,000 rev/mg), 9-methyl-10-aza-benzo(a)pyrene (30,000 rev/mg) and 10-azabenz(a)pyrene (130,000 rev/mg). The purposes in synthesizing two nitrogen isologs of benzo(a)pyrene was, first, to confirm the higher mutagenic activity of multi-ring aza-arenes, which comprise a large portion of the acetone subfraction, and to compare their activities with the mutagenic activity of benzo(a)pyrene. 10-azabenz(a)pyrene is two times more active than benzo(a)pyrene. A methyl group on the 9 position of azabenz(a)pyrene, decreases the mutagenic activity. This might be explained by steric hindrance toward the forming of an epoxide at the 7 and 8 position.

The presence of aromatic amines in the active subfraction from both oil samples was first suggested from their IR spectra. Bands at 3220 cm^{-1} and 3370 cm^{-1} , which are normally found in the IR spectra of aromatic amines, are characteristic of the amino compounds in the fraction. By acetylation of the acetone subfraction, we isolated large amounts of primary aromatic amides from the acetone subfraction. A mixture of ten compounds consisting of 4 aza-arenes and 6 aromatic amines (2,4,6-trimethylpyridine, quinoline, acridine, dibenz(a,h)acridine, N, N-dimethylaniline, N-methylaniline, N-phenyl-2-naphthylamine, aniline, 2-naphthylamine, and 1-aminopyrene) was separated on a basic alumina column followed with a Sephadex LH-20 column. All primary amines (1,2, and 4-ring compounds), quinoline and dibenz(a,h)acridine were concentrated in the acetone subfraction. This finding may mean that the primary aromatic amines as well as multi-ring aza-arenes are producing the mutagenic activities of the acetone subfractions. A logical extension of this work is to further separate the acetone subfraction into primary amines and multi-ring aza-arenes. This should lead to some important conclusions regarding the mutagenic effects of these classes of compounds.

References

1. J. R. Morandi and R. E. Poulson, A.C.S. Prepr., Div. Petrol. Chem., **20**(2), 162 (1975).
2. Unpublished results, I.B. Rubin, Oak Ridge National Laboratory, Oak Ridge, TN.
3. H. L. Lochte and E. R. Littmann, "The Petroleum Acids and Bases," Chemical Publishing Co., Inc., New York, NY, 291 (1955).
4. C. E. Searle, Ed., "Chemical Carcinogens," ACS Monograph 173, ACS, Washington, DC (1976).
5. A. R. Jones, M. R. Guerin and B. R. Clark, Anal. Chem. **49**, 1766 (1977).
6. B. R. Clark, "Oil Shale and Shale Oil-Organic Characterization," presented at the 2nd Workshop on Oil Shale Environmental Research, Nov. 2, 1977, Richland, WA.
7. R. E. Poulson, C. M. Frost and H. B. Jensen, in Advances in Chemistry Series, T. F. Yen, Ed., **1** (1978).
8. R. E. Poulson, H. B. Jensen, and G. L. Cook, A.C.S. Prepr., Div. Petrol. Chem. **16**(1), A49 (1971).
9. A. P. Swain, J. E. Cooper, and R. L. Stedman, Cancer Res. **29**, 579 (1969).
10. B. N. Ames, J. McCann and E. Yamasaki, Mutat. Res. **31**, 347 (1975).
11. T. K. Rao, A. A. Hardigree, J. A. Young, W. Lijinsky and J. L. Epler, Mutat. Res. **56**, 131 (1977).
12. I. B. Rubin, M. R. Guerin, A. A. Hardigree, and J. L. Epler, Environ. Res. **12**, 358 (1976).
13. M. E. Snook, R. F. Arrendale, H. C. Higman and O. T. Chortyk, Anal. Chem. **50**, 88 (1978).
14. M. R. Guerin, J. L. Epler, W. H. Griest, B. R. Clark, and T. K. Rao, in Carcinogenesis, Vol. 3: Polynuclear Aromatic Hydrocarbons, edited by P. W. Jones and R. I. Freudenthal, Raven Press, New York (1978).

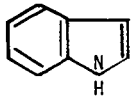
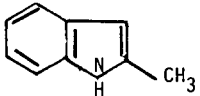
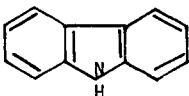
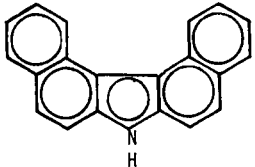
15. M. R. Guerin, B. R. Clark, C.-h. Ho, J. L. Epler, and T. K. Rao, "Short-Term Bioassay of Complex Organic Mixtures, Part I. Chemistry," Symposium on Application of Short-Term Bioassays in the Fractionation and Analysis of Complex Environmental Mixtures, Williamsburg, VA, February 21-23, 1978.

Table 1. Weight Distribution of Neutral Fractions*

	Weight % Distribution	
	<u>Shale Oil</u>	<u>Coal-Derived Oil</u>
Aliphatic and Polymeric (AP)	85.1	35.1
Aromatic (AROM)	14.9	62.9
PAH (I)	10.1	35.9
Neutral Aza-arene (II)	1.4	9.5
Polar (III)	4.3	17.7

* Acid-base extraction yield 89.6% by weight of neutral fraction from shale oil and 56% from coal-derived oil.

Table 2. Mutagenic Activities of the Neutral Subfractions of a Coal-Derived Oil and Some Neutral Aza-arene Compounds

<u>Fraction/Compound</u>	<u>Specific Activity (rev/mg)*</u>
Aliphatic and Polymeric Fraction (AP)	0
PAH Fraction (I)	1390
Neutral Aza-arene Fraction (II)	3250
Polar Fraction (III)	3380
	0
	0
	0
	0
	**

*Tested on TA98 with Aroclor S-9.

** Four-fold increase over spontaneous reversion at dose below 25 μ g/plate. Toxic effect developed at higher dose.

Table 3. Distribution of Mutagenic Activity in Basic Subfractions

Subfraction	Shale Oil Base Fraction			Coal-Derived Oil Base Fraction		
	Average ¹ Weight (%)	Average Specific Activity (rev/mg)	Average ² Relative Activity (%)	Average ¹ Weight (%)	Average Specific Activity (rev/mg)	Average ² Relative Activity (%)
Benzene	78	0	0	76	850	2
Isopropanol	13	277	1	12	0	0
Acetone	9	25,000	92	12	220,000	88
TOTAL	100		93	100		90

¹ Percentage by weight of the basic fraction.

² Percentage of mutagenic activity (TA98, S9, Aroclor 1254) of the basic fraction accounted for in the sub-fraction.

Table 4. Mutagenicity of Basic Aromatic Compounds*

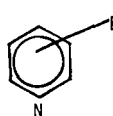
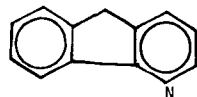
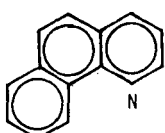
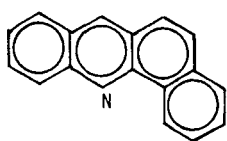
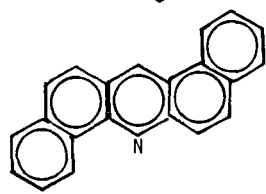
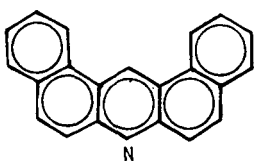
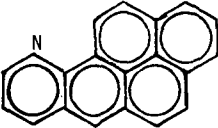
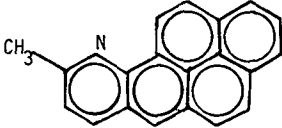
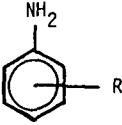
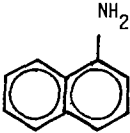
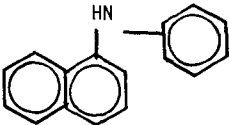
Compound Type - Basic Aza-arene	Specific Activity (rev/mg)
 <p>R = H, CH₃, C₂H₅, C₃H₇, C₉H₁₉</p>	0
	340
	0
	0
	0
	6,000
	13,000

Table 4. Continued

Compound Type - Basic Aza-arene (cont'd)	Specific Activity (rev/mg)
	130,000
	30,000
Aromatic Amine	
	R = H, CH ₃ , C ₂ H ₅
	4,660
	0

*Aroclor induced.

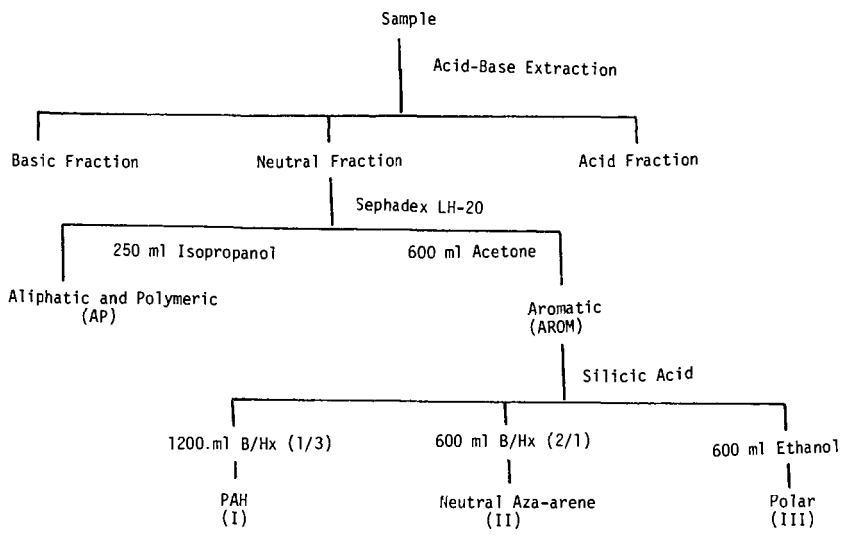


Figure 1. Isolation of Neutral Aza-arenes from Synfuels.

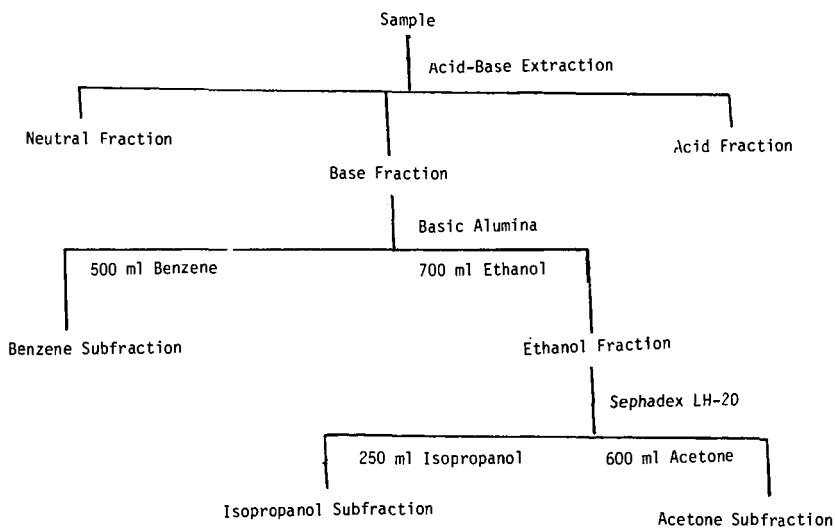


Figure 2. Subfractionation of the Basic Fraction of Synfuels.

MICRO-ANALYSIS of POLYNUCLEAR AROMATIC HYDROCARBONS in PETROLEUM

Hidetsuru Matsushita

Department of Community Environmental Sciences, National Institute of Public Health, 4-6-1, Shirogane-dai, Minato-ku, Tokyo, Japan, 108

It is well known that petroleum and related oils are largely used in our communities and that these oils contain many kinds of polynuclear aromatic hydrocarbons (PAH) in trace amounts. Some PAH are carcinogenic to experimental animals and are suspected to be carcinogenic to man. In fact, occupational cancer has been observed in various types of worker groups having an occupational contact with petroleum and related products such as fuel oil, lubricating oil, paraffin oil, waxes and so on (1). These indicate the need of a reliable method for determining PAH in petroleum and related oils. We have devised dual band thin-layer chromatography (TLC). This TLC has been proved to be useful as a tool for routine microanalysis of PAH in various samples such as heavy oil (2), kerosene (2), gasoline (3), air-borne particulates (4,5), cigarette smoke (6), asbestos (7), coal tar (8,9), pitch (9) and so on.

This paper describes two analytical methods for analysing PAH in petroleum and related oils. The first method, multiple PAH analysis, is useful for analysing many kinds of PAH. The second method, major component analysis, is useful for determining 5 - 10 PAH which are prevalent in petroleum and related oils.

1. Multiple PAH Analysis

Multiple PAH analysis consists of the following 3 procedures; selective extraction of PAH by a series of liquid - liquid partition, separation of the extract into each component by two dimensional dual band TLC, and identification and quantitative determination of the separated compounds by spectrofluorometry.

A known amount of petroleum are dissolved in cyclohexane. PAH in this solution is selectively extracted by a series of liquid - liquid partition of the cyclohexane solution - dimethyl sulfoxide (DMSO), [DMSO + (1 + 4) Hydrochloric acid, 1:1,v/v] - cyclohexane, 70% sulfuric acid - cyclohexane, and 5% sodium hydroxide aqueous solution - cyclohexane.

At the first partition, aromatic fraction in the sample is extracted to DMSO phase, remaining aliphatic fraction in cyclohexane phase. The aromatic fraction contain PAH, aromatic quinones, acidic and basic aromatic compounds. At the 2nd partition, PAH, aromatic quinones and some of acidic compounds are extracted to cyclohexane phase, and separated from basic aromatic compounds and water soluble acidic compounds. Aromatic quinones and trace amounts of basic aromatic compounds in the cyclohexane phase are removed by the 3rd liquid - liquid partition. Acidic aromatic compounds are removed by the 4th partition. The final cyclohexane solution thus obtained contains PAH selectively. Table 1 shows the partition coefficients for 30 aromatic compounds in these liquid - liquid partitions, and also shows the number of times required for extracting 99% or more of these compounds.

The cyclohexane solution which contains very rich PAH is washed with water. After removing the residual water in the solution by adding small amounts of sodium sulfate anhydride, the solution is dried up at a low temperature (40°C) under a reduced pressure. The residue is dissolved in a known amount of benzene (0.5 to 1.0 ml).

PAH in this benzene extract are separated into each component by two dimensional dual band TLC. The TLC plate consists of an aluminum oxide layer (4 x 20, cm) and a 26% acetylated cellulose layer (16 x 20,cm). The acetylated cellulose was prepared by acetylation of microcrystalline cellulose for TLC (Avicel SF) using the method of Wieland et al (10). After the application of a few microliters of the benzene extract onto the aluminum oxide layer, the first development is

carried out with n-hexane - ether (19:1,v/v) to the 15 cm mark on the aluminum oxide layer. This is done at about 20% relative humidity, easily achievable by placing a container of saturated aqueous solution of potassium acetate in a developing chamber. Developing time is about 35 min.

PAH on the aluminum oxide layer are then separated into each component on the acetylated cellulose layer by the second development with methanol - ether - water (4:4:1,v/v). It requires about 60 min. for the developer to reach 10 cm from the layer boundary.

PAH separated on the acetylated cellulose layer are detected as small spots by their fluorescence under UV ray (253 & 365 nm). Detection limit is very low and nanogram order of PAH are usually detectable. Most of PAH are stable on the acetylated cellulose layer. Fig. 1 shows two dimensional dual band thin-layer chromatograms of the benzene extracts from a heavy oil C and an ethylene bottom oil. Heavy oil C, which is widely used as a fuel oil, contained 42 PAH and the ethylene bottom oil contained 69 PAH. PAH in each spot can be analysed by spectrofluorometry. At the present time, 10 PAH in the heavy oil C and 21 PAH in the ethylene bottom oil have been identified as shown in Fig.1. Many PAH in the spots on the chromatograms are left for future identification mainly due to the difficulty in getting the reference substances.

This multiple PAH analysis has revealed that various kinds of PAH are contained in petroleum and related oils such as kerosenes (22 - 39 PAH), heavy oils (32 - 42 PAH), paraffin oil (66 PAH) and gasoline (76 PAH).

2. Major Component Analysis

It is often necessary to analyse 5 - 10 PAH which are abundant in petroleum and related oils. These PAH can be analysed by the major component analysis. This method differs from the multiple PAH analysis only in separation procedure. That is, a one dimensional dual band TLC is used instead of the two dimensional dual band TLC mentioned above. The one dimensional dual band TLC has the following advantages as compared with the usual one dimensional TLC: 1) It has a higher separation efficiency. 2) Separation efficiency is not affected by the spot size at the origin. 3) Sample solution up to a few milliliters can be tested. 4) Quantitative sample application is easily achievable. 5) Detectability of PAH is very high. Therefore, this method is especially useful for the analysis of a sample which contains very low amounts of PAH.

The dual band TLC plate used consists of a kieselguhr layer (4 x 20,cm) and a 26% acetylated cellulose layer (16 x 20,cm). The former layer is used for the application of a sample and the latter layer for separating the sample. Fig. 2 shows a one dimensional dual band thin-layer chromatogram of PAH in a gasoline. In this case, gasoline sample was applied to the kieselguhr layer without any purification by liquid-liquid partition, because gasoline sample evaporated rapidly leaving PAH and related compounds on the layer. Development was carried out with methanol - ether - water (4:4:1,v/v) until the developer reach 10 cm from the layer boundary. It required about 60 min. PAH and related compounds in a gasoline are usually separated into 21 - 24 rectangular spots on the acetylated cellulose layer.

After extraction with 4 ml of DMSO, PAH in each spot is identified by spectrofluorometry in due consideration of its R_f value. Spectrofluorometry is useful for the identification of PAH in a spot containing several kinds of PAH and related compounds. For example, PAH in the spot C in the chromatogram in Fig. 2 were easily identified as pyrene and fluoanthene. In this method, 10 PAH are usually identified from a gasoline sample. They are benzo(a)pyrene, chrysene, benzo(b)fluoranthene, benz(a)anthracene, anthanthrene, benzo(k)fluoranthene, perylene, pyrene, fluoanthene, and benzo(ghi)perylene. The first 4 PAH are carcinogen and the last 3 PAH are cocarcinogen.

The identified PAH except benzo(b)fluoranthene can be determined quantitatively by a narrow base line method (6). Benzo(b)fluoranthene can be analysed after complete separation with benzo(a)pyrene by repeat development with methanol

- ether - water (4:4:1,v/v). The narrow base line method has been proved to be very effective in eliminating interference from other PAH and related compounds coexisting in a test solution. For example, pyrene in a solution which also contained fluoranthene, perylene and benzo(e)pyrene was analysed by this method. Observed value of pyrene differed by only 3% from the theoretical values, even when the concentrations of the latter 3 PAH (100 ng/ml) were 5 times higher than pyrene (20 ng/ml). It was also found that observed value of benzo(a)pyrene in a mixed PAH solution differed only 0.8% from the theoretical value, even when the solution contained benzo(b)fluoranthene, chrysene, anthanthrene and dibenzo(a,h)pyrene in 10 times higher concentration than benzo(a)pyrene.

Table 2 shows contents of 9 PAH in regular and premium gasolines as well as coefficient of variation for each PAH obtained in this analysis. The coefficient of variation is low for all PAH analysed. Furthermore, this method is so sensitive that it can analyse PAH quantitatively at a concentration of 1 ng/ml or less.

Another major component analysis is achievable by high speed liquid chromatography instead of one dimensional dual band TLC. A spectrofluorometer is used as a detector of a high speed liquid chromatograph. Fig. 3 demonstrates an example in which a liquid-liquid partition extract from a gasoline is separated and detected at the spectrofluorometric condition for analysing benzo(a)pyrene, benzo(k)fluoranthene, benzo(ghi)perylene and anthracene. The other PAH in the extract can also be analysed in a suitable spectrofluorometric condition. It has been proved that this major component analysis is useful for analysing several kinds of PAH in petroleum and related oils as well as combustion products of these oils.

These analytical methods described in this paper have a wide range of uses, producing reliable data on PAH in petroleum and related oils. These methods will be useful for analysing PAH in various kinds of samples in the environment.

References

1. W.C. Hueper: Occupational and Environmental Cancers of the Respiratory System, pp.118 - 125, Springer-Verlag, Berlin Heidelberg New York (1966).
2. H. Matsushita, Y. Esumi, A. Suzuki: Japan Analyst, 21, 331 (1972).
3. H. Matsushita, K. Arashidani, M. Koyano, T. Handa: J. Jap. Soc. Air Pollution, 11, 44 (1976).
4. H. Matsushita, Y. Esumi, K. Yamada: Japan Analyst, 19, 951 (1970).
5. H. Matsushita, K. Arashidani, T. Handa: Japan Analyst, 25, 263 (1976).
6. H. Matsushita, K. Kawai, K. Arashidani: Proceedings of the 29th annual meeting of Chem. Soc. Japan, I, p.142 (1973).
7. H. Matsushita, K. Arashidani: Proceedings of the 46th annual meeting of Jap. Assoc. Ind. Health, p.172 (1973).
8. H. Matsushita, Y. Esumi, S. Suzuki, T. Handa: Japan Analyst, 21, 1471 (1972).
9. H. Matsushita, K. Arashidani: Japan Analyst, 25, 76 (1976).
10. Th. Wieland, G. Lüben, H. Determan: Experientia, 18, 432 (1962).

Table 1. Partition Coefficients of Aromatic Compounds

Substance		A Phase		DMSO		Cyclohexane		Cyclohexane		Cyclohexane	
		B Phase		Cyclohexane		DMSO + (1+4)		70% H ₂ SO ₄		5% NaOH	
		K	N	K	N	K	N	K	N	K	N
Hydrocarbon	Anthracene	3.9	3	>100	1	>100	1	>100	1	>100	1
	Phenanthrene	3.9	3	40	2	>100	1	14	2		
	Fluorene	7.9	3	>100	1	>100	1	>100	1		
	Pyrene	4.6	3	>100	1	>100	1	>100	1		
	Chrysene	9.8	2	>100	1	>100	1	>100	1		
	Benzo(a)pyrene	13	2	>100	1	>100	1	>100	1		
	Fluoranthene	5.3	3	>100	1	>100	1	>100	1		
	Benzo(b)fluoranthene	10	2	>100	1	>100	1	>100	1		
	Benzo(ghi)perylene	14	2	66	2	>100	1	>100	1		
	Coronene	14	2	40	2	>100	1	>100	1		
Quinone	Anthraquinone	12	2	49	2	0.77	9	>100	1		
	Benzanthrone	20	2	30	2	0.017	270	>100	1		
	Benz(a)anthraquinone	13	2	>100	1	19	2	>100	1		
	p-Benzoquinone	—	—	0.26	7	0.010	460	0.0035	1300		
	1,2-Naphthoquinone	>100	1	0.13	38	0.052	91	—	—		
	1,4-Naphthoquinone	22	2	2.9	4	0.078	62	0.0015	3100		
	Nicotinic Acid	—	—	0.051	92	—	—	0.027	180		
Acid	o-Hydroxybenzoic Acid	—	—	0.115	43	0.086	56	0.001	4600		
	Terephthalic Acid	—	—	0.032	150	—	—	0.031	150		
	Phenazine	4.0	3	4.6	3	—	—	14.5	2		
Base	Carbazole	>100	1	0.83	8	0.14	36	>100	1		
	Lepidine	6.2	3	0.047	100	—	—	—	—		
	Benzo(h)quinoline	7.0	3	0.019	240	—	—	—	—		
	Benzo(f)quinoline	12	2	<0.001	>4600	—	—	—	—		
	Acridine	8.8	3	<0.001	>4600	0.016	290	—	—		
	1-Naphthylamine	55	2	0.007	660	0.001	4600	—	—		
	2-Aminoanthracene	>100	1	0.077	63	—	—	—	—		
	2-Naphthylamine	>100	1	<0.001	>4600	—	—	—	—		
	2-Aminofluorene	>100	1	<0.001	>4600	—	—	—	—		
	2-Aminochrysene	>100	1	0.001	4600	0.055	87	—	—		

K: Partition Coefficient (Concentration in A/ Concentration in B)

N: Number of times required for extracting 99% or more of a compound from B phase to A phase

Table 2. Contents of polynuclear aromatic hydrocarbons in gasoline

Sample No.	Pyrene Mean C.V.	Fluoranthene Mean C.V.	Chrysene Mean C.V.	Benz(a)anthracene Mean C.V.	Benzo(a)pyrene Mean C.V.	Benzo(k)fluoranthene Mean C.V.	Perylene Mean C.V.	Anthracene Mean C.V.	Benzo(ghi)perylene Mean C.V.
1	2.9*	1.4*	0.24	0.20	0.05*	0.04	0.02	0.02	0.25
2	5.8*	2.2*	0.75	0.40	0.18*	0.09	0.06	0.04	0.74
3	14.6*	2.6*	0.58	0.20	0.16*	0.02	0.01	0.04	1.09
4	4.8	1.3	0.38	0.28	0.19**	0.05	0.02	0.05**	0.52
5	11.4	2.8	0.93	0.64	0.32	0.09	0.06	0.05	1.07
6	2.5	1.0	0.34	0.22	0.12	0.06	0.03	0.03	0.28
7	16.4	0.6	0.56	0.25	0.22	0.03	0.02	0.05	1.36
8	1.3	2.3	0.11	0.10	0.05	0.03	0.01	0.02	0.13
1	4.6*	1.8*	0.54	0.34	0.06*	0.07	0.03	0.03	0.38
2	10.6*	4.1*	1.07	0.46	0.25*	0.11	0.08	0.08	0.80
3	17.1*	2.9*	0.79	0.26	0.17*	0.02	0.01	0.04	1.65
4	3.4	3.5	0.45	0.39	0.15*	0.04	0.01	0.03**	0.39
5	16.9	1.7	1.31	1.14	0.50	0.15	0.10	0.11	1.22
6	3.4	0.5	0.50	0.29	0.18	0.09	0.03	0.05	0.43
7	20.0	0.8	0.86	0.35	0.35	0.04	0.02	0.09	2.00
8	14.3	3.7	1.28	1.00	0.56	0.23	0.11	0.22	1.64

Mean of 4 determinations, * Mean of 3 determinations, ** Mean of 7 determinations,

C.V.: Coefficient of variation (%)

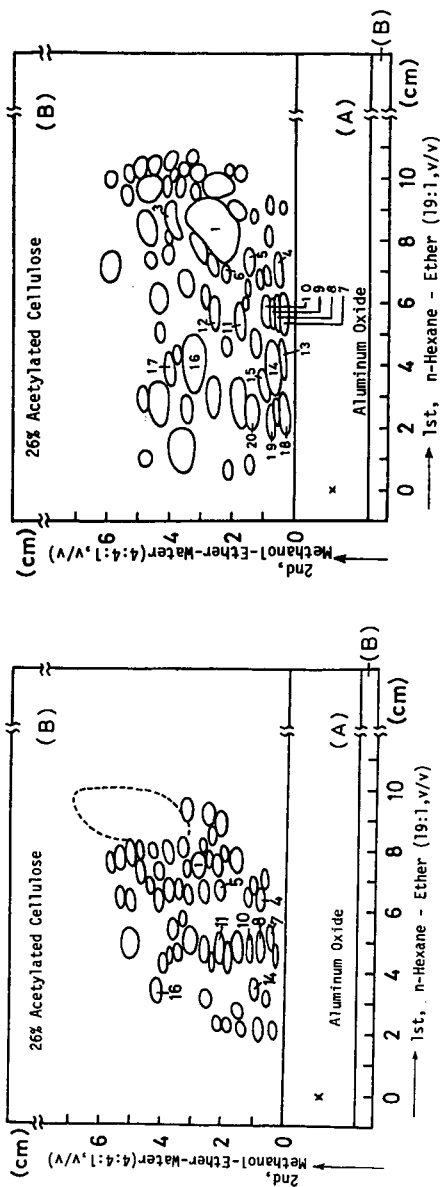


Fig. 1. Two dimensional dual band thin-layer chromatograms of the benzene extracts from heavy oil C (left) and ethylene bottom oil (right)

Identified polynuclear aromatic hydrocarbons and their spot numbers: pyrene and fluoranthene (spot 1), methyl derivatives of pyrene and fluoranthene (3), chrysene (4), benz(a)anthracene (5), benzo(b)fluorene (6), benzo(a)pyrene (7), benzo(b)fluoranthene (8), benzo(j)fluoranthene (9), benzo(k)fluoranthene (10), perylene (11), benzo(e)pyrene (12), anthanthrene (13), indeno(1,2,3-cd)pyrene (14), benzo(b)chrysene (15), benzo(ghi)perylene (16), coronene (17), dibenzo(a,h)pyrene (18), dibenzo(a,i)pyrene (19), and tribenzo(a,e,i)pyrene (20).

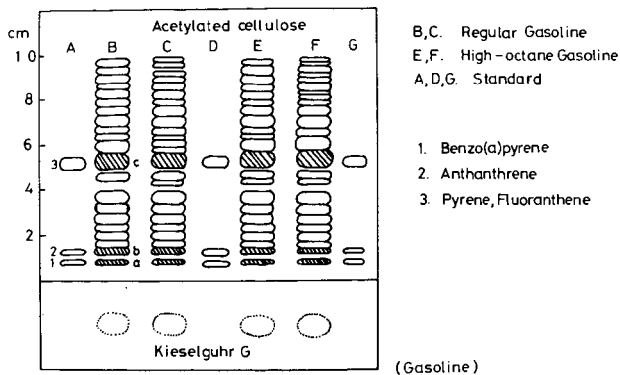


Fig. 2. One dimensional dual band thin-layer chromatogram of gasoline

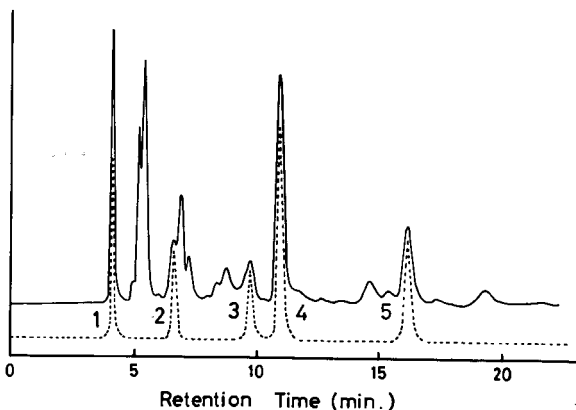


Fig. 3. High speed liquid chromatograms of the liquid-liquid partition extract from gasoline (—) and standard solution having 16 PAH

Column: Zorbax ODS (4.6mm x 25cm), Mobile phase: Methanol-Water (85:15,v/v), Detector: Spectrofluorometer (excitation 370nm, emission 410nm), 65°C, 1100psi.
 1. anthracene, 2. 9-phenylanthracene, 3. benzo(k)fluoranthene, 4. benzo(a)pyrene, 5. benzo(ghi)perylene
 Standard solution is a mixture of 1 - 5 PAH, naphthalene, fluorene, 3,4-benzofluorene, fluoranthene, chrysene, 7-ethylchrysene, benz(a)anthracene, 7-methylbenz(a)anthracene, perylene, benzo(b)fluoranthene and benzo(e)pyrene.

TRACE ELEMENT DISTRIBUTIONS IN COAL GASIFICATION PRODUCTS

D.W. Koppelaar*, H. Schultz, R.G. Lett, F.R. Brown, H.B. Booher, and E.A. Hattman

Pittsburgh Energy Technology Center
U.S. Department of Energy
Pittsburgh, PA 15213

and

S.E. Manahan

Department of Chemistry
University of Missouri
Columbia, MO 15201

INTRODUCTION

The determination of the fate and distribution of trace elements during coal conversion is an important and prerequisite task if such an industry is to be implemented on a massive scale. Considering the overwhelming abundance of native coal resources, an implementation of this magnitude is a distinct possibility in the near future. Coal gasification is currently under investigation by many organizations in the U.S. as an alternative source of environmentally acceptable fuels. In conjunction with ongoing coal gasification studies at this laboratory, trace element investigations have been performed to help assess potential environmental impacts of coal gasification processes. This work presents preliminary findings of trace and minor element distributions in the process streams of the SYNTHANE Gasifier Process Development Unit located at this laboratory.

EXPERIMENTAL

Three separate gasification runs were made with the SYNTHANE Gasifier PDU using Montana sub-bituminous 'C' coal. The SYNTHANE Gasifier characteristics and operating conditions have been described previously (1-3). Maximum average temperatures attained in this unit are typically 950-1000°C. A schematic diagram of the PDU is presented in Figure 1.

An integral part of this study was the sampling of the process streams of the gasification unit. Samples collected for subsequent analysis included the feed coal and feed water (major input streams) and gasifier char, filter fines, and condensable water and tars (major output streams). Sampling points in the PDU are illustrated in Figure 1. The feed coal was systematically thieved during the loading of the gasifier hopper in order to obtain representative samples of this process stream. Feed water (for generation of process steam) was also periodically sampled during the gasification runs. The gasifier char, condensable tars and water, and particulate matter from the gas product stream were collected after each run. The weights of the process streams sampled are reported in Table 1. Also shown are the weight percentages that the samples represent relative to the total amount of the process stream consumed or produced. In most cases, the entire process stream was collected. This procedure ensured representative sampling of these process streams.

Considerable efforts were required to homogenize these samples. The solid process streams were riffled, ground and further comminuted to manageable sizes. In some cases, further grinding to -325 mesh was required. Condensate water analytical samples were taken while vigorously stirring the bulk sample. The con-

*Present address: Institute for Mining and Minerals Research, Kentucky Center for Energy Research Laboratory, University of Kentucky, Lexington, Kentucky 40583

densate tar process stream presented unique sampling problems. This process stream consists of organic and aqueous phases, in addition to a considerable amount of solid material. Due to the immiscibility of these phases, it was not possible to withdraw homogenous samples by merely mixing the process stream. This problem was overcome by adding tetrahydrofuran to the sample to render the various phases miscible.

Samples were analyzed by spark-source mass spectrometry (SSMS) and atomic absorption spectrophotometry (AAS). Approximately 65 elements were semi-quantitatively determined in each process stream by SSMS 'survey' analyses. The feed coal, char, and filtered particular matter process streams were low-temperature ashed, mixed with high purity graphite, and formed into electrodes. Unashed samples were also analyzed for the determination of volatile elements. Aqueous and wet-ashed samples were mixed with graphite and gently dried under an infrared lamp. Photoplate detection was utilized with computer assisted quantitation by means of the Hull equation (4). Figure 2 illustrates a typical SSMS 'survey' analysis of the feed coal process stream. Such analyses are generally accurate to within a factor of three and are especially valuable for the complete inorganic characterization of these process streams.

Isotope dilution spark-source mass spectrometric (ID-SSMS) determinations were also performed. Samples were solubilized by means of Parr acid digestion bombs (5-7) after addition of enriched isotopes. Elements of high environmental interest (Ni, Cu, Se, Cd, Pb, and Tl) were preconcentrated by means of electrodeposition onto high-purity gold electrodes. These electrodes were then sparked in the spectrometer. Quantitation was accomplished using the isotope dilution equation of Paulsen (8-10). Results of ID-SSMS measurements on the three solid process streams are presented in Table 2. Quadruplicate analyses were made, with the precision of such measurements ranging from 2-15% (relative standard deviation).

Atomic absorption determinations of seven elements (Mn, Ni, Cu, Cr, As, Pb, and Cd) were also made. Samples were solubilized by means of high temperature ashing and lithium metaborate fusion for the determination of Mn, Ni, Cu, and Cr (11). Digested sample solutions were aspirated into the atomic absorption spectrometer and quantitated by the method of standard additions. Pb and Cd were preconcentrated by extracting their iodide complexes into methyl isobutyl ketone (MIBK) prior to aspiration into the spectrometer. Arsenic was determined using hydride evolution AAS after wet-ashing of the samples. Results of the AAS determinations of the solid process streams are shown in Table 3. The precision of these determinations ranged from 2-20% r.s.d.

DISCUSSION

All process streams were surveyed for approximately 65 elements by conventional SSMS analyses. Such analyses, although semi-quantitative, provide quick multi-element analyses that are valuable when the inorganic composition of the process streams are unknown and/or unsuspected. This type of analysis is especially useful for process monitoring applications, resulting in an almost complete inorganic characterization of process streams from such a conversion unit. This kind of characterization is especially useful in delineating potential problems and pointing out the need for more accurate analyses of specific elements. As an example of the kind of information that can be extracted from such data, an enrichment ratio can be calculated for various elements based on their concentrations in the filter fines process stream relative to their concentrations in the feed coal (after correcting for the varying ash contents in the two process streams). Table 4 presents the enrichment ratios for a number of elements. An enrichment ratio of unity indicates no enrichment, while ratios greater than unity indicate enrichment in the filter fines process stream. If an enrichment ratio of three or greater is assumed to be significant (to take into account the uncertainty limitations of the technique), then elements can be classified as either enriched or not enriched. Table 4 shows that many elements are shown to be enriched to a great degree. Presumably, such enrichment is due to a volatilization of these elements in the

high temperature zone of the reactor and subsequent condensation of these volatilized elements in the cooler sections of the gasification unit. Although such a mechanism has been shown to be operative in high temperature coal combustion (12-13), this may be the first work showing such a mechanism to be operative during coal gasification. Preliminary SSMS analyses of size-separated filter fines fractions substantiates this finding.

Both the SSMS survey results and the more accurate, precise results obtained by ID-SSMS and AAS show the gasifier char to be the major elemental 'sink' for most elements. This has important environmental ramifications in that this material may be utilized as a combustion material for production of process steam. The fate of the environmentally important elements during this combustion will need to be determined. On the other hand, if the char is disposed of as an alternative to its by-product utilization, significant solid waste problems will almost certainly occur.

Selenium, as determined by ID-SSMS, showed a distribution among the process streams that was markedly different from the bulk of the other elements studied. The major elemental sink for Se was the condensate water process stream. Significant quantities of this element were also found in the condensate tar. This finding can be rationalized in terms of the high volatility of this element. Arsenic, as determined by AAS, does not exhibit such behavior, in contrast to what one might expect for this element. The major sink for this element is the gasifier char. This fact seems to indicate that the arsenic is present in the coal in a non-volatile form and that it is not converted to a volatile form during the gasification process.

Mass balances of elements across a conversion unit may be valuable in predicting the release rates of certain elements to the environment. Such balances can be calculated knowing the concentration of the element in each process stream and the mass of the respective process stream. Mass balances of 100% at the trace level are generally exceedingly difficult to obtain in such complex, open systems as a gasification reactor. Results of such mass balances are shown in Table 5. The data were calculated using the AAS and/or the ID-SSMS concentration values for the elements in the major process streams. The data indicate that the bulk of most elements (Cu, Ni, Mn, Pb, Cr) are being retained within the unit. However, other elements cannot be fully recovered (i.e., Cd and Se) and careful considerations of the fate of these elements must be made in view of their environmental and toxicological hazards.

ACKNOWLEDGMENT

One of the authors (D.W.K.) gratefully acknowledges support from Oak Ridge Associated Universities in the form of a Laboratory Graduate Participantship at the Pittsburgh Energy Technology Center.

REFERENCES

1. Gasior, S.J., R.G. Lett, J.P. Strakey, W.P. Haynes. ACS Div. Fuel Chem. Preprints, 23, (2), 88 (1978).
2. Gasior, S.J., A.J. Forney, W.P. Haynes, R.F. Kenny. Chem. Eng. Prog., 71 89 (1975).
3. McMichael, W.J., et. al. "Synthane Gasifier Effluent Streams", PERC/RI-77/4, 1977.
4. Hull, C.W. Proc. 10th Ann. Conf. Mass Spectrom. Allied Topics, New Orleans, LA, 1962.
5. Bernas, B. Anal. Chem., 40, 1682 (1968).

6. Hartstein, A.M., R.W. Friedman, D.W. Platter. Anal. Chem., 45, 611 (1975).
7. Bulletin No. 4745. Parr Instrument Co., Moline, Ill., 1976.
8. Paulsen, P.J., R. Alvarez, D.E. Kelleher. Spectrochim. Acta, 24B, 535 (1969).
9. Alvarez, R., P.J. Paulsen, D.E. Kelleher. Anal. Chem., 41, 955 (1969).
10. Paulsen, P.J. In: NBS Special Publication 492, U.S. Gov't. Printing Office, Washington, D.C., 1977, p. 33-47.
11. Schultz, H., et. al. "The Distribution of Some Trace Elements in the 1/2 Ton Per Day Synthoil Process Development Unit". PERC/RI-77/2, Pittsburgh Energy Research Center, Pittsburgh, PA, 1977.
12. Davison, R.L., D.F.S. Natusch, J.R. Wallace, C.A. Evans, Jr. Env. Sci. Tech., 8, 1107 (1974).
13. Campbell, J.A., J.C. Laul, K.K. Nielsen, R.D. Smith. Anal. Chem., 50, 1033 (1978).

Table 1

Description of Sample Sizes Taken from SYNTHANE Process Development Unit
for Trace Element Studies

<u>Sample</u>	<u>Run Number</u>		
	<u>293</u>	<u>294</u>	<u>295</u>
Feed Coal, kg	7.7 (11.0) ¹	5.9 (8.0)	6.1 (8.6)
Feed Water, kg	4.9 (5.4)	4.2 (4.8)	4.2 (4.4)
Gasifier Char, kg	17.0 (100)	16.9 (100)	17.0 (100)
Condensate Tar/Water, kg	14.6 (100)	15.5 (100)	15.2 (100)
Condensate Water, kg	52.8 (100)	53.1 (100)	53.5 (100)
Filter Fines, kg	0.4 (100)	0.4 (100)	0.5 (100)
Product Gas, kl	1.7 (1.5)	1.7 (1.4)	1.6 (1.4)

¹Data in parentheses indicate the percentage of the process stream that was taken for preparation and analysis.

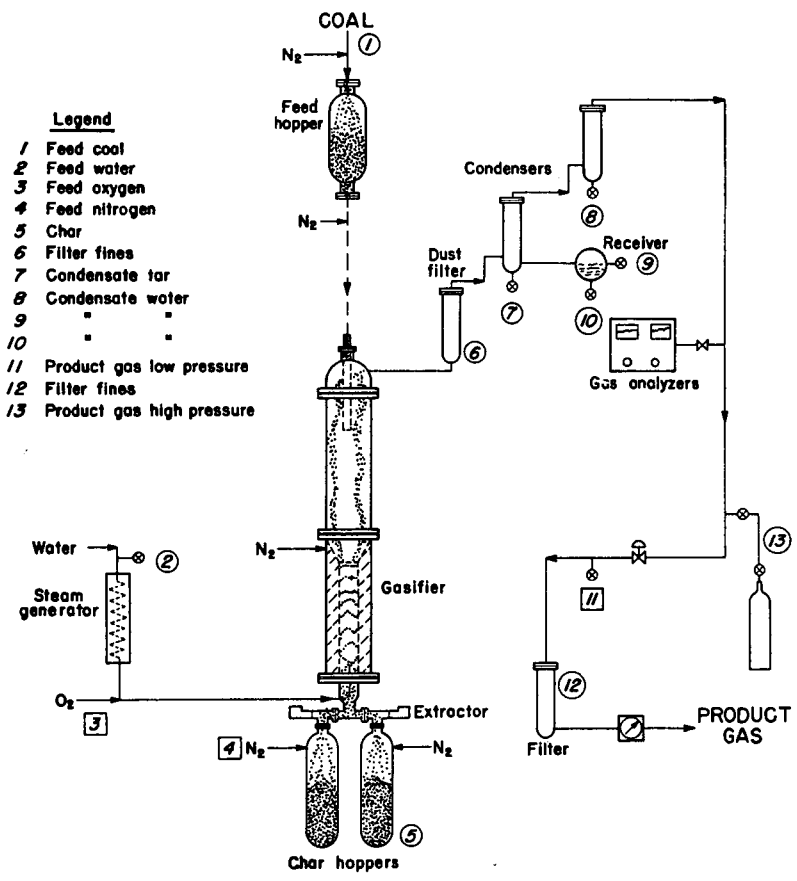


Figure 1 Sampling points on the PETC SYNTHANE Process Development Unit.

Table 2 - Element Concentrations (ppm, wt.) in Gasifier Samples by ID-SSMS Analysis

<u>Sample</u>	<u>Element</u>	<u>Run Number</u>		
		<u>293</u>	<u>294</u>	<u>295</u>
Feed Coal	Ni	2.83	2.56	2.39
	Cu	7.50	7.52	7.24
	Se	0.56	0.54	0.54
	Cd	0.12	0.12	0.14
	Tl	0.05	0.04	0.04
	Pb	5.14	4.80	4.77
Gasifier Char	Ni	11.6	9.06	11.6
	Cu	25.5	24.2	27.8
	Se	0.14	0.21	0.19
	Cd	0.10	0.12	0.13
	Tl	0.11	0.12	0.15
	Pb	21.2	17.1	19.3
Filter Fines	Ni	10.3	11.5	10.0
	Cu	105	150	131
	Se	0.65	0.94	0.74
	Cd	2.16	2.88	1.81
	Tl	0.09	0.11	0.10
	Pb	13.7	13.5	12.47

Table 3 - Element Concentrations (ppm, wt.) in Gasifier Process Streams by AAS Analysis

<u>Sample</u>	<u>Element</u>	<u>Run Number</u>		
		<u>293</u>	<u>294</u>	<u>295</u>
Feed Coal	Cr	7.1	6.6	7.9
	Mn	547	512	646
	Ni	2.2	2.7	2.4
	Cu	10.2	9.7	10.4
	As	1.6	1.5	2.0
	Cd	0.07	0.07	0.09
	Pb	5.5	4.6	5.3
	Cr	32.4	33.5	30.3
Gasifier Char	Mn	2510	2350	2430
	Ni	10.8	8.5	8.0
	Cu	33.0	23.8	27.0
	As	6.3	6.0	5.7
	Cd	0.06	0.05	0.05
	Pb	19.6	18.2	18.9
	Cr	12.4	18.5	20.7
	Mn	519	530	503
Filter Fines	Ni	10.0	12.5	10.6
	Cu	114	154	142
	As	9.1	7.9	11.0
	Cd	1.86	2.25	1.75
	Pb	14.1	13.8	15.6

Table 4 - Enrichment Ratios (E_r) for Various Elements

<u>Non-Enriched Elements</u>		<u>Enriched Elements</u>	
<u>Element</u>	<u>E_r</u>	<u>Element</u>	<u>E_r</u>
Na	2.0	K	3.1
Mg	2.7	Rb	6.5
Al	1.0	Co	4.1
Si	1.2	Ni	3.0
Ca	0.8	Zn	7.0
Ti	1.1	Cu	9.3
Zr	2.9	Ga	4.7
Fe	0.8	Ge	11.0
Cr	1.6	As	6.2
Be	2.4	Br	11.0
Sr	1.2	Sn	3.3
Ba	1.1	Sb	5.7
Hf	1.5	I	14.0
Gd	0.8	Mo	7.3
		Pb	3.8
		Cd	6.5

Table 5 - Elemental Mass Balances

<u>Element</u>	<u>Mass Balance, %</u>		
	<u>293</u>	<u>294</u>	<u>295</u>
Cu (ID-SSMS)	103	92	110
Cr (AAS)	112	118	96
Ni (AAS)	122	75	85
Se (ID-SSMS)	45	44	46
Cd (AAS)	36	35	27
Cd (ID-SSMS)	36	46	33
Pb (ID-SSMS)	102	84	101
Pb (AAS)	88	92	89
As (AAS)	99	95	74

The Effect of Trace Element Associations and
Mineral Phases on the Pyrolysis Products from Coal

J. K. Kuhn, R. A. Cahill, R. H. Shiley, D. R. Dickerson and C. W. Kruse

Illinois State Geological Survey
Urbana, IL 61801

The initial mode of occurrence of trace and minor elements in coal influences their ultimate fate during the processing and/or utilization of coal materials. A float-sink procedure and an acid-leaching procedure have been developed independently and used to estimate the trace and minor element associations with the organic and mineral phases in coal. Values obtained by the two methods were in agreement within the limits of analytical error. Ion exchange studies and internal surface area studies indicated that major differences that were observed could be explained in terms of exchangeable and/or chelated elements on the exposed surfaces of the coal. When these two factors were considered, results from these two methods were sufficiently reliable to allow their values to be used as indicators of an element's organic association.

Representative data for 50 elements from 9 coals are presented for both methods. The mean values for the same elements determined in the acid demineralized coals are given for 27 coals from 3 geographical areas. These values were compared to elemental values for crustal abundance and plant material; only S, Se, and Te had concentrations of organically associated elements significantly in excess of Clarke values (by factors of 20 to 50). Other elements, such as Pb, varied from virtually no organic association, to those, such as Ga, which averaged about 40 to 50 percent organic association.

Although many elements had some organic association, the major amounts of accessory elements in coal were present in the mineral phases. Semiquantitative mineral analysis of the low-temperature ashes (plasma ashing at $<150^{\circ}\text{C}$) was performed on the coals; clay, ranging from 20 to 80 percent and a mean of about 50 percent, was the predominant mineral phase in the inorganic fractions. The sulfide minerals were second and carbonates generally were the third most abundant mineral phase. In any particular coal, however, this order may be mixed or even inverted. Also frequently present in the coals is quartz and many other minerals in lesser amounts.

The mobilities during pyrolysis of the various elements were determined at 450°C , 600°C , and 700°C through the use of both batch and continuous-feed processes. This range in temperature was selected in order to produce chars with minimum sulfur content and with both maximum and minimum surface areas. The coals reached their most plastic (fluid?) state within this temperature range.

The concentrations of 50 elements were determined in 6 whole coals, also their corresponding char residues and condensed volatile products. For most of the coals studied, the data showed significant increase in mobility (volatilization) during pyrolysis for P, Cl, S, As, Br, I, Se, Te, and Zn. Elements that exhibited less significant mobility included Cd, Cr, Cu, Dy, Ga, Hf, La, Li, Pb, Sb, Sc, Sm, U, and Y. Those elements that generally exhibited no mobility during pyrolysis included Si, Al, K, V, Mg, Ca, Fe, Na, Ti, Ba, Ce, Co, Cs, Eu, Lu, Mn, Ni, Rb, Sr, Ta, Tb, and Th. Because of their extremely low concentrations, elements such as Ag, Au, In, Mo, W, and Sn were generally not detected at levels where any reasonable conclusions could be drawn.

Correlation of element mobility and organic association showed that elements associated with the organic material were the same elements that showed losses during pyrolysis. Two exceptions to this general rule were: (1) The alkali and alkaline earth elements generally were not lost during pyrolysis. These same elements were usually present to some extent in an exchangeable ion form and often showed a very high organic association. (2) The group of primarily sulfide elements, which include Pb, Zn and As, normally showed little or no organic association. The mechanism for mobility probably involved a thermal breakdown of the mineral itself. Iron usually occurred as the predominant sulfide mineral, but it was immobile.

The dissociation of pyrite when heated in a reducing atmosphere is well known. In coal, however, this reduction of pyrite to pyrrhotite takes place at relatively low temperatures, occurring at less than 450°C. During this process, two types of pyrrhotite were produced, one of which had magnetic properties. The material formed was susceptible to either chemical or magnetic cleaning. Mössbauer spectroscopy was used to identify four species of Fe^{+2} in the chars, only two species have been identified similarly in the raw coal.

The condensed volatile components from the pyrolysis of the coal were analyzed further to determine the organic composition of the products. Separation of the condensed organics into acid, base, and neutral fractions indicated that the components in the acid fraction predominated at the lower pyrolysis temperatures, and the components contained in the base fraction predominated at the higher temperatures. The distribution of constituents making up the organic fractions were shown to be strongly influenced by the temperature at which the pyrolysis was conducted. Furthermore, removal of virtually all of the mineral phases from the coal prior to heating significantly altered the proportion of tar to light fractions in the product; much less tar was produced when mineral phases were absent.

Correlations of mineral-phase content and the distribution of organic fractions at a given temperature indicated that the temperature at which the process was operated had a dominant effect on the product composition; nevertheless, the composition also was affected significantly by the kinds of mineral phases present. Individual effects of minerals on the distribution of organic constituents in condensed pyrolysis products are still being studied, but it is evident that knowledge of the organic associations and mineral phases present in an individual coal is necessary before a satisfactory evaluation of coal performance during utilization can be made.

Chemical and Mineralogical Characterization of Coal Liquefaction Residues

G. B. Dreher, Suzanne, J. Russell, and R. R. Ruch

Illinois State Geological Survey, Natural Resources Bldg., Urbana, Illinois 61801

The Illinois State Geological Survey, with support from the U.S. Department of Energy, is characterizing the residues from several advanced-stage coal liquefaction processes. Coal liquefaction in plants of commercial size, if developed on a large scale, will eventually result in the production of large tonnages of waste materials. It is desirable to know the compositions of these residues for possible evaluation as sources of valuable metals and also to know whether they are potential environmental hazards. A major objective of this project is to determine whether the residues from several coal liquefaction processes consistently contain recoverable amounts of valuable elements and can, therefore, be reliably classified as potential secondary source reserves for these elements. In this study the concentration levels of some 70 major, minor, and trace constituents have been determined and, where possible, the mineralogy for certain elements has been ascertained. An economic evaluation of the data will be made. The chemical and mineralogical data will aid in predicting the behavior of various elements during certain liquefaction processes.

Sampling and pretreatment. The processes from which samples were obtained are Clean Coke at United States Steel Research, Monroeville, PA; H-Coal, Hydrocarbon Research, Inc., Trenton, NJ; Lignite Project, University of North Dakota, Grand Forks, ND; Solvent Refined Coal, Southern Company Services, Wilsonville, AL (SRC-Ala); Solvent Refined Coal, Pittsburgh and Midway Coal Company, Ft. Lewis, Wash. (SRC-Wash); and Synthoil, Pittsburgh Energy Research Center, Bruceton, PA. In addition, one residue sample from the COED process has been obtained and analyzed. Each of these processes has been described elsewhere (1). Seventy constituents have been determined in 18 sample sets consisting of feed coal, corresponding residue, and where available, product material. The residues as we have received them are not envisioned to be the ultimate waste products; further processing of the materials beyond that which was being conducted when the samples were taken is anticipated for most processes.

The following coals have been used in the sample sets studied: feed coals from the Herrin (No. 6) coal of Illinois; composite samples of No. 9 and No. 14 coal beds and No. 9, No. 11, No. 12, and No. 13 coal beds of western Kentucky; the Pittsburgh No. 8 coal; Wyodak seam from Wyoming; and a lignite from North Dakota.

Residue samples from the liquefaction processes are often intractable mixtures of product oil, partially reacted coal, and unreacted coal. To produce samples that are more easily handled, more homogeneous, and convenient to use in low-temperature ashing procedures, the product oil portion was separated from the mineral matter portion by extraction with tetrahydrofuran (THF). The unextracted residues, however, have been found to be generally homogeneous, and the extracted residues have primarily been used in producing low-temperature (150°C) ashes for mineralogical analyses. The high temperature ash contents of the unextracted ash samples compare favorably with those recovered from the THF soluble and insoluble portions for most samples, indicating that the samples are fairly homogeneous with respect to ash content.

Methods of analysis. The analytical techniques used (shown in Table 1) are atomic absorption spectrometry (AA), instrumental neutron activation analysis (INAA), direct-reading optical emission spectrometry (OED), photographic optical emission spectrography (OEP), energy dispersive X-ray fluorescence spectrometry (XES), wavelength dispersive X-ray fluorescence spectrometry (XRF), radio-chemical separation followed by neutron activation analysis (RC), ion selective electrode (ISE), and standard ASTM methods (ASTM). Mineralogical studies were made by X-ray diffraction analysis and scanning electron microscopy using low-temperature ash samples prepared in an activated oxygen plasma asher. These methods have been described elsewhere (2). Sample pretreatment is summarized in Figure 1.

Results and discussion. All results on "as received" feed coal and residue samples were corrected for moisture and calculated to the 500°C ash basis. It was assumed that (a) the oxidized inorganic material (the 500°C ash) from a feed coal is comparable to that from the corresponding residue, and (b) that the feed coal sample is representative of the coal used to generate a particular residue. When the ash-basis data for a residue is compared to that for the feed coal, an indication is given as to whether an element is lost, retained, or possibly increased during the liquefaction processes. The "ash-basis" data are used to calculate the percentage of change of each element for which data are available.

Ranges for estimating whether an element was retained were calculated by taking into account an average sampling error and the random error of the particular analytical method used for that element. The "retention range" for an element is arbitrarily defined as twice the overall standard deviation of possible errors in analysis of the feed coal and residue. An element is indicated as having undergone a gain if results for that element exhibit a percentage of change (residue, concentration relative to feed coal concentration on the ash-basis in a given process) which is greater than the upper limit of the retention range. Elements undergoing losses exhibit the opposite tendency. All other elements are said to have been "retained" during the liquefaction process. Figures 2 and 3 are bar graphs showing representative gain-loss data for mercury and manganese in the 18 sample sets, and Figure 4 summarizes the gain-loss data obtained for most elements detected in a SRC(Wash) set.

Some general conclusions can be drawn about the mobilities of various elements in the liquefaction processes studied. In many cases only limited conclusions are possible because of a combination of low elemental concentrations coupled with a moderate-to-high analytical uncertainty of measurement. In addition it should be emphasized that these sample sets, in most cases, represent one-time, short-interval sampling under equilibrium conditions, where possible, and may not be fully representative of long-term continuous operation.

1. Ca, S, Ti, As, B, F, Hg, La, Sc, and Zn are generally ($\geq 51\%$ of the sample sets in which the element was determined) lost during the liquefaction process. Dy, Eu, Tb, and Yb are lost or retained in the liquefaction processes in approximately equal numbers.
2. Most of the elements determined show general retention during the liquefaction processes. These are: Fe, K, Si, Ba, Be, Br, Ce, Cl, Co, Cr, Cs, Cu, Ga, Ge, Hf, Li, Lu, Mn, Mo, Ni, Pb, Rb, Sb, Se, Sm, Sn, Sr, Ta, Th, Tl, U, V, W, and Zr.
3. Four elements, Al, Mg, Na, and P behave randomly, exhibiting no clear pattern.
4. Observed gains, where present, most probably reflect contamination or degradation of equipment.
5. Some elements generally occur at concentrations too low to be accurately measured by the methods used and, thus are too low to be considered in the gain-loss data evaluation. These include Ag, Bi, Cd, In, Nd, Pt, Te, Au, and Pd.

In particular, three sample sets from the SRC-Ala process and two sets from the SRC-Wash process exhibit the greatest apparent losses. Elements which exhibit apparent losses in three or more of these sample sets are Al, Fe, Mg, S, Ti, As, B, Be, Br, Co, Dy, Eu, F, Hg, La, Lu, Mn, Mo, Sc, Se, Sm, Ta, Tb, Th, Yb, and Zn. Elements which exhibit increases in concentration in two or more of these five liquefaction processes are Na, P, Si, Cr, and Cs. Filtering aid materials were used in conjunction with all five SRC-Ala sample sets (Johns-Manville 7A, consisting of 92.5 percent diatomaceous earth and 7.5 percent asbestos) and the first two SRC-Wash sample sets. It is probable that at least Na, P, Si, and Cr increases are due to the filtering aids. Diatomaceous earth consists primarily of silicon dioxide and

asbestos minerals which contain the elements Na and Si among others. These materials have been detected by scanning electron microscope analysis of the SRC-Ala residues.

Mineralogical analysis. In addition to the chemical analyses, mineralogical analyses have comprised a major portion of this study. They have yielded information about the modes of occurrence of some elements and may shed some light on the behavior of certain chemical elements during the liquefaction processes.

The major mineralogical change which takes place in the liquefaction processes is the transformation of pyrite (FeS_2) in the feed coal to pyrrhotite (Fe_{1-x}S , where $x = 0. \text{ to } 0.2$) in the residue by the reaction $2\text{FeS}_2 \rightarrow 2\text{Fe}_{1-x}\text{S} + 2\text{S}$. Sulfur probably is evolved as H_2S . Pyrrhotite occurs in the residues primarily as fine-grained (crystal size about $1 \mu\text{m}$) aggregates sometimes incorporating other mineral matter. It also occurs as a fine granular layer on mineral particles.

A small amount of wollastonite, CaSiO_3 , formed by the reaction $\text{CaCO}_3 + \text{SiO}_2 \rightarrow \text{CaSiO}_3 + \text{CO}_2$, was detected by scanning electron microscopy in one residue from an H-Coal set. Some calcite particles found in the residue have a spongy texture similar to that seen in calcined carbonates (3). It appears that some dissociation of the calcite occurred, enabling a small amount of CaO to combine with SiO_2 . In a closed system, calcite, quartz, and wollastonite are stable together under the pressures and temperatures present in liquefaction process preheaters and reactors, if the CO_2 partial pressure is not appreciable (4).

A qualitative summary of mineral matter detected by X-ray diffraction analysis in feed coals and residues is presented in Table 2. An "X" indicates the presence of a mineral in a sample. A question mark indicates uncertainty in the presence of a mineral as determined from the diffraction patterns. Marcasite, a dimorph of pyrite, has been observed in only one feed coal sample. It is also transformed to pyrrhotite during liquefaction. Other minerals may be present in the samples in quantities below the detection limits.

Semi-quantitative X-ray diffraction data for quartz, calcite, pyrite, and pyrrhotite in the low temperature ash samples of several feed coals and their corresponding residues are shown in Table 3. Inclusion of quartz and calcite in pyrrhotite aggregates contributes to an apparent decrease in quartz and calcite from the feed coals to the residues. A decrease in the pyrrhotite concentration in the residue with respect to the pyrite concentration in the feed coals is due to the loss of sulfur from pyrite in the transformation to pyrrhotite. In samples which show the presence of calcite in the residues but not in the corresponding coal, calcite and some pyrite have broken down to form sulfate minerals during storage of the coal. This is a common reaction in coals exposed to moisture (5).

Conclusions. Data from the limited number of sample sets covering several liquefaction processes indicate that relatively few elements (e.g. Hg, S, As, Br, and B) are consistently lost to any significant degree from the resultant residues. Only a few mineralogical changes occur during the processes in which the transformation of pyrite to pyrrhotite most consistently occurs. These experimental observations, including the general range of elemental concentrations found in the residues, along with extensive trace element distribution data now available (2,6) from analyses of many coals from the various U.S. coal fields, will be used for an economic evaluation for many metals. Trace element concentrations for such economically significant metals such as Au, Ag, Pt, Pd, Ta, etc. in most cases will probably be too low for consideration as resources. In some cases, however, such as Zn, there are areas (7) where concentrations are high enough for serious consideration. The more abundant metals in coal--such as Al, Fe, Si, and possibly Ti--although perhaps currently not economical to extract may require attention in the future.

Acknowledgment. This work is supported in part by the U.S. Department of Energy under Contract EY-76-C-21-8004, in which Mrs. Patricia Barnes is Technical Project Officer.

References.

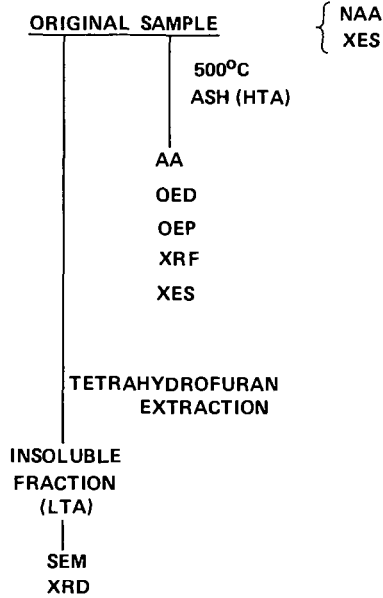
1. Energy Research and Development Administration, "Coal Liquefaction," Quarterly Report, April-June, 1976, ERDA 76-95/2 (1976).
2. Gluskoter, H. J., R. R. Ruch, W. G. Miller, R. A. Cahill, G. B. Dreher, and J. K. Kuhn: Trace Elements in Coal: Occurrence and Distribution, Illinois State Geological Survey Circular 499 (1977).
3. Harvey, R. D.: Petrographic and Mineralogical Characteristics of Carbonate Rocks Related to Sorption of Sulfur Oxides in Flue Gases, An Interim Report to the National Air Pollution Control Administration, Contract No. CPA 22-69-65, (1970).
4. Harker, R. I. and Tuttle, O. F.: Experimental Data on the P_{CO_2} -T Curve for the Reaction: Calcite + Quartz \rightleftharpoons Wollastonite + Carbon Dioxide, American Journal of Science, 254 (4), 239-256 (1956).
5. Rao, C. P. and Gluskoter, H. J.: Occurrence and Distribution of Minerals in Illinois Coals, Illinois State Geological Survey Circular 476 (1973).
6. Swanson, V. E., J. H. Medlin, J. R. Hatch, S. L. Coleman, G. H. Wood, S. D. Woodruff, and R. T. Hildebrand: Collection, Chemical Analysis, and Evaluation of Coal Samples in 1975, USGS Open File Report 76-468 (1976).
7. Cobb, J. C., J. D. Steele, C. G. Treworgy, J. F. Ashby, and S. J. Russell: The Geology of Zinc in Coals of the Illinois Basin, Final Report U.S. Department of Interior Grant 14-08-0001-G-249, August (1978).

Table 1
 Selection of Methods for Determining Various Elements
 In Coal Liquefaction Feed Coals and Residues

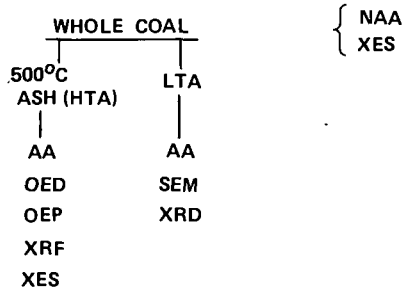
Element	AA	INAA	OED	OEP	XES	XRF	ASTM	ISE	RC	Element	AA	INAA	OED	OEP	XES	XRF	ASTM	ISE	RC
Al					X					Hf		X							
C						X				Hg									X
Ca					X					Ho									X
Fe	X	X			X					I					X				
H						X				In		X							
K		X			X					La		X							
Mg					X					Li		X							
N						X				Lu		X							
Na		X								Mn		X		X					
O					X					Mo			X						
P					X					Nd		X							
S						X				Ni	X	X	X	X	X				
Si					X					Pb		X							
Ti					X					Pd									X
Ag		X		X						Pt									X
As		X								Rb			X						
Au		X						X		Sb		X							
B			X							Sc		X							
Ba					X					Se		X							
Be				X						Sm		X							
Bi				X						Sn			X		X				
Br		X								Sr		X*	X						
Cd		X								Ta		X							
Ce		X								Tb		X							
Cl		X								Te					X				
Co		X	X	X						Th		X							
Cr		X	X							Tl			X						
Cs		X								Tm									X
Cu		X	X	X						U		X							
Dy			X							V			X	X					
Er								X		W		X							
Eu		X								Y					X				
F								X		Zn		X							
Ga		X								Zr									X
Ge			X																

*Strontium results by INAA are satisfactory above 10 ppm.

A. FLOW SHEET OF RESIDUE SAMPLE PRETREATMENT



B. FLOW SHEET OF WHOLE COAL SAMPLE PRETREATMENT



ISGS 1978

Figure 1 - Flow sheets of sample pretreatments.

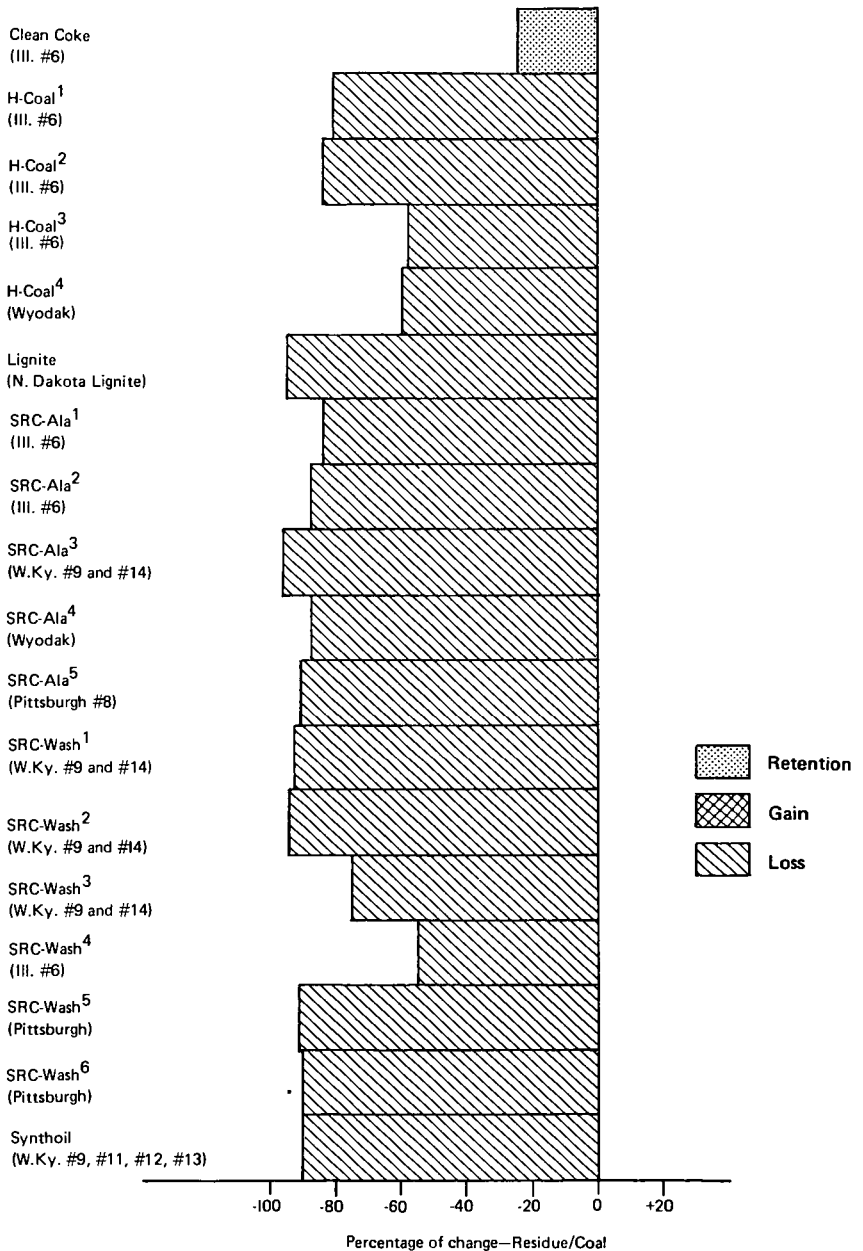
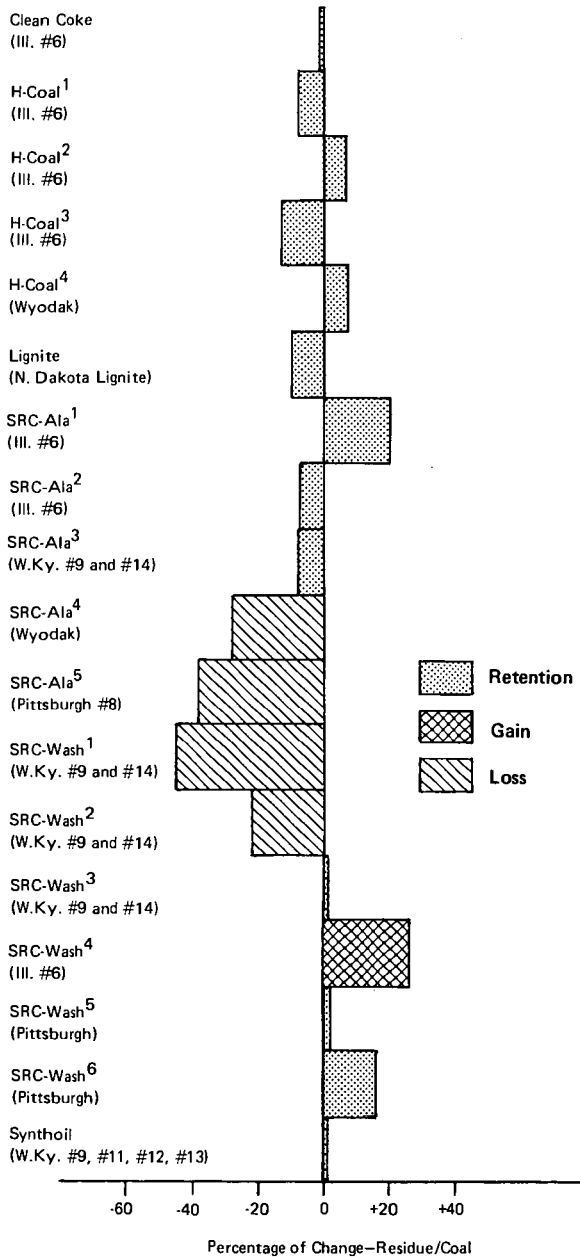


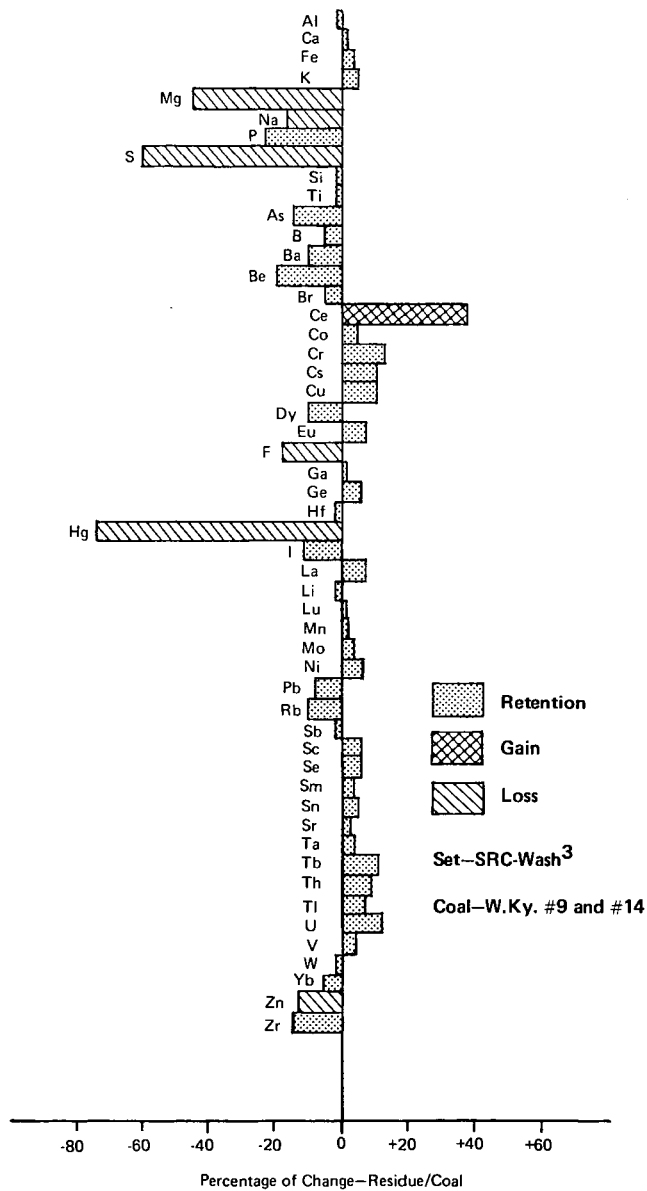
Figure 2 - Summary of percentage of change in elemental composition (500°C ash basis) for Hg in several liquefaction processes from feed coal to residue.

ISGS 1978



ISGS 1978

Figure 3 - Summary of percentage of change in elemental composition (500°C ash basis) for Mn in several liquefaction processes from feed coal to residue.



ISGS 1978

Figure 4 - Summary of percentage of change in elemental composition (500°C ash basis) from feed coal to residue.

Table 2

Mineral Matter Detected in Low Temperature Ash
of Liquefaction Samples by X-ray Diffraction Analysis

Lab No.	Sample Set	Anhydrite	Bassanite	Calcite	Coquimbite	Feldspar	Gypsum	Illite	Jarosite	Kaolinite	Marcasite	Pyrite	Pyrrhotite	Quartz
C-19660	Clean Coke			X				X		X		X		X
C-19661A		X	X	X		X		X		X			X	X
C-18903	H-Coal 1	X		X	X			X		X		X		X
C-18941A		X		X				X		X			X	X
C-19194	H-Coal 2	?		X	X			X		X		X		X
C-19196A		?		X		X		X		X			X	X
C-19916	H-Coal 3			X	?					X		X		X
C-19917A		X		X				X	?	X			X	X
C-20021	H-Coal 4		X	X						X		X		X
C-20022A			X	X		X		X		X			X	X
C-19590	Lignite		X	X								X		X
C-19591			?	X		X							?	X
C-19702	SRC-Ala 1			X				X		X		X		X
C-19703				X			X	X		X		?	X	X
C-19705	SRC-Ala 2	X			X	?		X	X	X				X
C-19706		?		X						X		X	X	X
C-19708	SRC-Ala 3				X					X		X		X
C-19709						X		X	X	X		X	X	X
C-19711	SRC-Ala 4	X	X							X		X		X
C-19712				X			X			X				X
C-19714	SRC-Ala 5		X	X		X		X		X		X		X
C-19715						X	X			X			X	X
C-19141	SRC-Wash 1				X					X	X	X		X
C-19142A								X		X			X	X
C-19488	SRC-Wash 2			?				X	X	X		X		X
C-19487		X						X	?	X			X	X
C-19899	SRC-Wash 3	X		X	X			X		X		X		X
C-19902A		X		X		X		X	X	X			X	X
C-20014	SRC-Wash 4			X				X		X		X		X
C-20015A				X				X		X			X	X
C-20016	SRC-Wash 5	X	X	X		X		X	X	X		X		X
C-20017A				X		X		X		X			X	X
C-20019	SRC-Wash 6	?					?	X	X	X		X		X
C-20020A				X				X	?	X			X	X
C-19276	Synthoil			X	X			X		X		X		X
C-19349A				X		X		X		X		X	X	X

Table 3

Average Percentage of Principal Minerals by X-Ray Diffraction
in Low Temperature Ash of Liquefaction Samples

Lab No.	Sample Set	Sample Type	Average Mineral Percentages, by weight, ± 7.5%, absolute			
			Quartz	Calcite	Pyrite	Pyrrhotite
C-19660	Clean Coke	Coal	21	11	19	N.D.
C-19661A		Residue	15	3	N.D.	16
C-18903	H-Coal 1	Coal	22	13	22	N.D.
C-18941A		Residue	17	8	N.D.	15
C-19194	H-Coal 2	Coal	22	9	25	N.D.
C-19196A		Residue	16	4	N.D.	18
C-19916	H-Coal 3	Coal	15	4	22	N.D.
C-19917A		Residue	14	5	N.D.	20
C-20021	H-Coal 4	Coal	11	*	9	N.D.
C-20022A		Residue	10	12	N.D.	*
C-19590	Lignite	Coal	7	*	10	N.D.
C-19591		Residue	12	28	N.D.	*
C-19702	SRC-Ala 1	Coal	22	3	21	N.D.
C-19703		Residue	15	<1	N.D.	13
C-19705	SRC-Ala 2	Coal	18	N.D.	N.D.	N.D.
C-19706		Residue	12	5	N.D.	12
C-19708	SRC-Ala 3	Coal	13	N.D.	23	N.D.
C-19709		Residue	13	N.D.	7	7
C-19711	SRC-Ala 4	Coal	16	*	6	N.D.
C-19712		Residue	16	12	N.D.	N.D.
C-19714	SRC-Ala 5	Coal	12	6	16	N.D.
C-19715		Residue	9	1	N.D.	10
C-19141	SRC-Wash 1	Coal	8	N.D.	39	N.D.
C-19142A		Residue	7	N.D.	N.D.	27
C-19488	SRC-Wash 2	Coal	9	N.D.	37	N.D.
C-19487		Residue	7	N.D.	N.D.	17
C-19899	SRC-Wash 3	Coal	18	2	29	N.D.
C-19902A		Residue	16	1	N.D.	20
C-20014	SRC-Wash 4	Coal	18	4	26	N.D.
C-20015A		Residue	15	3	N.D.	17
C-20016	SRC-Wash 5	Coal	16	5	21	N.D.
C-20017A		Residue	14	3	N.D.	19
C-20019	SRC-Wash 6	Coal	15	N.D.	22	N.D.
C-20020A		Residue	11	3	N.D.	14
C-19276	Synthoil	Coal	15	7	27	N.D.
C-19349A		Residue	13	6	N.D.	22

*Mineral present, but cannot be quantified due to the interference of other mineral peaks.

N.D. = Not Detected

The Development and Application of a Non-Dispersive X-ray Sulfur Analyzer with Mechanisms for Non-linear Approximation and for All Other Matrix Effect Corrections

Akiyoshi Masuko*, Fumio Imai* and Toyotsugu Yamano**

*Nippon Oil Company Ltd., Central Technical Research Laboratory
8, Chidoricho, Nakaku, Yokohama 231, Japan

**Rigaku Corporation, Osaka
14-8, Akaouji, Takatsuki 569, Japan

Introduction

Precise determination of sulfur contents in fuel oils has become more important for quality control by refineries and quality monitoring by environmental agencies.

Of the many test methods used for determining sulfur contents in fuel oils, the bomb method (ASTM D 129) is considered to be the world-wide standard. However, this method requires several hours running time, and the results can vary greatly depending upon the skill of the analyst running the test.

A rapid and exact method is required to routinely analyze sulfur contents in fuel oils, and the method should be easy to operate and to maintain. To meet these requirements, non-dispersive x-ray sulfur analyzers which utilize either a radioisotope such as ^{55}Fe or a small x-ray tube as the fluorescent x-ray generator have been developed by many manufacturers. This kind of analyzer is reportedly superior in terms of speed, accuracy, economy and ease of operation and maintenance as compared to a combustion method such as the bomb method (1). However, the accuracy of the results in the x-ray method cannot be better than that of the standards with which the unknowns are compared. Also, it was found during our research that fairly large errors can arise from the following items. (It should be noted, however, that these errors, though large, rarely exceed the allowable errors cited in ASTM methods):

- (i) Peak overlapping between the S-KX spectrum and Cl-KX spectrum,
- (ii) The use of a linear approximation for the working curve, and
- (iii) Differences in composition between the standards and the unknowns, especially in the carbon-hydrogen weight ratio (C/H) of the hydrocarbon portion of these oils.

With respect to item (i), most manufacturers have already solved the problem. The most straightforward way of doing this is by inserting a sulfur-containing film between the sample and the x-ray detector, since the Cl-KX spectrum is filtered out by such film. However, other methods have also been successful.

The error due to item (ii), can be reduced by narrowing the interpolation range of the standards to be used for the calibration. In fact, many laboratories where sulfur contents of the samples to be analyzed are limited to a certain range can apply the linear approximation without noticeable loss of accuracy. However, in analyzing samples which spread over a wide range of sulfur contents, recalibrations should be made several times a day so that the working range of the approximation is small enough to insure the accuracy desired. The recalibration itself is very troublesome for analysts in routine analysis.

With respect to item (iii), the error can be corrected either theoretically or experimentally if the compositions of both the standards and the samples are known. However, it is tedious to determine these compositions.

To correct these errors automatically, a new type of analyzer was developed. In this paper, the improvements in this analyzer compared to the prototype (Rigaku Sulfur-X) will be reported. In addition to this, the results of tests on a variety of samples will also be described.

Instrument

The non-dispersive x-ray sulfur analyzer discussed in this paper consists of the prototype plus additional components as described below. Figure 1 is a schematic diagram of the apparatus with the broken lines denoting newly installed components, i.e. '9', '10', '13' and '16'. Component '10' calculates the ratio between the S-KX spectrum intensity ('8') and the scattered radiation intensity ('9'). Since the factors influencing the absolute intensity of the S-KX spectrum (e.g., differences in composition, instrumental variables, and atmospheric changes) also influence the scattered radiation intensity to the same degree, using the ratio instead of the absolute intensity corrects for these factors.

Block '17' calculates the values of the constants in the calibration equation shown below (Eq.1).

$$S = a I^2 + b I + c \quad 1)$$

where S is the sulfur content, I is the x-ray intensity ratio between the S-KX spectrum and the scattered radiation, and a, b and c are constants. To determine these constants, three standard samples whose sulfur contents are exactly known are sequentially measured with the analyzer set on mode 'C' (see Fig.1). These constants, once determined and stored in the memory of the calculator, can be used for about one year without loss of accuracy, since the ratio calculator '10' seems to be also effective in correcting the long term drift of the analyzer.

Preliminary Tests

To compare the performance of the modified analyzer to that of the prototype, analyses were made on prepared samples. The samples consisted of white oil plus di-butyl di-sulfide (DBDS). Di-butyl di-sulfide has recently been officially certified by the Japanese government as the sulfur compound for x-ray calibration purposes and is now widely used in Japan.

As can be seen in Fig.2, the relationship between the content and the intensity is not linear. Thus, if the working curve is approximated with a straight line, for example, ranging from 0 wt% to 6 wt%, the maximum error reaches 0.31 wt% at the mid point of the curve, as illustrated in Fig.3(b). It was recognized that the relationship shown in Fig.2 can be more accurately expressed by a quadratic equation rather than a linear equation. Thus, a quadratic approximation was set up using calibration standards containing 0, 3 and 6 wt% sulfur. The results shown in Fig.3(b) clearly indicate that the use of this quadratic approximation greatly reduced the difference between the measured value and actual value of the sulfur content. The maximum error observed was 0.01 wt%.

As shown in Fig.4(a), fairly large errors were observed when samples of high C/H were analyzed by using calibration standards of low C/H. In this case, the standards were prepared from decalin (C/H=6.7) plus DBDS, while the unknowns were prepared from tetralin (C/H=10.0) plus DBDS.

It was previously reported by one of the authors (2) that this error could be corrected by using the following empirical equation,

$$\Delta S = -0.013 S \left(\frac{C/H}{C/H_{std}} - \frac{C/H}{C/H_{unkn}} \right) \quad 2)$$

where S is the observed sulfur content and ΔS the value to be added to the observed sulfur content. In the above-referenced study, the factor 0.013 was determined experimentally by using the prototype x-ray analyzer. To use Eq.2, one must know C/H values for both the standards and the unknowns. An alternative expression can also be obtained by using the specific gravity ρ instead of C/H, since it was found that C/H is roughly related to ρ as follows:

$$C/H = 8.82 \rho - 1.06 \quad 3)$$

$$\text{thus, } \Delta S = 0.115 S \Delta \rho \quad 4)$$

where $\Delta\rho = \rho_{\text{std}} - \rho_{\text{unkn}}$

5)

It has been reported(3) that the error due to the C/H difference in the standards and the unknowns can be effectively eliminated by using the scattering intensity of the sample as an internal standard. In the modified analyzer, the effect of the compositional differences between the standards and the unknowns are automatically compensated by installing a scaler for the scattered radiation('9') and a ratio calculator ('10'). Figure 4(b) shows the results obtained by using the modified analyzer for testing the same combination of standards and unknowns tested on the prototype. Since the errors observed using the modified analyzer were much smaller than those observed using the prototype, we feel that the modified analyzer can be used in a wider range of applications than was previously possible.

The results illustrated in Fig.5(a) indicate that the magnitude of the effect due to the coexistence of chlorine is very small, and that the effect of the Cl-KX spectrum is adequately reduced by the filter. Without a filter, or other device for eliminating the Cl-KX spectrum, errors can be very large as seen in Fig.5(b).

Test Results

To examine practical usage of the analyzer, analyses were made on a variety of fuel oils whose characteristics are outlined in Table 1. Sulfur contents for these samples had been previously determined by the quartz tube method(JIS K 2541-1971) in several inter-laboratory tests. The standard samples for calibration were made from white oil plus DBDS. Sulfur contents of these standards were 0, 1.5 and 3.0 wt%. In this series of measurements, three 100 sec integrations were made for each sample, and the results were averaged. The results of the analyses are shown in Fig.6, where the horizontal axis indicates the sulfur content determined by the quartz tube method, and the vertical axis indicates the difference between the sulfur level determined by the x-ray method and that determined by the quartz tube method(in the case of fuels used in inter-laboratory tests) or that certified by NBS or JPI(in the case of standard reference materials).

It can be seen from Fig.6 that the errors are within ± 0.01 wt% for most of the samples analyzed, and within ± 0.02 wt% for all of the samples analyzed(ranging up to 3.3 wt% sulfur contents).

Since the observed errors are so small, we can conclude that standard samples prepared from white oil plus DBDS can be used for calibration without loss of accuracy, in spite of the fact that there are many differences in composition between the standards and the unknowns, such as C/H, quantity of ash, chlorine content, etc.

Conclusion

A non-dispersive x-ray sulfur analyzer which consists of the prototype "Rigaku Sulfur-X" plus additional mechanisms for correcting various matrix effects was developed.

Test results made on a variety of fuel oils indicated that the modified analyzer can accurately measure sulfur contents of fuel oils(within ± 0.01 wt% of the actual value) by using calibration standards prepared from white oil plus di-butyl di-sulfide.

References

- (1) G.Frechette, J.C.Herbert, T.P.Thinh and Y.A.Miron; Hydrocarbon Processing, vol.54, 109 (1975).
- (2) A.Masuko; J. Japan Petrol. Inst., vol.20, 909 (1977), in Japanese.
- (3) G. Andermann and J.W.Kemp; Anal. Chem., vol.30, 1306 (1958).

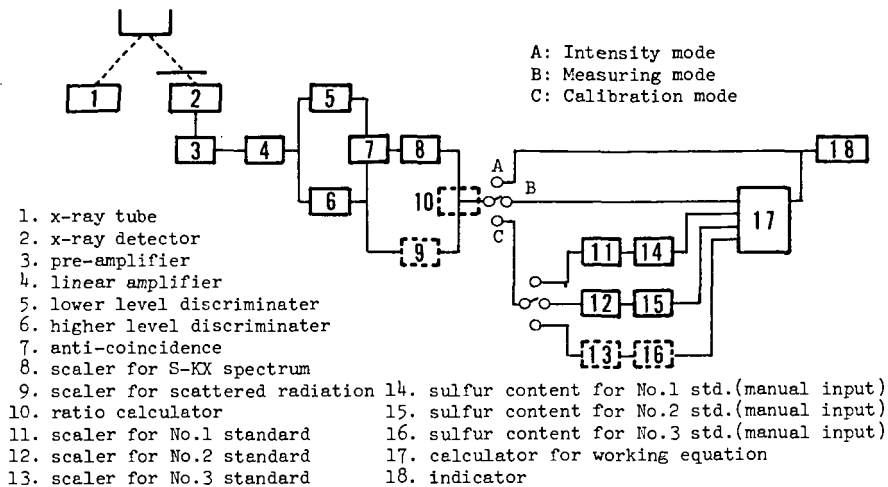


Fig.1 Schematic diagram of the non-dispersive x-ray sulfur analyzer

Note: the blocks surrounded by solid lines are those of the prototype.

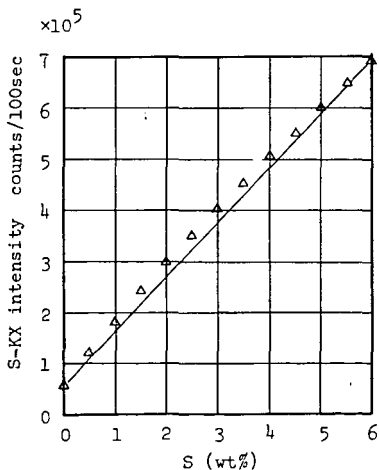


Fig.2 Relation between sulfur content and S-KX intensity

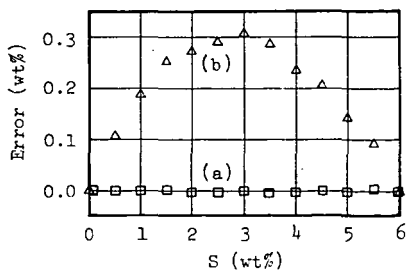


Fig.3 Comparison of linear approximation and quadratic approximation

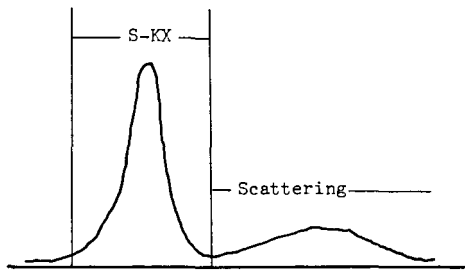
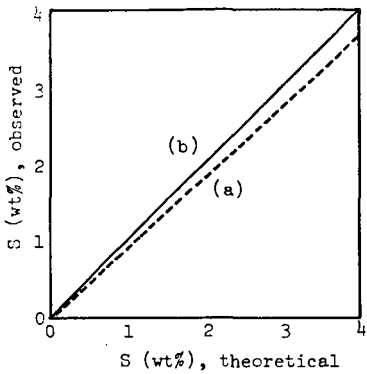


Fig.4 Comparison of absolute method(S-KX intensity) and ratio method(S-KX intensity/scattering intensity)

C/H of the standards: 6.7
 C/H of the unknowns :10.0

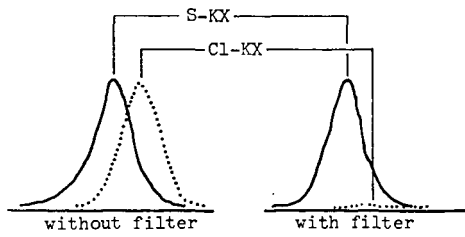
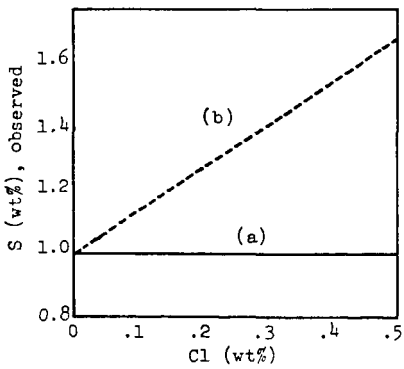


Fig.5 Error due to peak overlapping, and the effect of filtering

Sulfur contents in the samples used in the experiment were 1.0wt%

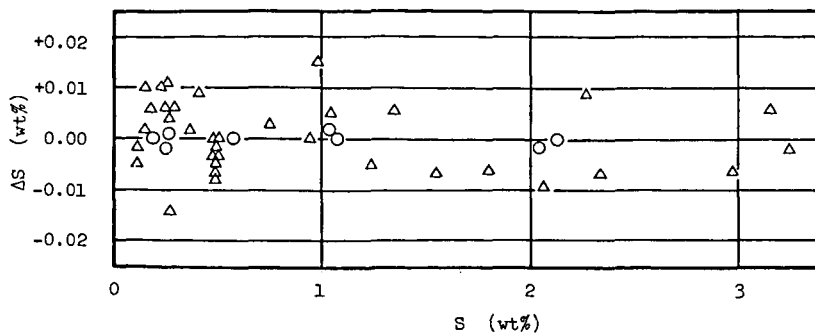


Fig.6 Analytical results for a variety of fuel oils

Δ: Samples which had been used and analyzed in inter-laboratory tests by quartz tube method(JIS K 2541-1971).
 O: Standard reference materials(NBS and JPI).

Horizontal axis: Sulfur content either determined by quartz tube method or certified by NBS or JPI.

Vertical axis : The difference ΔS (wt%) given by following equations,

$$\Delta S = S_{\text{quartz}} - S_{\text{x-ray}}$$

$$\Delta S = S_{\text{SRM}} - S_{\text{x-ray}}$$

Table 1. Characteristics of the sample oils* analyzed

Term	Range
C/H (wt%/wt%)	6.0 - 8.5
Sulfur content (wt%)	0.1 - 3.4
Ash (wt%)	0.01 - 0.2
Pour point (°C)	-10 - +35
Viscosity, @50°C (cSt)	2.5 - 200
Specific gravity (15/4°C)	0.84 - 0.95
Chlorine content**(wt%)	0 - 0.5

* These samples had been analyzed previously in inter-laboratory tests.

** Chlorinated paraffins were added to some of the sample oils for the adjustment of Cl contents.